Supplementary Information

Ortho-functionalized pyridinyl-tetrazines break the inverse correlation between click reactivity and cleavage yields in click-to-release chemistry

Ron M. Versteegen[1], Raffaella Rossin[2], Ivo A.W. Filot[3], Freek J.M. Hoeben[1], Arthur H.A.M. van Onzen[2], Henk M. Janssen[1†], Marc S. Robillard[2,*]

[1] SyMO-Chem B.V., Den Dolech 2, 5612 AZ Eindhoven, The Netherlands. [2] Tagworks Pharmaceuticals, Toernooiveld 1, 6525 ED Nijmegen, The Netherlands. [3] Eindhoven University of Technology, Den Dolech 2, 5612 EZ Eindhoven, The Netherlands.
* Corresponding author: marc.robillard@tagworkspharma.com
† Dedicated to co-author Henk Janssen, who passed away on October 21, 2024.

Table of Contents

Section S1: Supplementary Methods

Materials

All reagents, chemicals, materials and solvents were obtained from commercial sources, and were used as received: Biosolve, Merck and Cambridge Isotope Laboratories for (deuterated) solvents, and Aldrich, Acros, ABCR, Merck, Fluka, and Fluorochem for chemicals, materials and reagents. All solvents were of AR quality. Dry THF was dispensed from an MBRAUN MB-SPS-800 system. Water was distilled and deionized (18 MΩcm) by means of a milli-Q water filtration system (Millipore). Monomethyl auristatin E (MMAE) and deuterated (d_8) MMAE were purchased from MedChemExpress. Sodium [^{125}I]iodide solutions were purchased from PerkinElmer. [^{111}In]Indium chloride solution was purchased from Curium. The Bolton-Hunter reagent (N-succinimidyl-3-[4-hydroxyphenyl]propionate, SHPP) and Zeba desalting spin columns (7 kDa MW cut-off, 0.5 mL) were purchased from Fisher Scientific. Mouse plasma was purchased from Innovative Research. 29-Amino-3,6,9,12,15,18,21,24,27-nonaoxanonacosan-1-ol was purchased from PurePEG. 3,6-Dimethyl-1,2,4,5-tetrazine and (*E*)-cyclooct-2-en-1-yl (4-nitrophenyl) carbonate [1], and *rel*-(1*R*,4*E*,6*R*,*pS*)-2,5-dioxopyrrolidin-1-yl-6-((((2,5-dioxopyrrolidin-1-yl)oxy)carbonyl)oxy)-1-methylcyclooct4-ene-1-carboxylate (axial isomer) [2] were prepared according to literature procedures. The anti-TAG72 diabody (TGW101-DB) was produced,functionalized with PEG-TCO-MMAE groups and charachterized as previously described [3], yielding an ADC with DAR=4.

General methods

Moisture- and oxygen-sensitive reactions were performed under an Ar atmosphere. In the synthetic procedures, equivalents (eq) are molar equivalents. ^{1}H-NMR and ^{13}C-NMR spectra were recorded on a Bruker Avance III HD (400 MHz for ^{1}H-NMR and 100 MHz for ^{13}C-NMR) spectrometer at 25°C. Chemical shifts are reported in ppm downfield from TMS at 25°C. Abbreviations used for splitting patterns are s=singlet, t=triplet, q=quartet, m=multiplet and br=broad. Reverse phase (RP) medium pressure liquid column chromatography was performed on a Biotage Isolera One MPLC system using a GracePure C_{18} RP column (40 gram), and acetonitrile / water mixtures (containing 0.1 v/v% formic acid) as the eluent. HPLC-MS/PDA was performed using a Shimadzu LC-20 AD VP series HPLC coupled to a diode array detector (Shimadzu SPD-M20A) and an Ion-Trap (LCQ Fleet, Thermo Scientific) MS-detector, employing a Phenomenex Kinetex 5µm EVO C_{18} 100 Å column using an injection volume of 1-10 µL, a flow rate of 0.3 mL/mL and typically a gradient (5% to 100% in 5 min, held at 100% for 1 min) of acetonitrile in H_2O (both containing 0.1 v/v% formic acid) at 20°C. Quantitative HPLC-SIM-MS was performed on a Shimadzu Nexera-i LC-2040C 3D HPLC equipped with a Shimadzu LCMS-2020 mass spectrometer. Preparative RP-HPLC (acetonitrile / H_2O with 0.1 v/v% formic acid) was performed using a Shimadzu SCL-10A VP coupled to two Shimadzu LC-8A pumps and a Shimadzu SPD-10AV VP UV-vis detector on a Phenomenex Gemini 5µ C_{18} 110A column. Radio-HPLC was performed on an Agilent 1100 system, equipped with a Gabi radioactive detector (Raytest). The samples were loaded on an Alltima C_{18} column (4.6 × 150mm, 5µ), which was eluted at 1 mL min-1 with a linear gradient of water (A) and acetonitrile (B) containing 0.1% v/v% TFA (4 min at 20% B followed by an increase to 70% B in 11 min). Radio-ITLC was performed on ITLC-SG strips (Varian Inc.) eluted with 200 mM EDTA in saline solution (^{111}In-labeling) or a 1:1 mixture of methanol/ethyl acetate (^{125}I-labeling). In these conditions the radiolabeled products remain at the base while unbound ^{111}In and [^{125}I]I-SHPP migrates with an R_f of 0.7-0.9. SDS-PAGE was performed on a Mini-PROTEAN Tetra Cell system using 4-20% precast Mini-PROTEAN TGX gels and Precision Plus Protein All Blue Prestained protein standards (BioRad Laboratories). The radioactivity distribution on ITLC strips and SDS-PAGE gels was monitored with a Typhoon FLA 7000 phosphor imager (GE Healthcare Life Science) using the AIDA software.

The ADC was labeled with ^{125}I using the Bolton-Hunter method as previously described [4] and the obtained radiolabeled product was analysed by radio-TLC and SDS-PAGE. The tetrazine probe was radiolabeled with ^{111}In as previously described [4] and the radiolabeled probe was analysed by radio-TLC and RP-HPLC.

Section S2: Synthetic procedures

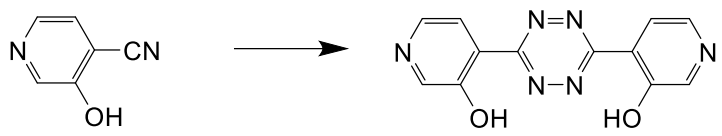

1b

4,4'-(1,2,4,5-Tetrazine-3,6-diyl)bis(pyridin-3-ol) (**1b**)

3-Hydroxyisonicotinonitrile (62 mg, 0.52 mmol), $Zn(OTf)_2$ (10 mg, 28 µmol, 0.05 eq), ethanol (80 µL) and hydrazine hydrate (0.3 mL, 5.3 mmol, 10 eq) were stirred at 60°C for 21 h. After removal of the volatiles in vacuo the solid was stirred in methanol (4 mL) for 5 min at room temperature. The suspension was filtered, the solid was washed with methanol (5×2 mL) and dried in vacuo yielding impure intermediate [2H]-TZ as an orange solid. The [2H]-TZ was stirred in acetic acid (4 mL) and $NaNO_2$ (32 mg, 0.45 mmol) in water (0.2 mL) was added dropwise (CAUTION: toxic fumes) causing an immediate color change from orange to red. After stirring at room temperature for 1 h the suspension was filtrated, the solid was washed with ethanol, water and ethanol (all 5×2 mL) and dried in vacuo. This yielded **1b** (10 mg, 37 µmol, 14 % overall) as a red solid. ^{1}H-NMR (DMSO-d6): δ = 10.89 (br, 2H, O*H*), 8.55 (s, 2H, Ar*H*), 8.37 (d, 2H, Ar*H*), 8.04 (d, 2H, Ar*H*) ppm. ESI-MS: *m/z* Calc. for $C_{12}H_8N_6O_2$ 268.07; Obs. $[M+H]^+$ 269.17, λ_{max} = 227, 271, 338 and 516 nm.

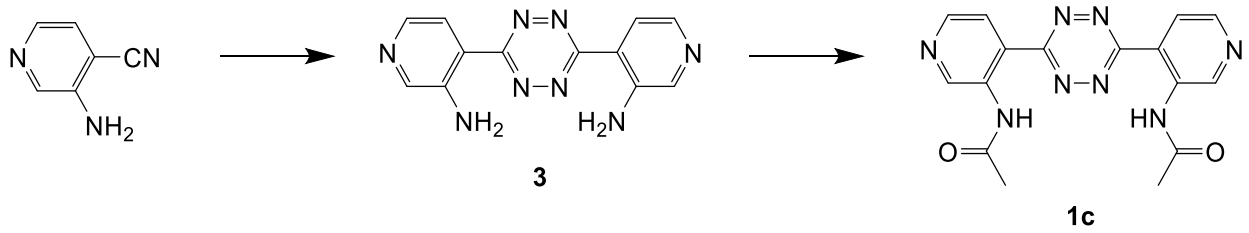

3 **1c**

4,4'-(1,2,4,5-Tetrazine-3,6-diyl)bis(pyridin-3-amine) (**3**)

3-Aminoisonicotinonitrile (200 mg, 1.6 mmol), sulfur (26 mg, 0.8 mmol, 0.5 eq) and hydrazine hydrate (0.46 mL, 8.1 mmol, 5 eq) were stirred at 100°C for 16 h. Cold water (2 mL) was added and the suspension was stirred at room temperature for 5 min, filtered and the solid was washed with cold water and cold ethanol (both 5×4 mL). Trituration of the solid in ethanol (20 mL) at 50°C for 15 min was followed by filtration. The solid was washed with ethanol (5×4 mL) and dried in vacuo yielding the intermediate [2H]-TZ **4** (144 mg, 0.54 mmol, 67%) as an orange solid. **4** was stirred in DMSO (5 mL) at 40°C for 16 h while bubbling through O_2. In time a color change occurred from orange to red. The reaction mixture was added dropwise to water (70 mL) and the resulting suspension was filtered. The solid was washed with water, ethanol and dichloromethane (all 5×4 mL) and dried in vacuo yielding pure **3** (130 mg, 0.49 mmol, 61% overall) as a red solid. ^{1}H-NMR (DMSO-d6): δ = 8.41 (br s, 2H, Ar*H*), 8.21 (d, 2H, Ar*H*), 7.95 (br d, 2H, Ar*H*), 7.16 (br s, 4H, NH_2) ppm. ^{13}C-NMR (DMSO-d6): δ = 162.7, 144.3 (br), 141.3, 135.9, 120.8 (br), 115.9 ppm. ESI-MS: *m/z* Calc. for $C_{12}H_{10}N_8$ 266.10; Obs. $[M+H]^+$ 267.17, λ_{max} = 240, 288 and 427 nm.

***N*,*N*'-(4,4'-(1,2,4,5-Tetrazine-3,6-diyl)bis(pyridine-4,3-diyl))diacetamide** (**1c**)

3 (22 mg, 83 µmol) was suspended in acetic anhydride (0.5 mL) and the suspension was heated at 50°C for 3 d. The mixture was precipitated in diethyl ether (6 mL) and the solution was decanted. Next, the solid was triturated with water (2 mL), the mixture was centrifuged at 12.7k rpm for 1 min and the solution was decanted. This trituration-centrifugation procedure was repeated using methanol and 2-propanol (both 2 mL). The resulting solid was dried in vacuo yielding pure **1c** (12 mg, 34 µmol, 41%) as a purple-red solid. ^{1}H-NMR (DMSO-d6): δ = 10.35 (s, 2H, N*H*), 9.01 (s, 2H, Ar*H*), 8.67 (d, 2H, Ar*H*), 8.02 (d, 2H, Ar*H*), 2.00 (s, 6H, CH_3) ppm. ^{13}C-NMR (DMSO-d6): δ = 168.7, 164.1, 146.4, 146.1, 132.4, 131.4, 123.7, 23.3 ppm. ESI-MS: *m/z* Calc. for $C_{16}H_{14}N_8O_2$ 350.12; Obs. $[M+H]^+$ 351.17, λ_{max} = 242 and 523 nm.

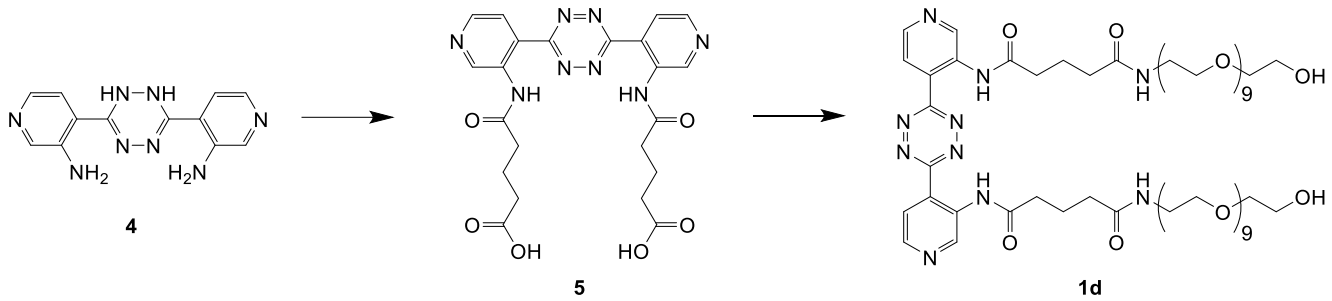

5,5'-((4,4'-(1,2,4,5-Tetrazine-3,6-diyl)bis(pyridine-4,3-diyl))bis(azanediyl))bis(5-oxopentanoic acid) (**5**)

4 (200 mg, 0.75 mmol) and glutaric anhydride (0.9 g, 7.5 mmol, 10 eq) were suspended in dry THF (2 mL) and the mixture was stirred under an Ar atmosphere at 52°C for 14 d. In time, the reaction mixture turned into a paste and additional THF was occasionally added to ensure that stirring continued. After ^{1}H-NMR confirmed close to full conversion, the paste was transferred to a round-bottom flask and the solvent was removed in vacuo. The compound was suspended in acetic acid (20 mL) and concentrated nitric acid (0.75 mL) was added dropwise (CAUTION: toxic fumes). The initially orange suspension turned red in seconds and the mixture was stirred at room temperature for 30 min. The suspension was filtered and the resulting solid was washed with acetic acid (3×4 mL). The solid was thoroughly broken up using a spatula, washed with diethyl ether (3×4 mL) and dried in vacuo at 30°C for 1 h. The dry solid was powdered using a spatula and stirred in methanol (6 mL) at room temperature for 30 min. The suspension was filtered and the resulting solid was washed with methanol (2×8 mL) and diethyl ether (5×8 mL). The solid was dried in vacuo at 30°C for 1 h yielding **5** (313 mg, 0.63 mmol, 85%) as a pink solid. ^{1}H-NMR (DMSO-d6): δ = 10.41 (s, 2H, N*H*), 9.05 (s, 2H, Ar*H*), 8.67 (d, 2H, Ar*H*), 8.04 (d, 2H, Ar*H*), 2.33 (t, 4H, CH_2), 2.24 (t, 4H, CH_2), 1.72 (qn, 4H, $CH_2CH_2CH_2$) ppm. ^{13}C-NMR (DMSO-d6): δ = 174.1, 171.2, 164.0, 145.1, 144.8, 132.9, 131.9, 124.3, 35.0, 32.8, 20.1 ppm. ESI-MS: *m/z* Calc. for $C_{22}H_{22}N_8O_6$ 494.17; Obs. $[M+H]^+$ 495.33, λ_{max} = 240, 328 and 525 nm.

***N*^{1},*N*$^{1'}$-(4,4'-(1,2,4,5-Tetrazine-3,6-diyl)bis(pyridine-4,3-diyl))bis(*N*^{5}-(29-hydroxy-3,6,9,12,15,18,21,24,27-nonaoxanonacosyl)glutaramide)** (**1d**)

29-Amino-3,6,9,12,15,18,21,24,27-nonaoxanonacosan-1-ol (53.5 mg, 0.12 mmol, 2.1 eq) was dissolved in DMF (1 mL) and **5** (27.5 mg, 56 mmol) was added. To this orange suspension was added *N*-methylmorpholine (37 mL, 0.33 mmol, 6 eq) and PyBOP (75 mg, 0.14 mmol, 2.5 eq). The mixture was stirred at room temperature for 90 min during which the suspension eventually cleared. The red solution was evaporated to dryness, redissolved in DCM (1 mL), and purified by column chromatography (flash SiO_2) using an elution gradient of 0% to 20% methanol in DCM, to yield pure product **1d** (36 mg, 56 mmol, 47%) as a red sticky solid. ^{1}H-NMR (DMSO-d6): δ = 10.35 (s, 2H, ArN*H*), 9.05 (s, 2H, Ar*H*), 8.66 (d, 2H, Ar*H*), 8.02 (d, 2H, Ar*H*), 7.80 (t, 2H, N*H*CH_2), 4.54 (t, 2H, O*H*), 3.53–

3.34 (m, 76H, OC*H*$_2$), 3.17 (q, 4H, NHC*H*$_2$), 2.29 (t, 4H, C*H*$_2$), 2.09 (t, 4H, C*H*$_2$), 1.72 (qn, 4H, CH$_2$C*H*$_2$CH$_2$) ppm. ^{13}C-NMR ($CDCl_3$): δ = 172.56, 171.54, 163.89, 145.73, 145.29, 133.81, 128.16, 122.44, 72.35, 70.5 – 69.7 (m), 61.50, 39.18, 36.56, 34.95, 21.30 ppm. ESI-MS: *m/z* Calc. for $C_{62}H_{104}N_{10}O_{24}$ 1372.72; Obs. $[2M+H]^+$ 687.75, $[M+H]^+$ 1373.75, λ_{max} = 237 and 526 nm.

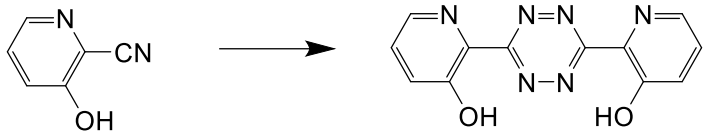

2b

2,2'-(1,2,4,5-Tetrazine-3,6-diyl)bis(pyridin-3-ol) (**2b**)

3-Hydroxypicolinonitrile (100 mg, 0.82 mmol) and hydrazine hydrate (0.28 mL, 4.9 mmol, 6 eq) were stirred at 90°C for 2 h. Ethanol (4 mL) was added and the suspension was stirred at room temperature for 5 min. The suspension was filtered and the solid was washed with ethanol (5×2 mL). Drying of the solid in vacuo yielded pure intermediate [2H]-TZ (59 mg, 0.22 mmol, 54%) as a yellow solid. The [2H]-TZ was suspended in acetic acid (6 mL) and $NaNO_2$ (75 mg, 1.1 mmol, 5 eq) in water (0.5 mL) was added dropwise (CAUTION: toxic fumes). The suspension was stirred at room temperature for 1 h during which a clear red solution was obtained and, eventually, a red precipitate arose. Chloroform and water (both 40 mL) were added and the layers were separated. The aqueous layer was extracted with chloroform (2×20 mL) and the combined organic layers were dried using Na_2SO_4. After filtration, the filtrate was evaporated to dryness yielding pure **2b** (55 mg, 0.21 mmol, 50% overall) as a red solid. ^{1}H-NMR (DMSO-d6): δ = 10.74 (br s, 2H, O*H*), 8.38 (m, 2H, Ar*H*), 7.57 (m, 4H, Ar*H*) ppm. ^{13}C-NMR (DMSO-d6): δ = 164.3, 154.3, 141.3, 137.5, 127.5, 125.3 ppm. ESI-MS: *m/z* Calc. for $C_{12}H_8N_6O_2$ 268.07; Obs. $[M+H]^+$ 269.17, $[2M+Na]^+$ 559.08, λ_{max} = 234, 258, 352 and 527 nm.

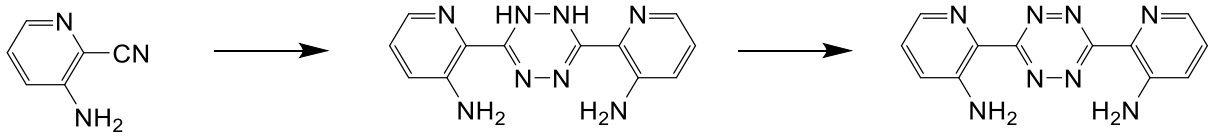

6 **7**

2,2'-(1,2,4,5-Tetrazine-3,6-diyl)bis(pyridin-3-amine) (**7**)

3-Aminopicolinonitrile (0.62 g, 5.2 mmol), 3-mercaptopropionic acid (0.46 mL, 5.2 mmol, 1 eq) and hydrazine hydrate (1.8 mL, 32 mmol, 6 eq) were stirred at 90°C for 18 h. Cold water (2 mL) was added and the suspension was stirred at room temperature for 5 min. Filtration, washing of the solid with cold water and cold ethanol (both 5×2 mL) and drying in vacuo yielded the intermediate [2H]-TZ **6** (0.66 g, 2.4 mmol, 94%) as an orange solid. To **6** (38 mg, 0.14 mmol) and $PhI(OAc)_2$ (75 mg, 0.23 mmol, 1.6 eq) dichloromethane (1 mL) was added and the suspension was stirred at room temperature for 3 h. In time a color change occurred from orange to red. The suspension was filtered, the solid was washed with dichloromethane (5×1 mL) and dried in vacuo yielding pure **7** (31 mg, 0.12 mmol, 77% overall) as a red solid. ^{1}H-NMR (DMSO-d6): δ = 8.13 (dd, 2H, Ar*H*), 7.36 (2dd, 4H, Ar*H*), 6.98 (br s, 4H, N*H*$_2$) ppm. ^{13}C-NMR (DMSO-d6): δ = 162.8, 146.6, 138.3, 129.5, 126.9, 124.5 ppm. ESI-MS: *m/z* Calc. for $C_{12}H_{10}N_8$ 266.10; Obs. $[M+H]^+$ 267.08, λ_{max} = 224 and 439 nm.

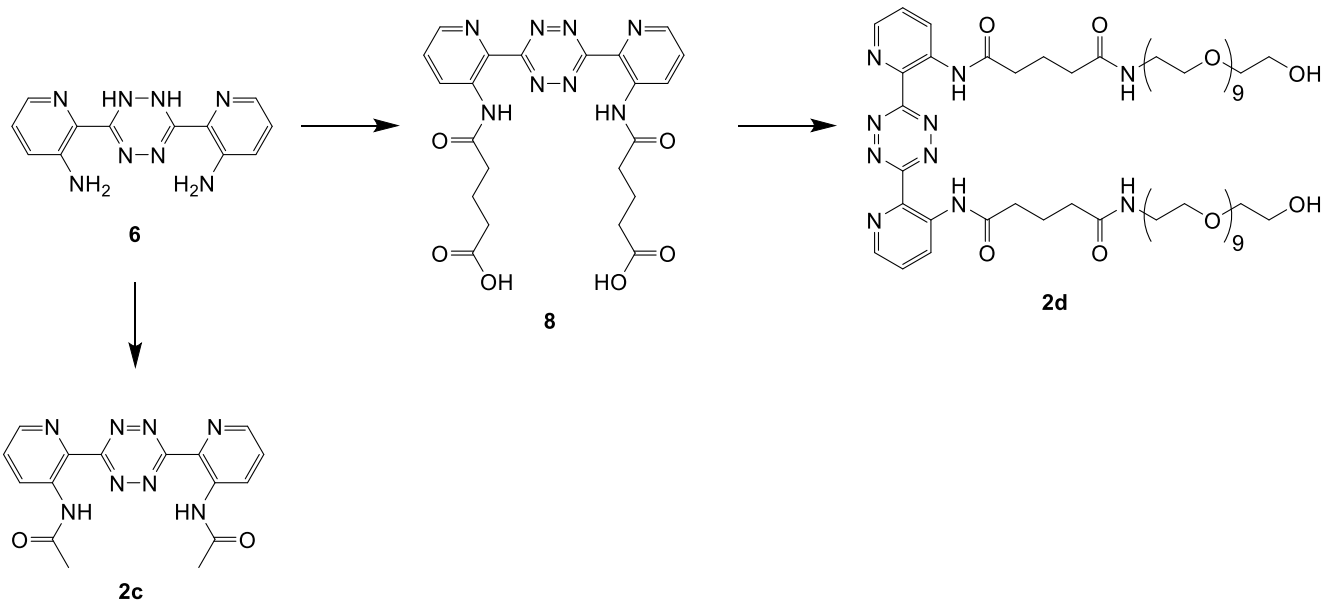

***N*,*N*'-(2,2'-(1,2,4,5-Tetrazine-3,6-diyl)bis(pyridine-3,2-diyl))diacetamide** (**2c**)

6 (52 mg, 0.19 mmol) was suspended in dry THF (0.8 mL), acetic anhydride (185 mL, 1.9 mmol, 10 eq) was added and the mixture was heated at 52°C for 22 h. The volatiles were removed in vacuo and the residue was suspended in acetic acid (1 mL). Concentrated nitric acid (5 drops) was added dropwise (CAUTION: toxic fumes) and the initially orange suspension turned red in seconds. After stirring at room temperature for 30 min, the suspension was filtered and the resulting solid was washed with diethyl ether (3×4 mL). This procedure was repeated for the supernatant, in which renewed precipitation occurred. The solids were combined and dried in vacuo for 20 h yielding pure **2c** (63 mg, 0.18 mmol, 93%) as a red solid. ^{1}H-NMR (DMSO-d6): δ = 10.16 (br s, 2H, N*H*), 8.66 (dd, 2H, Ar*H*), 8.29 (dd, 2H, Ar*H*), 7.72 (dd, 2H, Ar*H*), 1.95 (s, 6H, CH_3) ppm. ^{13}C-NMR (DMSO-d6): δ = 168.6, 164.5, 145.8, 142.3, 134.6, 132.2, 126.2, 23.4 ppm. ESI-MS: *m/z* Calc. for $C_{16}H_{14}N_8O_2$ 350.12; Obs. $[M+H]^+$ 351.17, $[2M+Na]^+$ 723.00, λ_{max} = 239, 321 and 525 nm.

5,5'-((2,2'-(1,2,4,5-Tetrazine-3,6-diyl)bis(pyridine-3,2-diyl))bis(azanediyl))bis(5-oxopentanoic acid) (**8**)

6 (200 mg, 0.75 mmol) and glutaric anhydride (0.9 g, 7.5 mmol, 10 eq) were suspended in dry THF (3 mL). Upon stirring at 52°C the suspension cleared and the mixture was stirred at 52°C for 19 h. The obtained suspension was filtered and the resulting solid was washed with diethyl ether (3×4 mL). The solid was transferred to a round-bottom flask and the solvent was removed in vacuo. The compound was suspended in acetic acid (8 mL) and concentrated nitric acid (6 drops) was added dropwise (CAUTION: toxic fumes). The initially orange suspension turned red in seconds and the mixture was stirred at room temperature for 30 min. The suspension was filtrated and the resulting solid was washed with acetic acid (3×4 mL) and diethyl ether (3×4 mL). The solid was dried in vacuo at 35°C for 2 h yielding pure **8** (327 mg, 0.66 mmol, 89%) as a red solid. ^{1}H-NMR (DMSO-d6): δ = 10.15 (s, 2H, N*H*), 8.65 (dd, 2H, Ar*H*), 8.32 (dd, 2H, Ar*H*), 7.71 (dd, 2H, Ar*H*), 2.27 (t, 4H, CH_2), 2.22 (t, 4H, CH_2), 1.70 (qn, 4H, $CH_2CH_2CH_2$) ppm. ^{13}C-NMR (DMSO-d6): δ = 174.1, 171.0, 164.5, 145.8, 142.2, 134.5, 132.0, 126.1, 35.0, 32.8, 20.1 ppm. ESI-MS: *m/z* Calc. for $C_{22}H_{22}N_8O_6$ 494.17; Obs. $[M+H]^+$ 495.33, λ_{max} = 240, 328 and 525 nm.

***N*^{1},*N*$^{1'}$-(2,2'-(1,2,4,5-Tetrazine-3,6-diyl)bis(pyridine-3,2-diyl))bis(*N*^{5}-(29-hydroxy-3,6,9,12,15,18,21,24,27-nonaoxanonacosyl)glutaramide)** (**2d**)

29-Amino-3,6,9,12,15,18,21,24,27-nonaoxanonacosan-1-ol (64.1 mg, 0.14 mmol, 2.1 eq) was dissolved in DMF (1 mL) and **8** (32.7 mg, 66 mmol) was added. To this orange suspension was added *N*-methylmorpholine (44 mL, 0.40 mmol, 6 eq) and PyBOP (92 mg, 0.17 mmol, 2.6 eq). The mixture was stirred at room temperature for 2 h during which the suspension eventually cleared. The red solution was evaporated to dryness, redissolved in DCM (1 mL), and purified by column chromatography (flash SiO_2) using an elution gradient of 0% to 20% methanol in DCM, to yield pure **2d** (57 mg, 41 mmol, 63%) as a red sticky solid. ^{1}H-NMR (DMSO-d6): δ = 10.16 (s, 2H, ArN*H*), 8.65 (dd, 2H, Ar*H*), 8.33 (dd, 2H, Ar*H*), 7.79 (t, 2H, N*H*CH_2), 7.71 (dd, 2H, Ar*H*), 4.54 (t, 2H, O*H*), 3.53–3.33 (m, 76H, OCH_2), 3.16 (m, 4H, NHCH_2), 2.23 (t, 4H, CH_2), 2.07 (t, 4H, CH_2), 1.70 (qn, 4H, $CH_2CH_2CH_2$) ppm. ESI-MS: *m/z* Calc. for $C_{62}H_{104}N_{10}O_{24}$ 1372.72; Obs. $[2M+H]^+$ 687.58, $[M+H]^+$ 1373.83, λ_{max} = 242 and 524 nm.

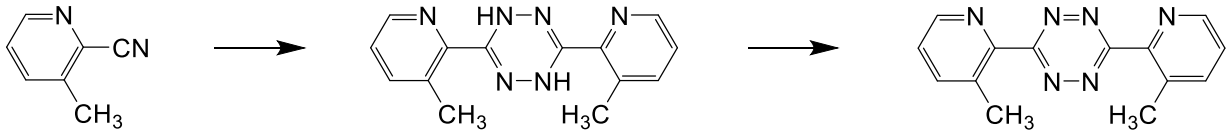

2e

3,6-Bis(3-methylpyridin-2-yl)-1,2,4,5-tetrazine (2e)

3-Methylpicolinonitrile (0.500 g, 4.24 mmol), hydrazine hydrate (1.8 mL, 40 mmol), and sulfur (0.100 g, 3.12 mmol) were stirred at 90°C for 3 h. The orange suspension was cooled to 20°C and filtered. The residue was washed with water (10 mL) and ethanol (30 mL) and dried in vacuo to give the crude intermediate [2H]-TZ (230 mg, 41%).

To the crude intermediate [2H]-TZ (100 mg, 0.38 mmol) was added THF (4 mL), acetic acid (3 mL), and water (1 mL). Sodium nitrite (202 mg, 2.93 mmol) was added, causing the yellow suspension to turn red, and the mixture was stirred at 20°C for 18 h, and subsequently filtered. The pink/red filtrate was concentrated, diluted with DCM (20 mL), and washed with 1 M sodium carbonate (3 mL). The organic layer was dried over sodium sulfate and concentrated in vacuo. The crude product was purified by column chromatography (flash SiO_2) using an elution gradient of 20% to 50% acetone in heptane, to yield pure **2e** (63 mg, 64%) as a pink solid. ^{1}H-NMR ($CDCl_3$): δ = 8.78 (d, 2H, *J* = 4.8 Hz), 7.80 (d, *J* = 7.8 Hz, 2H), 7.47 (dd, *J* = 7.8, 4.7 Hz, 2H), 2.68 (s, 6H) ppm. ^{13}C-NMR ($CDCl_3$): δ = 165.51, 149.59, 148.14, 139.88, 135.10, 125.46, 19.99 ppm. ESI-MS: *m/z* Calc. for $C_{14}H_{12}N_{16}$ 264.11; Obs. $[M+H]^+$ 265.08, λ_{max} = 291 and 524 nm.

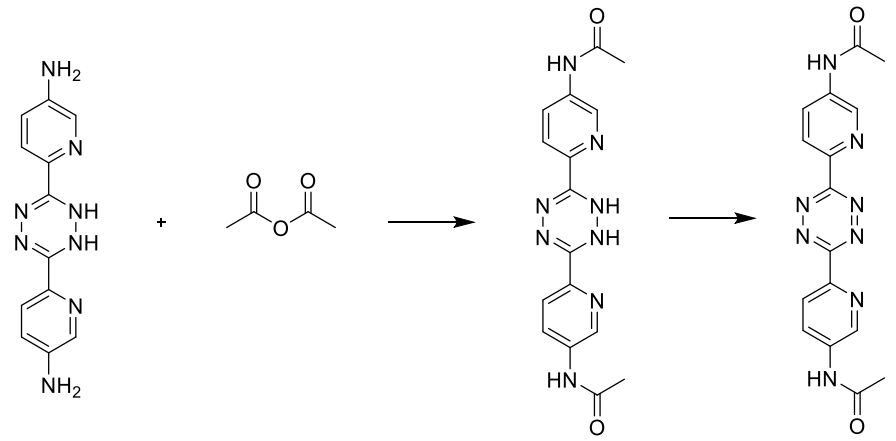

2f

***N,N'*-((1,2,4,5-Tetrazine-3,6-diyl)bis(pyridine-6,3-diyl))diacetamide (2f)**

3,6-Di(5-amino-pyridin-2-yl)-1,2-dihydro-1,2,4,5-tetrazine {Selvaraj, 2014 #1753} (100 mg, 0.373 mmol) was suspended in THF (2 mL). Acetic anhydride (114 mg, 1.12 mmol) was added, and the yellow suspension was stirred at room temperature for 18 h. To the intermediate product acetic acid (3 mL) was added, followed by sodium nitrite (58 mg, 0.84 mmol). The red suspension was stirred at room temperature for 1 h, and then filtered, washed with water (10 mL) and ethanol (10 mL), and dried in vacuo to yield product **2f** as a pink solid (74 mg, 57%). ^{1}H-NMR (DMSO-d6): δ = 10.59 (s, 2H), 9.01 (s, 2H), 8.58 (d, 2H), 8.41 (d, 2H), 2.16 (s, 6H) ppm. ESI-MS: *m/z* Calc. for $C_{16}H_{14}N_8O_2$ 350.12; Obs. $[M+H]^+$ 351.00, λ_{max} = 338 and 530 nm.

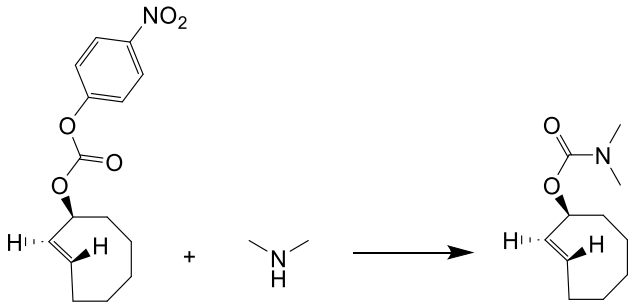

9

(*E*)-Cyclooct-2-en-1-yl dimethylcarbamate (axial isomer) (9)

(*E*)-Cyclooct-2-en-1-yl (4-nitrophenyl) carbonate (axial isomer) {Versteegen, 2013 #1443}v(109 mg, 0.374 mmol) was dissolved in THF (2 mL), and a solution of dimethylamine (0.468 ml, 2 M in THF) was added. After 1 h the solution was evaporated to dryness and the residue was dissolved in chloroform (5 mL) and washed with subsequently 1 M aqueous citric acid (2x2 mL) and 1 M aqueous NaOH (3x2 mL). The organic layer was dried over sodium sulfate, filtered and evaporated to dryness to yield **9** as a colorless oil (69 mg, 93%). ^{1}H-NMR ($CDCl_3$): δ = 5.80 (m, 1H), 5.55 (dd, 1H), 5.36 (d, 1H), 2.97 (s, 3H), 2.93 (s, 3H), 2.47 (m, 1H), 2.01 (m, 3H), 1.79 (m, 1H), 1.68 (m, 2H), 1.43 (m, 1H), 1.08 (m, 1H), 0.82 (m, 1H) ppm. ^{13}C-NMR ($CDCl_3$): δ = 155.81, 131.70, 131.63, 74.35, 40.85, 36.04, 35.90, 30.33, 29.16, 24.18 ppm. ESI-MS: *m/z* Calc. for $C_{11}H_{19}NO_2$ 197.14; Obs. $[M+H]^+$ 198.17, λ_{max} < 200 nm.

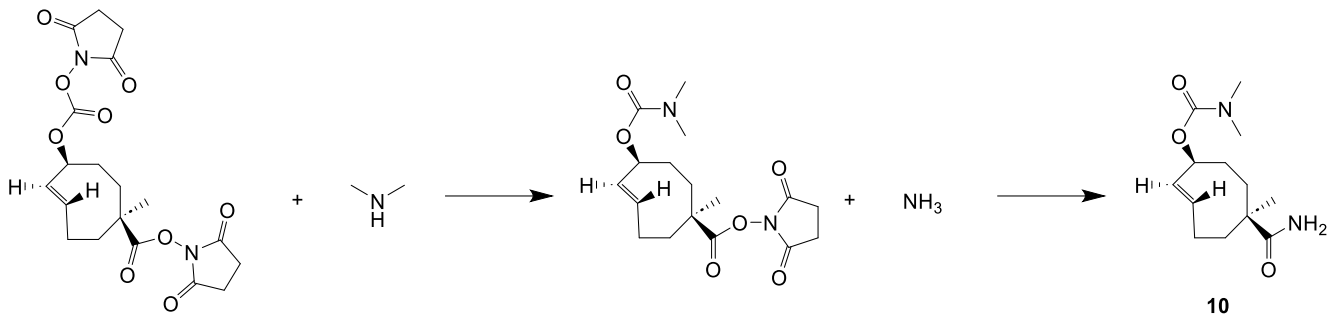

***rel*-(1*S*,6*S*,*E*,*pS*)-6-Carbamoyl-6-methylcyclooct-2-en-1-yl dimethylcarbamate** (**10**)

rel-(1*R*,4*E*,6*R*,*pS*)-2,5-Dioxopyrrolidin-1-yl-6-((((2,5-dioxopyrrolidin-1-yl)oxy)carbonyl)oxy)-1-methylcyclooct4-ene-1-carboxylate {Rossin, 2016 #1615} (100 mg, 0.237 mmol) was dissolved in acetonitrile (3 mL) and the solution was cooled to 0°C. Then, DIPEA (61 mg, 0.474 mmol) and a solution of dimethylamine (0.180 mL 2 M in THF, 0.36 mmol) were added. The solution was stirred for 5 min at 0°C, and subsequently, a solution of ammonia (1 mL 7 M in methanol, 7 mmol) was added. The turbid mixture was stirred at 20°C for 18 h, and then filtered. The filtrate was concentrated and the remaining oil was dissolved in chloroform (5 mL) and washed with subsequently 1 M aqueous citric acid (2x1.5 mL), and 1 M aqueous Na_2CO_3 (1.5 mL). The organic layer was dried over sodium sulfate, filtered and evaporated to dryness to yield **10** as a colorless oil (58 mg, 96%). ^{1}H-NMR ($CDCl_3$): δ = 5.89 (m, 1H), 5.62 (dd, 1H), 5.52 (br. s, 1H), 5.38 (br. s, 1H), 5.21 (s, 1H), 2.99 (s, 3H), 2.93 (s, 3H), 2.4 – 2.0 (4H), 2.0 – 1.8 (3H), 1.71 (dd, 1H), 1.15 (s, 3H) ppm. ESI-MS: *m/z* Calc. for $C_{13}H_{22}N_2O_3$ 254.16; Obs. $[M+Na]^+$ 277.17, λ_{max} < 200 nm.

Section S3: Component stability and reactivity

Activator stability

The assessment of activator stability was performed in PBS at room temperature and in 50% mouse plasma at 37°C in triplicate.

PBS: tetrazine solutions in DMSO (2.5 mM, 20 µL) were diluted with PBS (3.00 mL), filtered, and incubated at room temperature. The decrease of the absorption band at 520 nm (specific for the tetrazine moiety) was monitored using UV spectroscopy. The rate of hydrolysis and half-life time was derived by fitting a monoexponential decay through these data.

50 % plasma: tetrazine solutions in DMSO (10 mM, 30 µL) were added to wells containing 50% mouse plasma in PBS (270 µL, filtered through 45 µm and pre-heated to 37°C) in a 96-well plate. After a short mixing (20 seconds), the plate was inserted into a plate reader (Tecan Infinite 200 PRO) and incubated at 37°C with UV measurements every 5 min. The absorbance values were corrected for background (plasma:PBS:DMSO 4.5:4.5:1) and averaged. The tetrazine half-live was derived by fitting a monoexponential decay through these data.

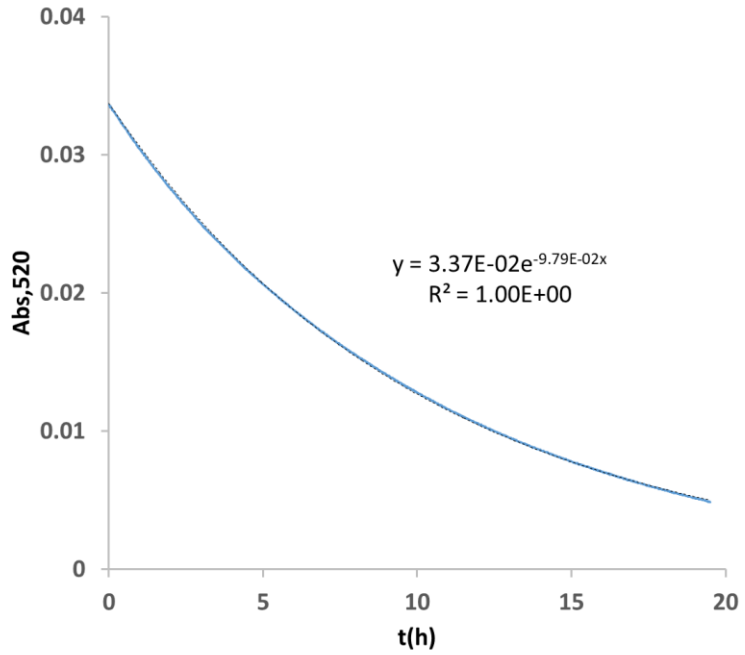

Supplementary Figure 1a. Decrease of the absorption at 520 nm of a solution of tetrazine **1b** in PBS at 20°C. Calculated half-life is 7.0 h (n=1).

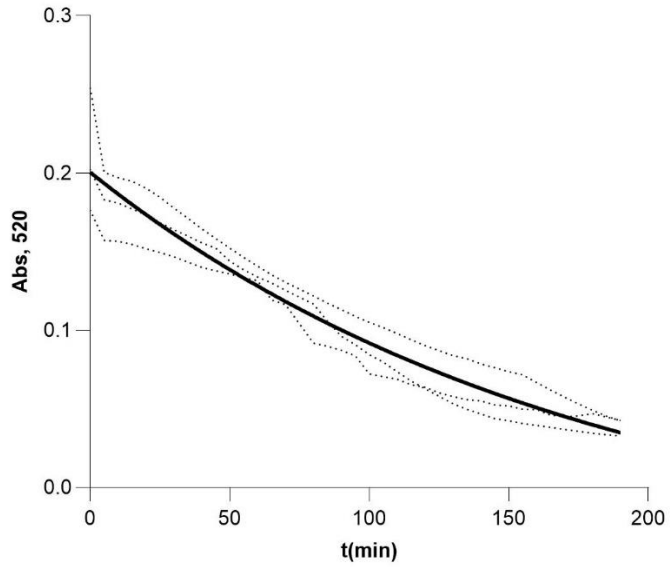

Supplementary Figure 1b. Decrease of the absorption at 520 nm (single plots, corrected for background, and fitted curve) of a solution of tetrazine **1b** in 50% mouse plasma at 37°C.

Supplementary Table 1. Half-lives of tetrazine activators in PBS at 20°C (n=3).

Activator	Half-life (h)
1b	6.5 ± 0.6
2b	37.8 ± 0.8
1d	4.2 ± 0.1
2d	8.7 ± 0.1

Kinetic measurements

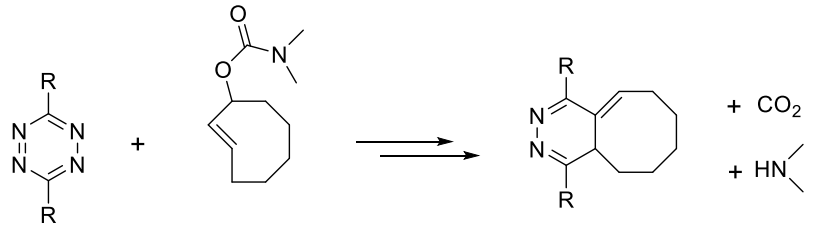

The second-order rate constant of the IEDDA reaction between model TCO **9** and activators **1b**, **2b** and **2e** in MeCN at 20°C was determined by UV-Vis spectrometry under second-order conditions. A cuvette was filled with a solution of activator (3 mL 0.083 mM in MeCN), and equilibrated at 20°C. Next, a solution of TCO **9** (10.0 µL 25 mM in DMSO) was added. The absorption at 540 nm (specific for the tetrazine moiety) was measured every second in a time course experiment. From the decay of this absorption, the conversion *x* was

calculated. The second-order rate constant k_2 was determined from the slope of the curve of a plot of 1/c-1/c0 versus time.

The second-order rate constant of the IEDDA reaction between model TCO **9** and activators **1b**, **1d**, **2b**, **2d** or bis-methyl tetrazine in 25% MeCN/PBS at 20°C was determined by stopped-flow UV-Vis spectrometry under pseudo first-order conditions. Tetrazine solutions (0.25 mM in 25% MeCN/PBS) and TCO **9** (3.45 mM in 25% MeCN/PBS) were mixed in a 1:1 volume ratio resulting in a concentration of 0.125 mM and 1.73 mM, respectively. The absorption at 520 nm was measured every 50 ms, and from the decay of this absorption the pseudo first-order rate constant k_1' was determined by a nonlinear Simplex regression analysis of the data points using BioKine software. The second-order rate constant k_2 was calculated: $k_2 = k_1' / c_{,TCO}$.

Supplementary Table 2. Calculated k_2 values ($M^{-1}s^{-1}$) for the reaction between tetrazine activators and TCO **9** in 25% MeCN/PBS (mean ± SD , n=5) and MeCN (n=1).

activator	25% MeCN/PBS	MeCN
1b	270 ± 11	10
2b	397 ± 4	68
1d	519 ± 12	--
2d	748 ± 20	--
2e	--	2.5
dimethyl-Tz	29.0 ± 0.4	--

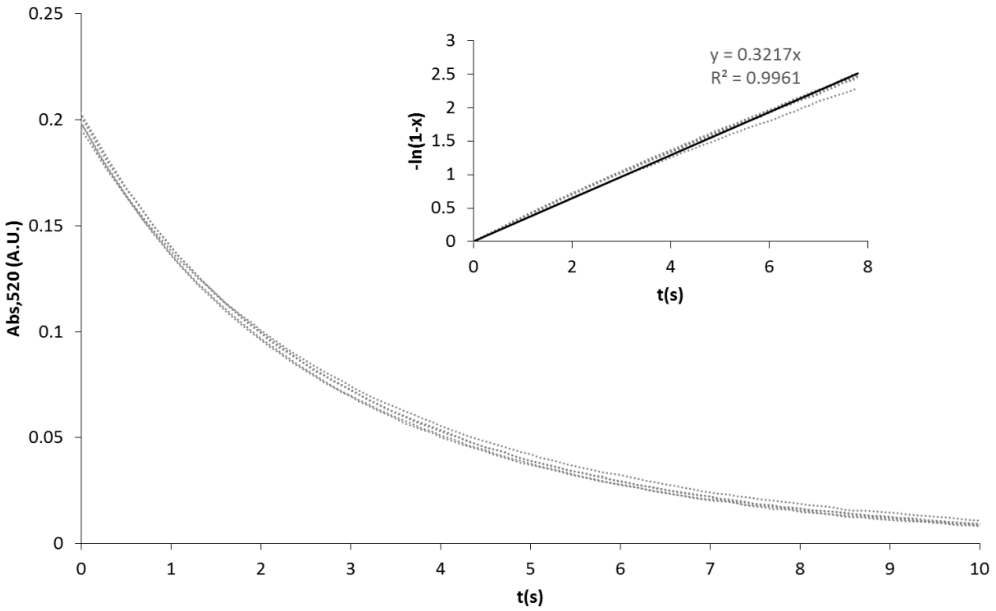

Supplementary Figure 2. Kinetic plots of reaction of **1b** (c=0.125 mM) with TCO **9** (c=1.17 mM) in 25% MeCN/PBS at 20°C. k_2 was calculated to be 270 ± 11 M^{-1} s^{-1} (n=5).

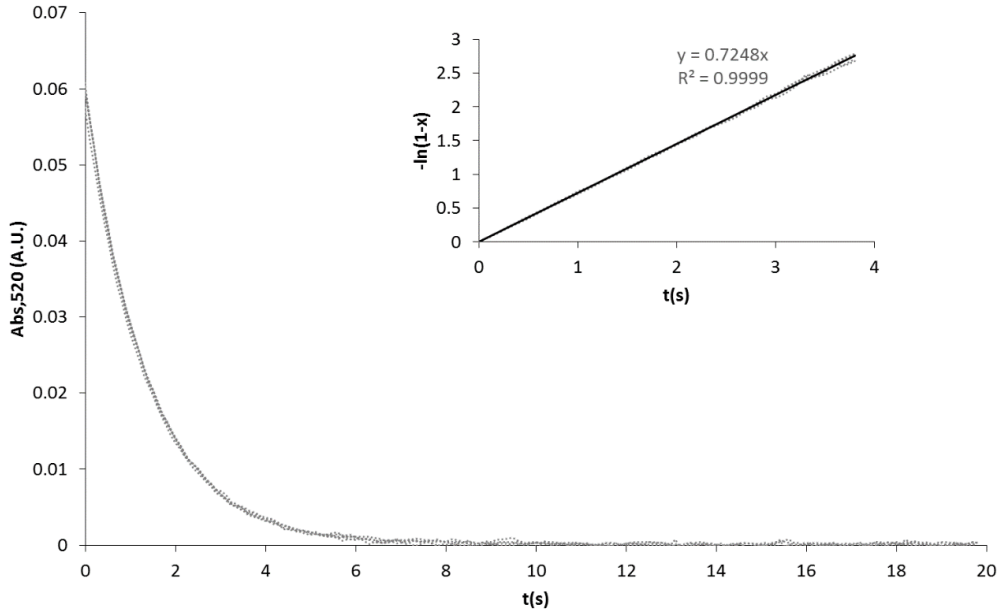

Supplementary Figure 3. Kinetic plots of reaction of **2b** (c=0.165 mM) with TCO **9** (c=1.73 mM) in 25% MeCN/PBS at 20°C. k_2 was calculated to be 397 ± 4 M^{-1} s^{-1} (n=5).

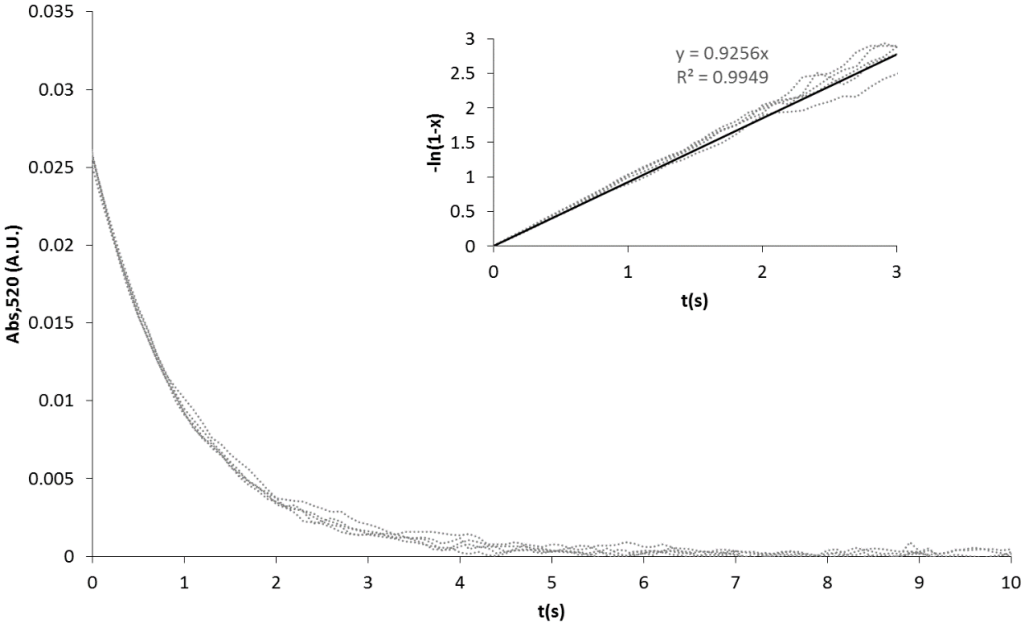

Supplementary Figure 4. Kinetic plots of reaction of **1d** (c=0.125 mM) with TCO **9** (c=1.78 mM) in 25% MeCN/PBS at 20°C. k_2 was calculated to be 519 ± 12 M^{-1} s^{-1} (n=5).

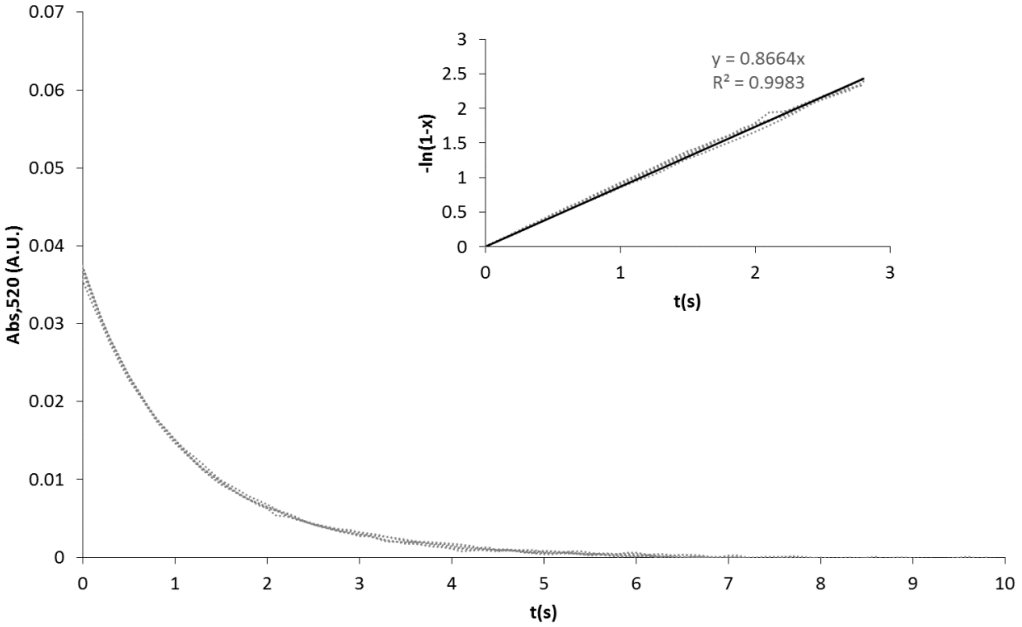

Supplementary Figure 5. Kinetic plots of reaction of **2d** (c=0.125 mM) with TCO **9** (c=1.17 mM) in 25% MeCN/PBS at 20°C. k_2 was calculated to be 748 ± 20 M^{-1} s^{-1} (n=5).

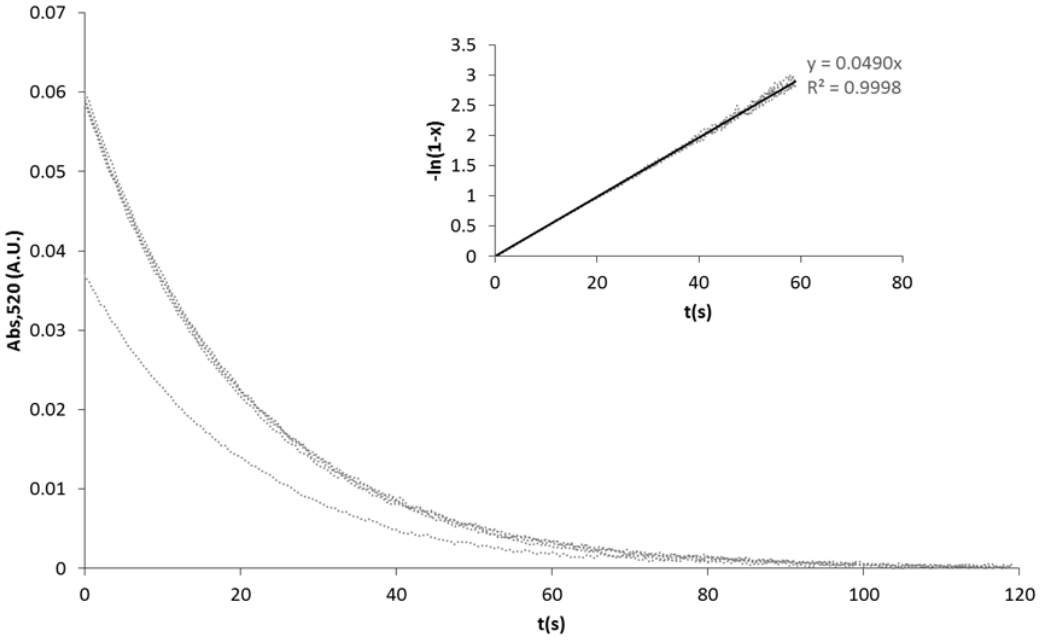

Supplementary Figure 6. Kinetic plots of reaction of 3,6-dimethyl-Tz (c=0.160 mM) with TCO **9** (c=1.68 mM) in 25% MeCN/PBS at 20°C. k_2 was calculated to be 29.0 ± 0.4 M^{-1} s^{-1} (n=5).

Section S4: UV-Vis spectroscopy of tetrazine activators in aqueous phosphate buffers

The UV-Vis spectra of tetrazine activators **2a**, **2b**, and **2c** were studied in aqueous phosphate buffers at various pH. These buffers where prepared from 100 mM dipotassium hydrogenphosphate, upon addition of either 1 M NaOH or 1 M HCl to reach the appropriate pH in a range of 2.0 – 10.0. A stock solution of the tetrazine (10 µL 25 mM in DMSO, 0.25×10^{-6} mol) was diluted with buffer (3 mL), and UV-Vis spectra of these solutions were measured.

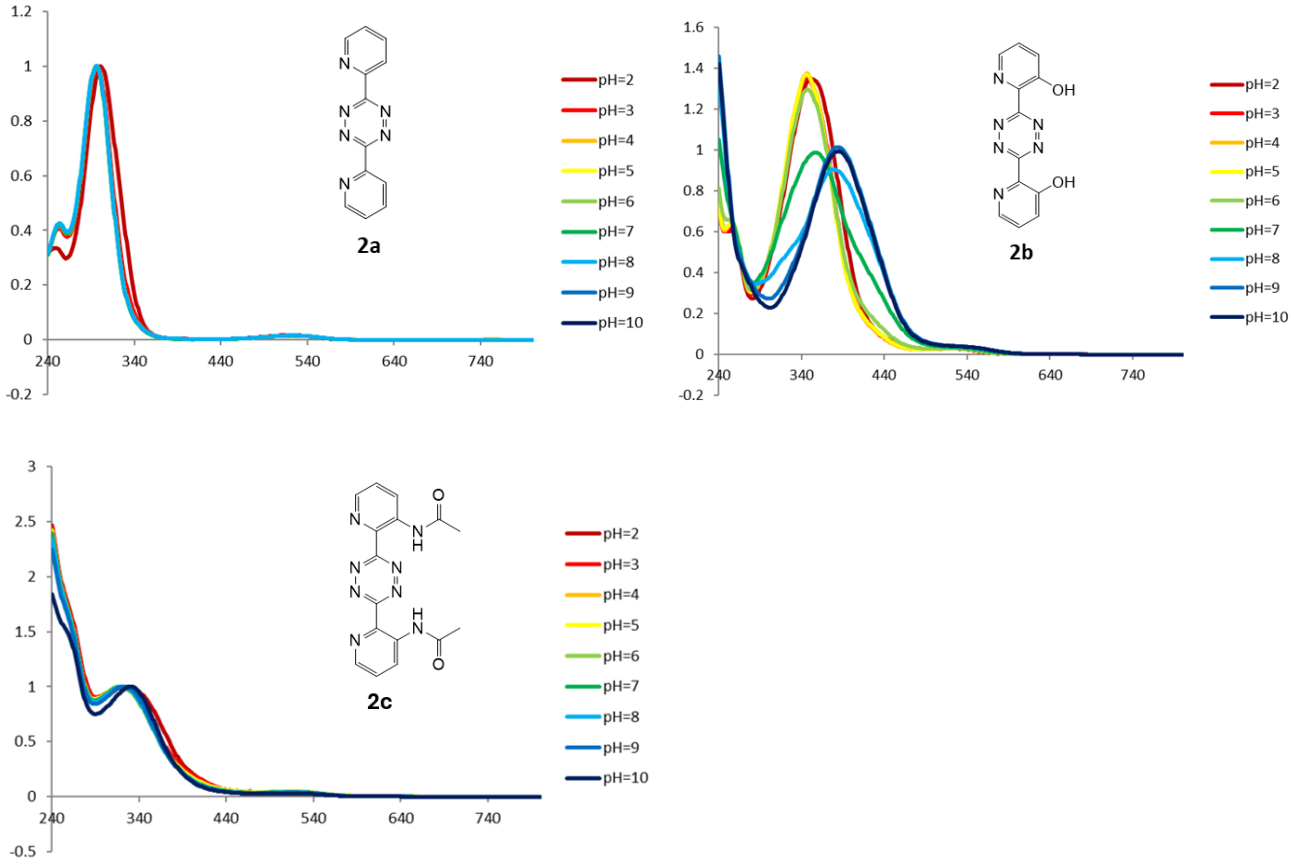

Supplementary Figure 7: UV-Vis spectra of tetrazine **2a**, **2b**, and **2c** in aqueous buffers of different pH

Section S5: Tautomerization Studies

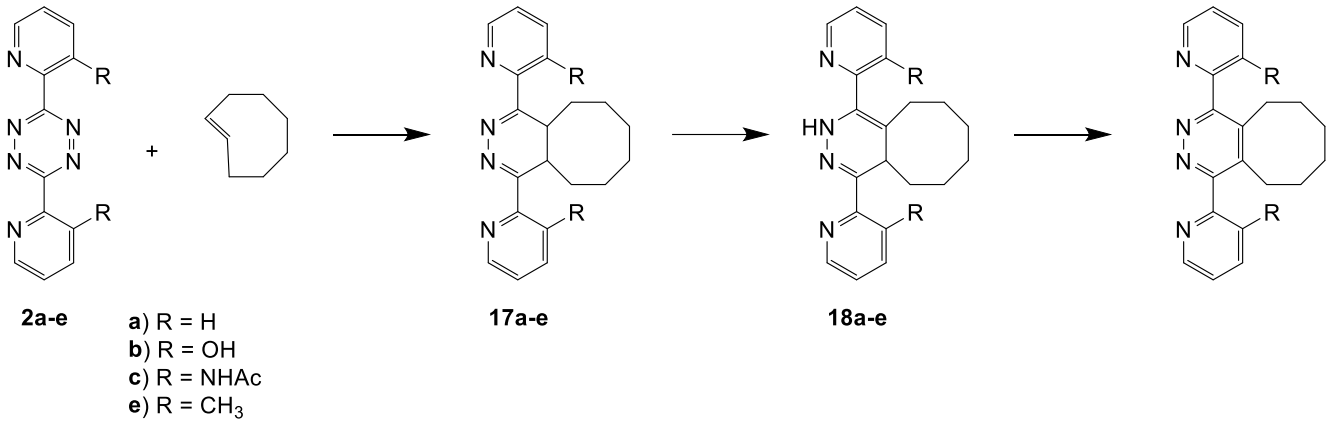

In order to study the rate of tautomerization of the IEDDA adducts of *trans*-cyclooctene and tetrazine activators **2a**, **2b**, **2c** and **2e**, reactions where performed in a variety of solvents, and the progress of the tautomerization was monitored over time by ^{1}H-NMR.

The study with tetrazine **2a** in $CDCl_3$ is given as a representative example.

Trans-cyclooctene (2.23 mg, 2.03×10^{-6} mol) was dissolved in $CDCl_3$ (0.6 mL). Tetrazine **2a** (4.79 mg, 2.03×10^{-6} mol) was dissolved in $CDCl_3$ (0.05 mL), and this pink solution was added to the solution of *trans*-cyclooctene. The mixture was homogenized and turned slight yellowish while gas bubbles evolved, indicating complete IEDDA reaction. After 3 min, the mixture was transferred to an NMR tube and analyzed by ^{1}H-NMR to prove the initial formation of 4,5-tautomer **17a**. The progress of tautomerization was monitored over time by ^{1}H-NMR, which showed the gradual formation of 1,4-tautomer **18a** (see Supplementary Figure 8 for details) with an estimated half-life of 50 min. After 6 h, the conversion to tautomer **18a** was complete.

4,5-Tautomer **17a**: ^{1}H-NMR ($CDCl_3$): δ = 8.69 (d, 2H), 8.35 (d, 2H), 7.78 (dt, 2H), 7.34 (dd, 2H), 4.01 (m, 2H, *H*4 and *H*5), 2.00 (m, 2H), 1.96 – 1.79 (br.m, 6H), 1.53 (m, 2H), 1.42 (m, 2H) ppm. FT-IR (ATR): ν = 2911, 2856, 1592, 1544, 1463, 782, 737 cm^{-1}.

1,4-Tautomer **18a**: ^{1}H-NMR ($CDCl_3$): δ = 8.78 (br.s, 1H, N*H*), 8.65 (d, 1H), 8.60 (d, 1H), 8.09 (d, 1H), 7.73. (dt, 1H), 7.65 (dt, 1H), 7.56 (d, 1H), 7.24 (dt, 1H), 7.18 (dt, 1H), 4.39 (t, 1H, *H*1), 2.90 (m, 1H, *H*4), 2.24 – 2.02 (br.m, 2H), 1.95 – 1.47 (br.m, 10H) ppm. FT-IR (ATR): ν = 3264 (NH), 2916, 2859, 1579, 1563, 1470, 1427, 779, 739 cm^{-1}.

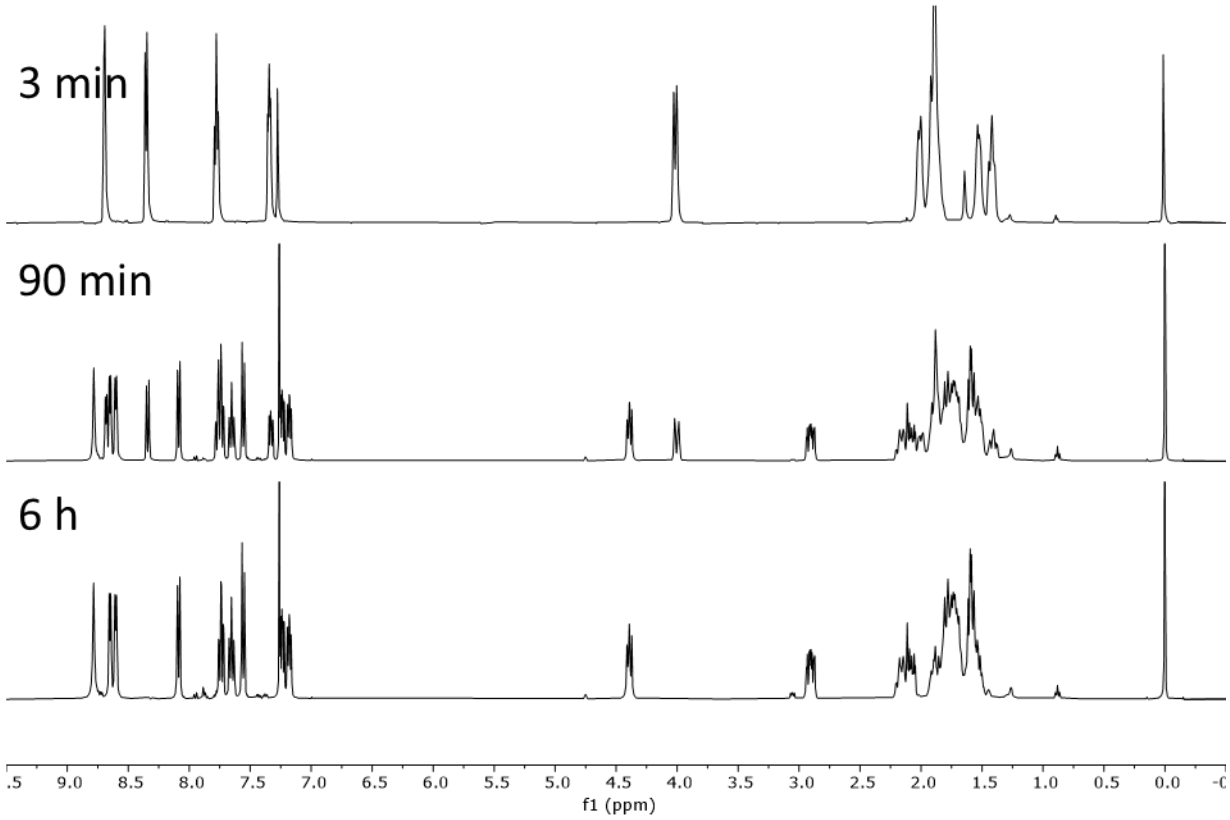

Supplementary Figure 8: ^{1}H-NMR spectra of the reaction mixture of *trans*-cyclooctene and tetrazine **2a** in $CDCl_3$. Top: after 3 min, showing the exclusive formation of 4,5-tautomer **17a**; middle: after 90 min, showing partial tautomerization; bottom: after 6 h, showing complete tautomerization to 1,4-tautomer **18a**.

Supplementary Table 3. Rate of tautomerization of IEDDA adducts of tetrazine activators and *trans*-cyclooctene

activator	solvent	Half-life
2a	$CDCl_3$	50 min
2a	CD_3CN	no tautomerization
2b	$CDCl_3$	< 2 min
2b	CD_3CN	15 min
2c	CD_3CN	31 min
2c	DMSO-d6	< 2 min
2e	CD_3CN	no tautomerization
2e	CD_3CN + 0.1 v% formic acid	12 min

Section S6: Release studies

Studies on the reaction of TCO 9 with tetrazine 2a

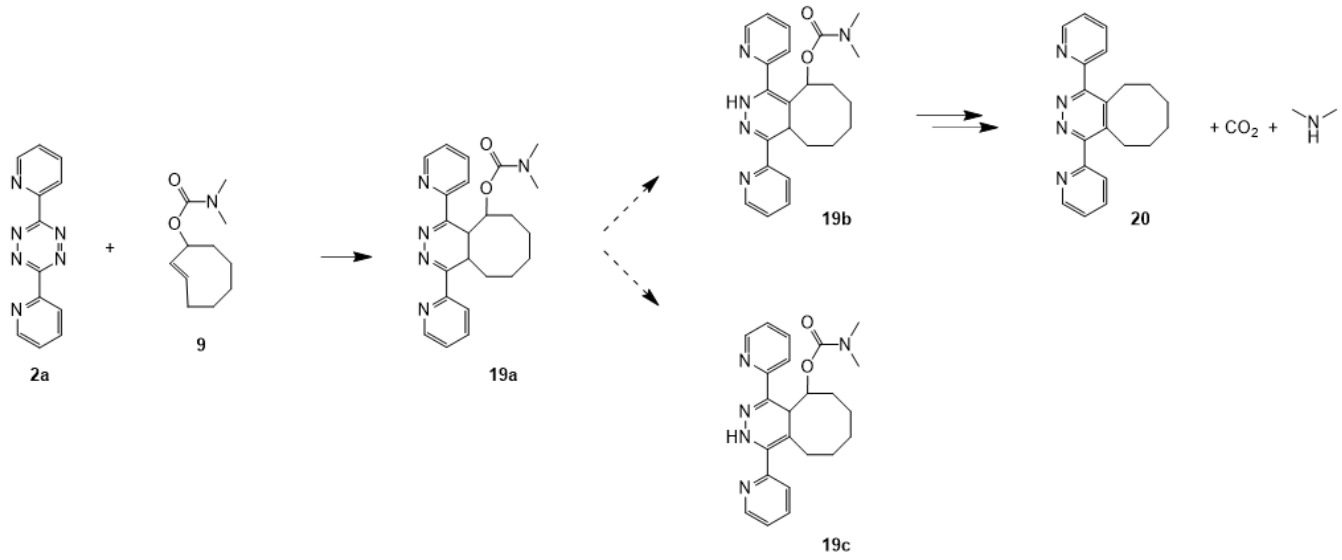

Reaction of TCO **9** and 3,6-di(pyridin-2-yl)-1,2,4,5-tetrazine (**2a**) as activator in $CDCl_3$

TCO **9** (5.00 mg, 25.4×10^{-6} mol) was dissolved in $CDCl_3$ (0.6 mL) and **2a** (6.00 mg, 25.4×10^{-6} mol) was added. The mixture was thoroughly mixed, and the pink solution turned yellowish while gas bubbles evolved. After 5 min, the sample was analyzed by ^{1}H-NMR, and this was repeated after 16 h (see Supplementary Figure 9). No change in the ^{1}H-NMR spectrum was observed during this timeframe, showing the kinetic stability of 4,5-tautomer **19a**. The sample was additionally analyzed by ^{13}C, COSY, HSQC, and HMBC NMR spectroscopy, and FT-IR to further characterize the 4,5-tautomer **19a** (see Section S9: Spectra). ^{1}H-NMR ($CDCl_3$): δ = 8.70 (d, 1H), 8.66 (d, 1H), 8.35 (d, 2H), 7.77 (dt, 2H), 7.33 (m, 2H), 5.23 (dt, 1H, C*H*O), 4.32 (dt, 1H, *H*4), 4.28 (t, 1H, H5), 2.68 (s, 3H), 2.46 (t, 1H), 2.42 (s, 3H), 2.12 – 1.87 (m, 4H), 1.87 – 1.72 (m, 2H), 1.64 – 1.36 (m, 3H) ppm. ^{13}C-NMR ($CDCl_3$): δ = 163.31, 159.99, 155.82, 154.25, 153.98, 149.10, 148.96, 136.49, 136.33, 124.84, 124.61, 122.76, 122.73, 76.17, 36.15, 35.68, 32.73, 31.80, 28.80, 27.86, 26.32, 25.18, 25.01 ppm. FT-IR (ATR): ν = 2926, 2854, 1697 (C=O), 1593, 1460, 1394, 1184, 1045, 787, 727 cm^{-1}. ESI-MS: *m/z* Calc. for $C_{23}H_{27}N_5O_2$ 405.22; Obs. $[M+H]^+$ 406.17, λ_{max} = 306 nm.

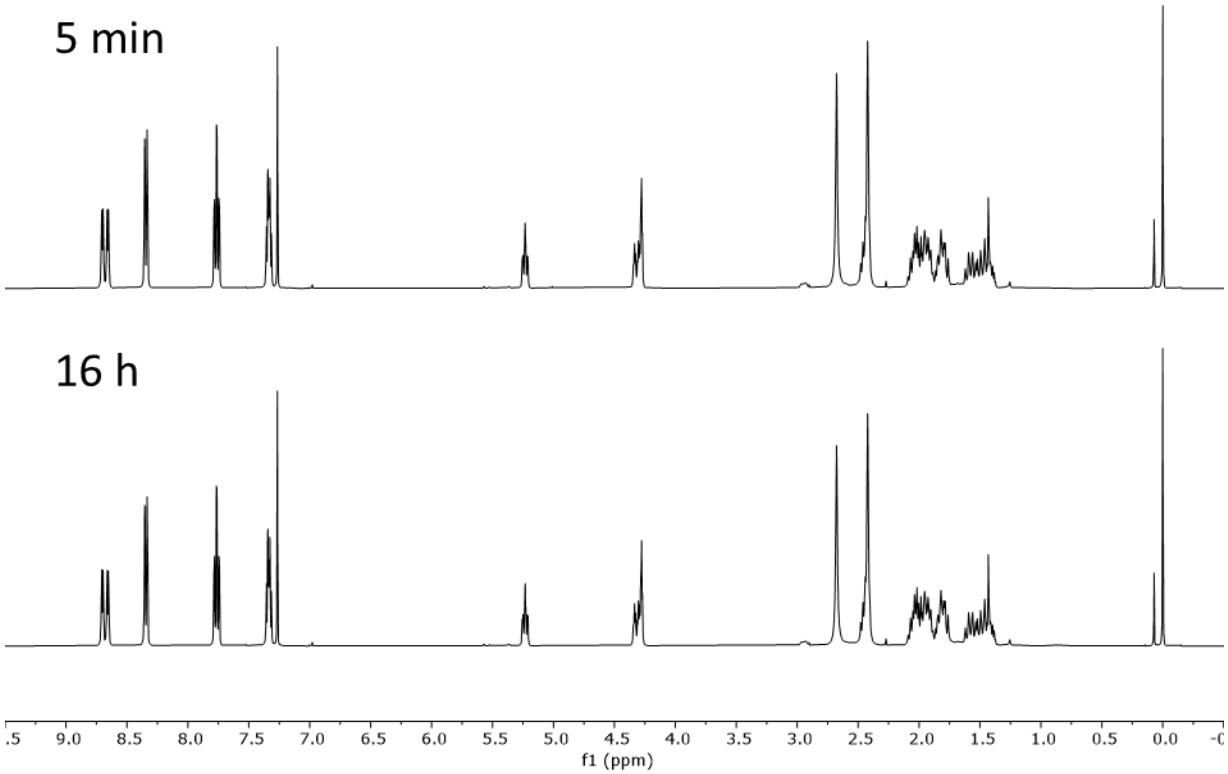

Supplementary Figure 9: ^{1}H-NMR spectra of the reaction mixture of TCO **9** and tetrazine **2a** in $CDCl_3$. Top: after 5 min; bottom: after 16 h, showing kinetically stable formation of 4,5-tautomer **19a**.

Tautomerization of 4,5-tautomer **19a** with acid, forming 2,5-tautomer **19c**

TCO **9** (4.3 mg, 21.8×10^{-6} mol) was dissolved in MeCN (1 mL), and water (1 mL) was added. Next, a solution of 3,6-di(pyridin-2-yl)-1,2,4,5-tetrazine (**2a**) (5.2 mg, 21.8×10^{-6} mol) was added, and the mixture was thoroughly mixed as the pink solution turned yellowish while gas bubbles evolved. After 5 min, formic acid (2.5 mg, 54×10^{-6} mol) was added to induce tautomerization, and the mixture was stirred at 20°C for 18 h. Subsequently, the solution was freeze dried, and the crude product purified by normal phase column chromatography (silica, ethyl acetate/heptane) to yield **19c**, which was characterized as the 2,5-tautomer (see Section S9: Spectra), as a yellow solid (3.1 mg, 35 %). ^{1}H-NMR ($CDCl_3$): δ = 8.70 (s, 1H), 8.65 (d, 1H), 8.55 (d, 1H), 8.06 (d, 1H), 7.76 (d, 1H), 7.67 – 7.56 (m, 2H), 7.28 (dd, 1H), 7.14 (dd, 1H), 5.16 (m, 1H), 4.65 (d, 1H), 2.95 (m, 1H), 2.74 (s, 6H), 2.13 (m, 1H), 2.07 – 1.70 (br. m, 8H) ppm. ^{13}C-NMR (CDCl3): δ = 156.34, 155.02, 152.72, 149.48, 148.54, 138.06, 136.33, 135.89, 135.80, 124.39, 122.80, 122.30, 120.71, 106.17, 77.21, 38.80, 36.15, 36.02, 32.28, 28.15, 27.39, 24.86, 21.37 ppm. FT-IR (ATR): ν = 3366 (NH), 2925, 2855, 1693 (C=O), 1582, 1466, 1189, 787, 732 cm^{-1}. ESI-MS: *m/z* Calc. for $C_{23}H_{27}N_5O_2$ 405.22; Obs. $[M+H]^+$ 406.17, λ_{max} = 425 nm.

Release from 2,5-tautomer **19c**

To study the release from the 2,5-tautomer, **19c** (0.10 mg, 2.5×10^{-7} mol) was dissolved in MeCN (0.2 mL) and diluted with PBS (0.8 mL). The solution was stirred at 20°C for 24 h, and then analyzed by HPLC-PDA/MS to show intact **19c** and no signs of elimination product **20**.

Studies on the reaction of TCO 10 with tetrazines 2a, 2b, and 2c

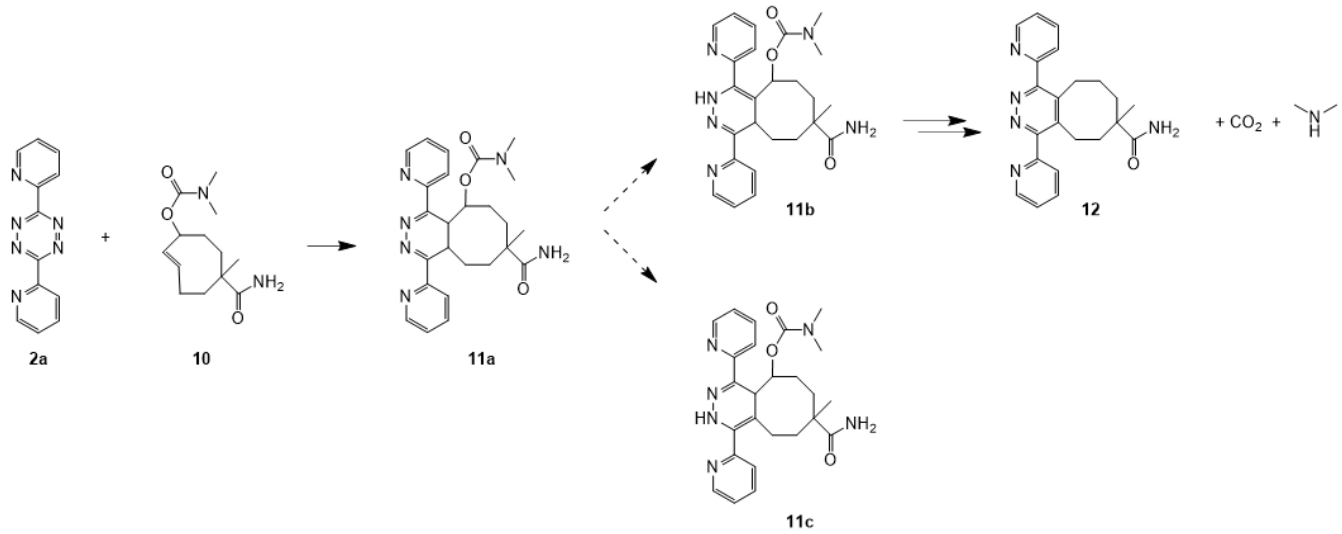

Reaction of TCO **10** and 3,6-di(pyridin-2-yl)-1,2,4,5-tetrazine (**2a**) as activator in $CDCl_3$

TCO **10** (6.09 mg, 24.0×10^{-6} mol) was dissolved in $CDCl_3$ (0.6 mL) and **2a** (5.66 mg, 24.0×10^{-6} mol) was added. The mixture was thoroughly mixed, and the pink solution turned colorless while gas bubbles evolved. After 10 min, the sample was analyzed by ^{1}H-NMR (Supplementary Figure 10), and this was repeated after 18 h. No change in the ^{1}H-NMR spectrum was observed. The sample was additionally analyzed by ^{13}C, COSY, HSQC, and HMBC NMR spectroscopy to further characterize the 4,5-tautomer **11a** (see Section S9: Spectra). ^{1}H-NMR ($CDCl_3$): δ = 8.67 (d, 1H), 8.55 (d, 1H), 8.31 (dd, 2H), 7.80 (dt, 2H), 7.36 (m, 2H), 5.93 (br.s, 1H), 5.35 (br.t, 1H), 4.59 (br.s, 1H), 4.10 (d, 1H), 2.71 (s, 3H), 2.68 (m, 1H), 2.49 (s, 3H), 2.43 – 2.22 (m, 2H), 2.04 (m, 2H), 1.86 (m, 2H), 1.71 (m, 1H), 1.47 (m, 1H), 1.33 (s, 3H) ppm. ^{13}C-NMR (CDCl3): δ = 179.71, 161.99, 159.65, 155.29, 153.94, 153.88, 148.79, 148.27, 137.03, 136.74, 125.16, 125.03, 123.36, 123.18, 73.22 (br.), 45.85, 36.29, 35.63, 28.13, 27.58, 25.68 ppm.

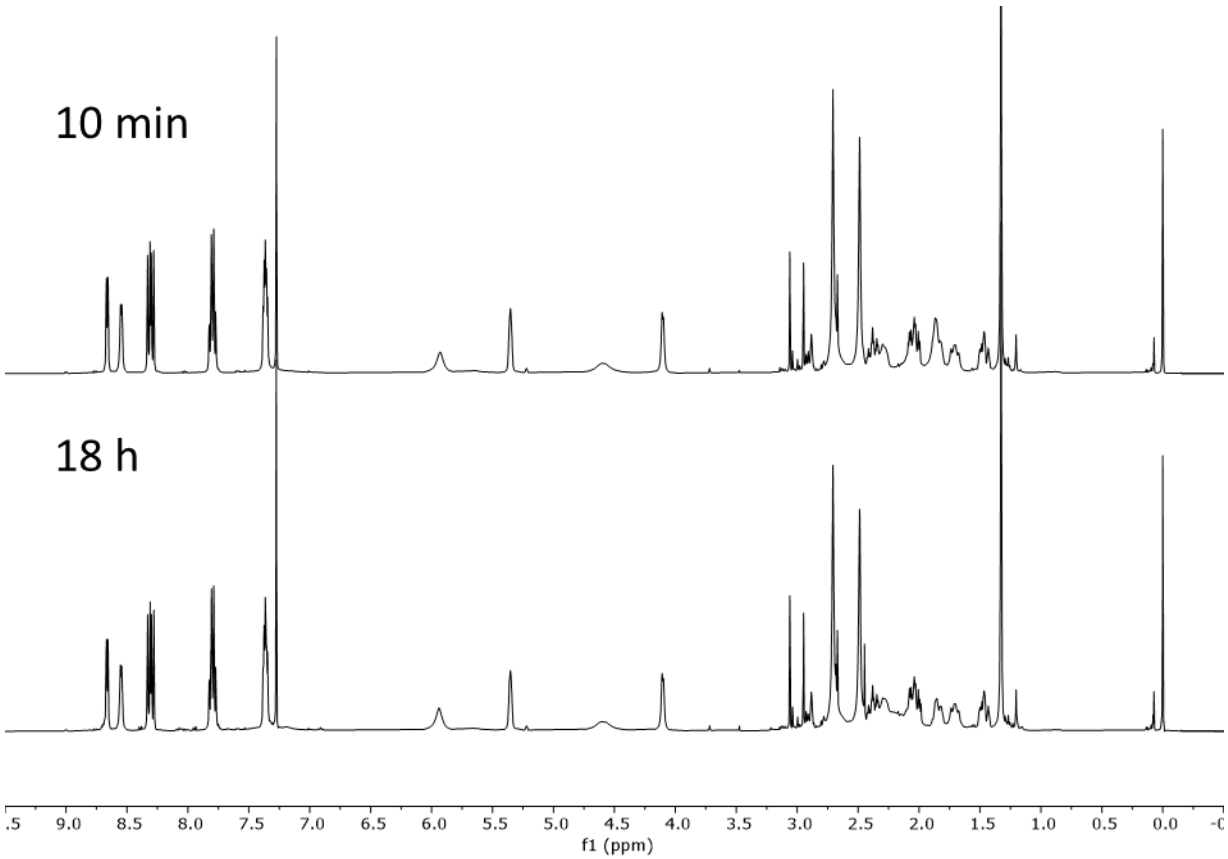

Supplementary Figure 10: ^{1}H-NMR spectra of the reaction mixture of TCO **10** and tetrazine **2a** in $CDCl_3$. Top: after 10 min; bottom: after 18 h, showing kinetically stable formation of 4,5-tautomer **11a**.

Reaction of TCO **10** and 3,6-di(pyridin-2-yl)-1,2,4,5-tetrazine (**2a**) as activator in DMSO-d6

TCO **10** (1.0 mg, 4.1×10^{-6} mol) was dissolved in DMSO-d6 (0.3 mL) and **2a** (0.97 mg, 4.1×10^{-6} mol) dissolved in DMSO-d6 (0.3 mL) was added. The mixture was thoroughly mixed, and the pink solution turned colorless. After 10 min, the sample was analyzed by ^{1}H-NMR, and this was repeated after 18 h, but no change in the ^{1}H-NMR spectrum was observed, indicating the exclusive formation of the 4,5-tautomer **11a** (Supplementary Figure 11).

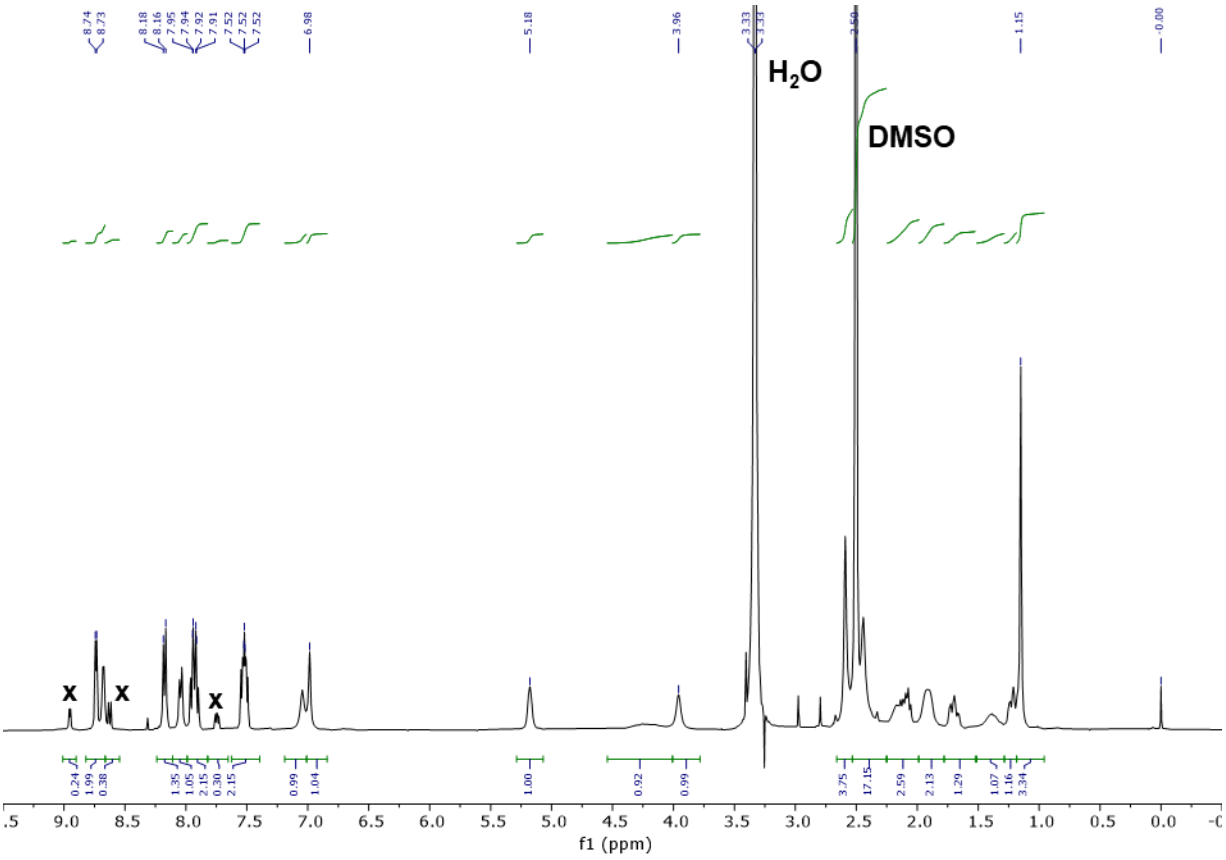

Supplementary Figure 11: ^{1}H-NMR spectrum of the IEDDA-adduct of TCO **10** and **2a** in DMSO-d6 after 10 min, demonstrating the exclusive formation of the 4,5-tautomer **11a** (**x** denotes excess tetrazine).

Reaction of TCO **10** and 3,6-di(pyridin-2-yl)-1,2,4,5-tetrazine as activator (**2a**) in a mixture of DMSO-d6 and D_2O-buffer (pD=7.4)

The D_2O-buffer was prepared by dissolving potassium dihyrogen phosphate (27.2 mg, 0.20 mmol) and dipotassium hydrogen phosphate (139 mg, 0.80 mmol) in D_2O (10 mL), resulting in pD=7.4.

To a solution of TCO **10** in 50/50 DMSO-d6 / D_2O-buffer (0.300 mL 15 mM, 4.5×10^{-6} mol) was added a solution of **2a** in 50/50 DMSO-d6 / D_2O-buffer (0.300 mL 15 mM, 4.5×10^{-6} mol). The pink solution was thoroughly mixed while the pink color fainted and gas evolved. After 3 min, the mixture was transferred to an NMR tube and the progress of the reaction was monitored over time by ^{1}H-NMR and HPLC-MS/PDA (Supplementary Figure 12, resp. 13). No significant change was observed indicating the exclusive formation of the 4,5-tautomer **11a**.

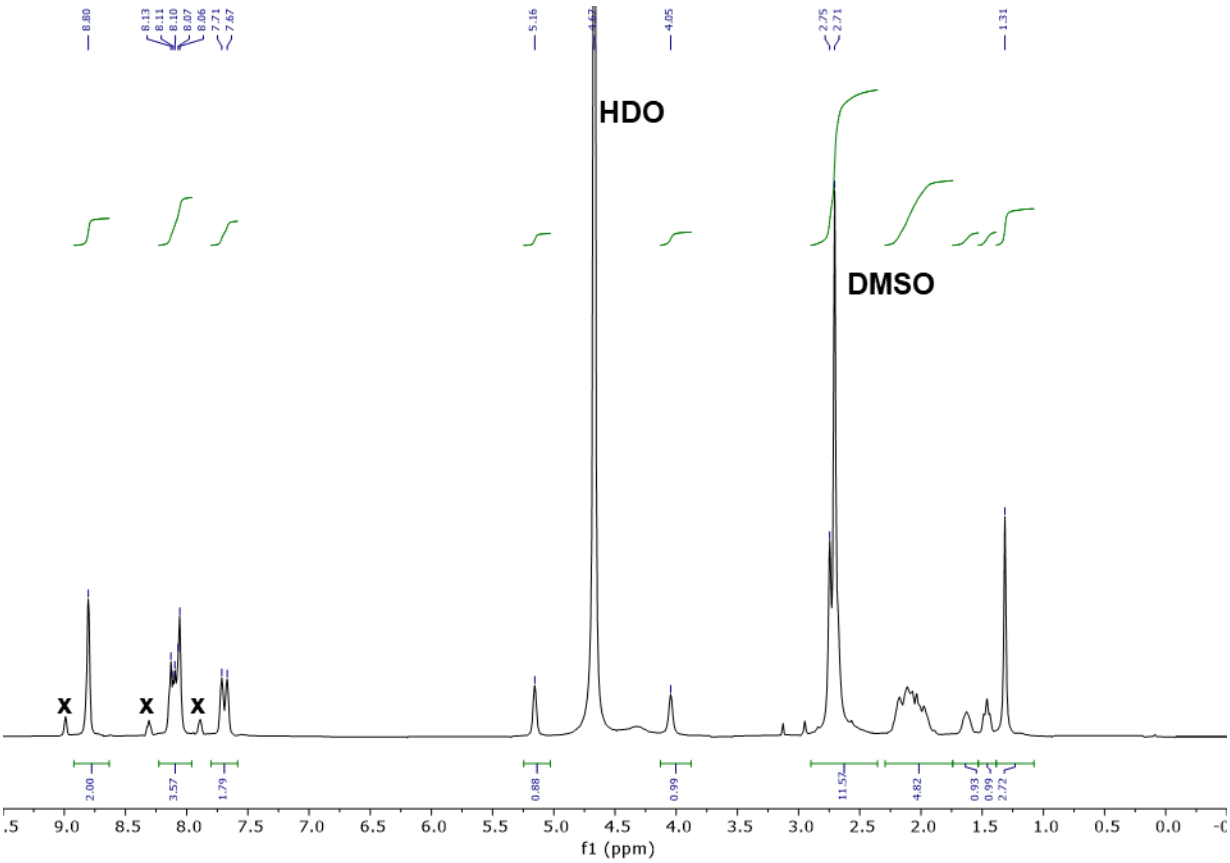

Supplementary Figure 12: ^{1}H-NMR spectrum of the IEDDA-adduct of TCO **10** and **2a** in 50/50 DMSO-d6 / D_2O-buffer after 7 min, demonstrating the exclusive formation of the 4,5-tautomer **11a** (**x** denotes excess tetrazine).

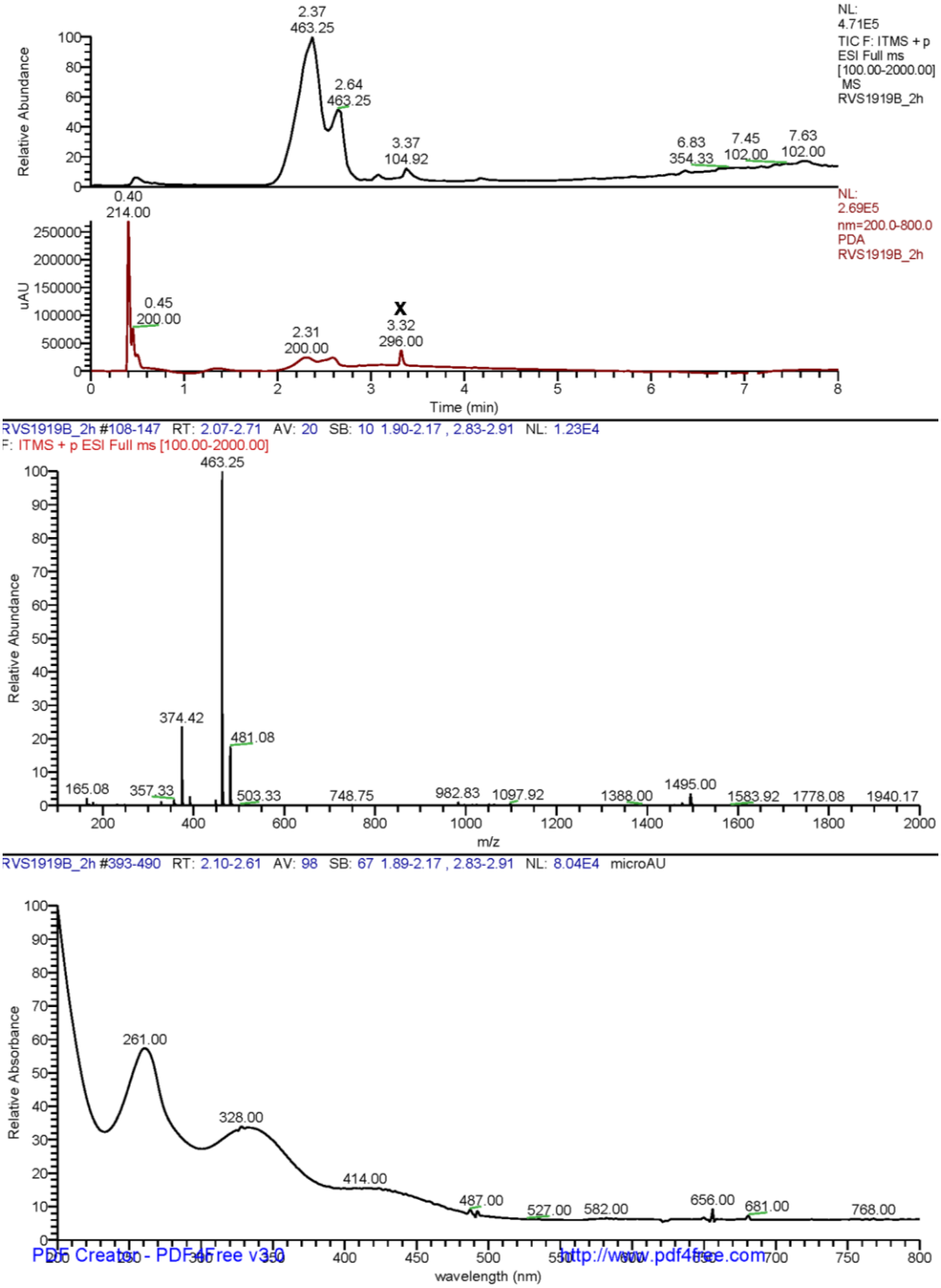

Supplementary Figure 13: HPLC-MS/PDA analysis of the IEDDA-adduct (MW=462.24) of TCO **10** and **2a** in 50/50 DMSO-d6 / D_2O-buffer after 45 min, demonstrating the absence of elimination product **12** (**x** denotes excess tetrazine).

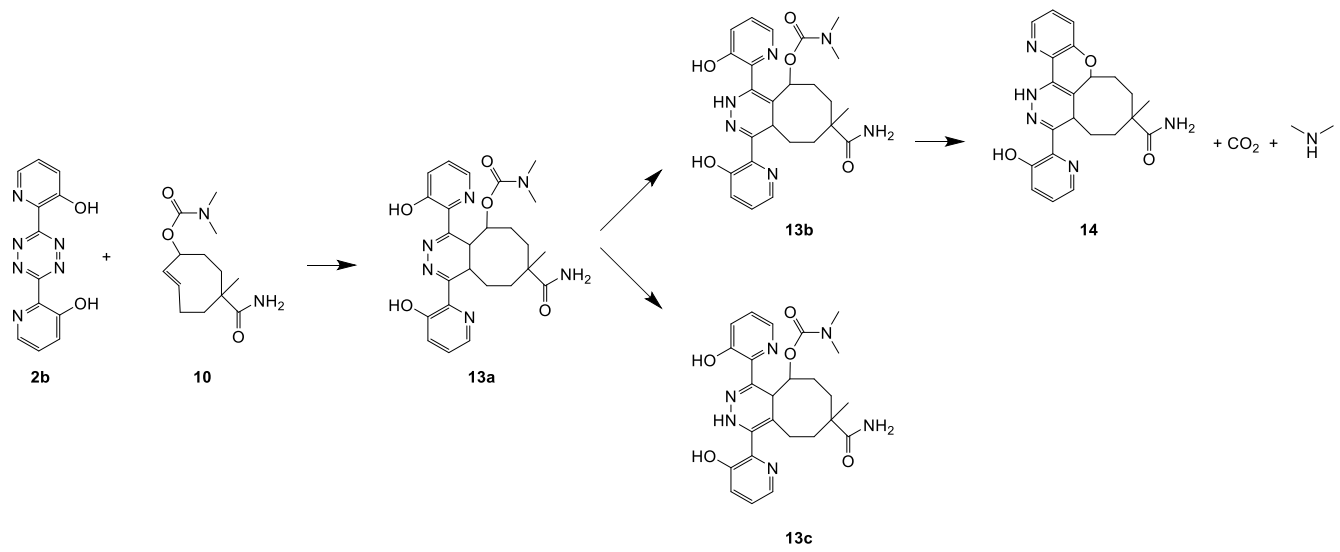

Reaction of TCO **10** and tetrazine **2b** as activator in a mixture of DMSO-d6 and D_2O-buffer (pD=7.4)

To a solution of TCO **10** in 50/50 DMSO-d6 / D_2O-buffer (0.300 mL 15 mM, 4.5×10^{-6} mol) was added a solution of tetrazine **2b** in 50/50 DMSO-d6 / D_2O-buffer (0.300 mL 15 mM, 4.5×10^{-6} mol). The red solution was thoroughly mixed while the color fainted and turned yellowish and gas evolved. After 3 min, the mixture was transferred to an NMR tube and the progress of the reaction was monitored over time by ^{1}H-NMR and HPLC-MS/PDA (Supplementary Figure 14, resp. 15), showing the immediate formation of elimination product **14** and N,N-dimethylamine.

After several hours, an off-white precipitate was formed, which was collected by filtration, and subsequently washed with water and dissolved in chloroform. The solution was dried with sodium sulfate and evaporated to dryness to yield elimination product **14** (1.4 mg, 77%). ^{1}H-NMR ($CDCl_3$): δ = 11.72 (s, 1H), 8.70 (s, 1H), 8.13 (dd, 1H), 8.03 (dd, 1H), 7.24 (d, 1H), 7.16 (dd, 1H), 7.06 (m, 2H), 5.63 (br. s, 1H), 5.32 (br. s, 1H), 5.24 (m, 1H), 4.25 (dd, 1H), 2.25 – 1.95 (m, 4H), 1.88 – 1.75 (m, 3H), 1.57 (m, 1H), 1.15 (s, 3H) ppm. ^{13}C-NMR ($CDCl_3$): δ = 179.93, 155.98, 149.69, 149.35, 140.69, 139.97, 135.88, 134.84, 129.33, 124.62, 124.26, 124.01, 122.19, 107.10, 78.94, 45.14, 41.02, 34.09, 32.53, 29.64, 29.55, 27.91, 26.86 ppm. ESI-MS: *m/z* Calc. for $C_{22}H_{23}N_5O_3$ 405.18; Obs. $[M+H]^+$ 406.33, λ_{max} = 330 nm.

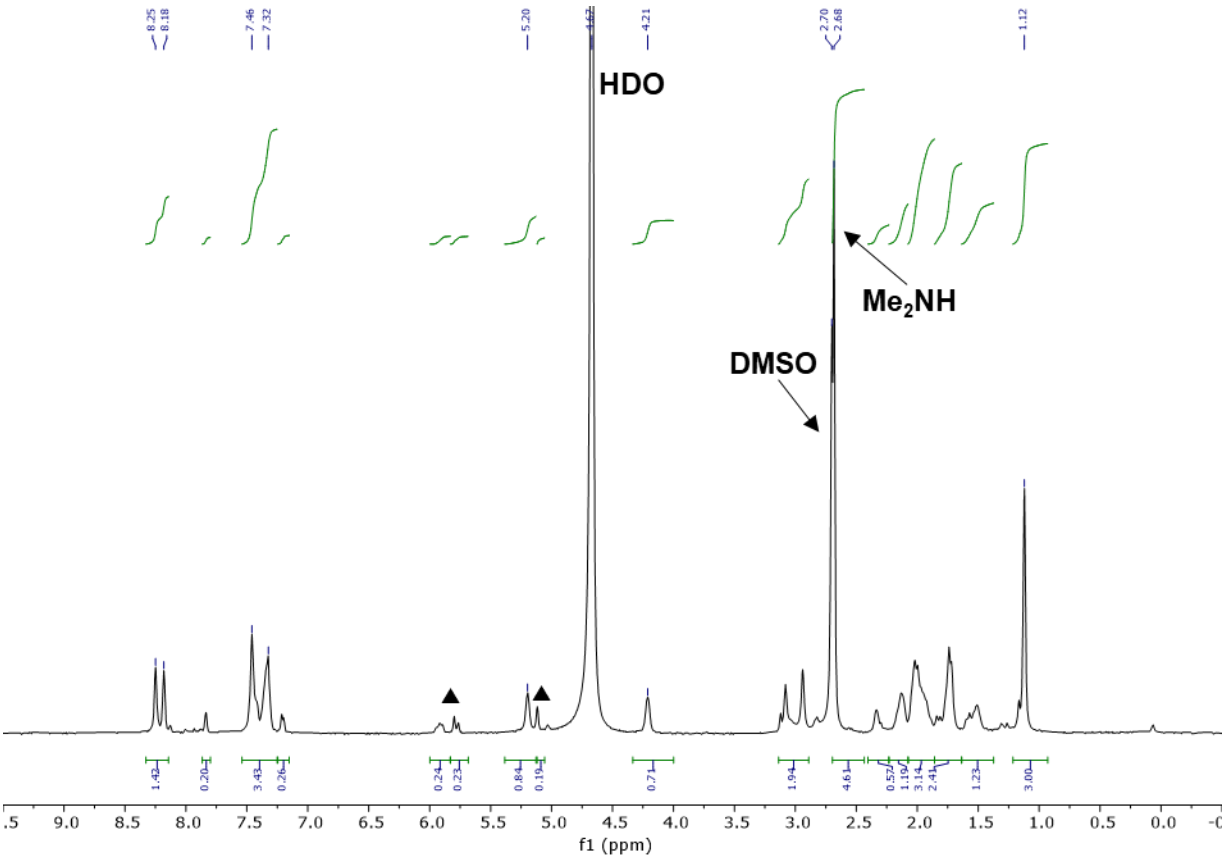

Supplementary Figure 14: ^{1}H-NMR spectrum of the reaction mixture of TCO **10** and tetrazine **2b** in 50/50 DMSO-d6 / D_2O-buffer after 10 min (▲ denotes excess **10**); Me_2NH singlet partially overlaps with DMSO peak.

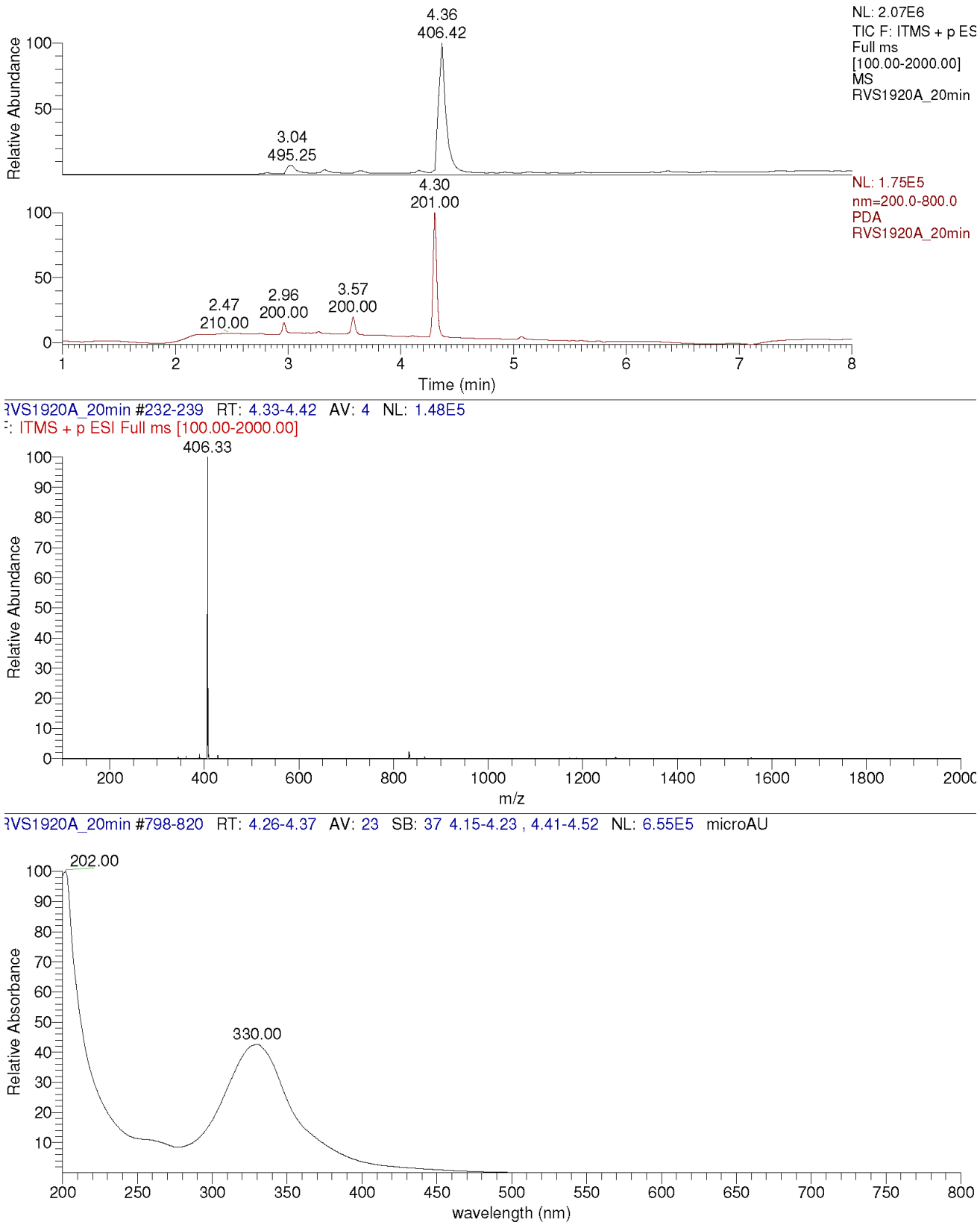

Supplementary Figure 15: HPLC-MS/PDA analysis of the reaction mixture of TCO **10** and tetrazine **2b** in 50/50 DMSO-d6 / D_2O-buffer after 20 min, demonstrating almost complete formation of elimination product **14** (MW=405).

Reaction of TCO **9** and tetrazine **2b** as activator

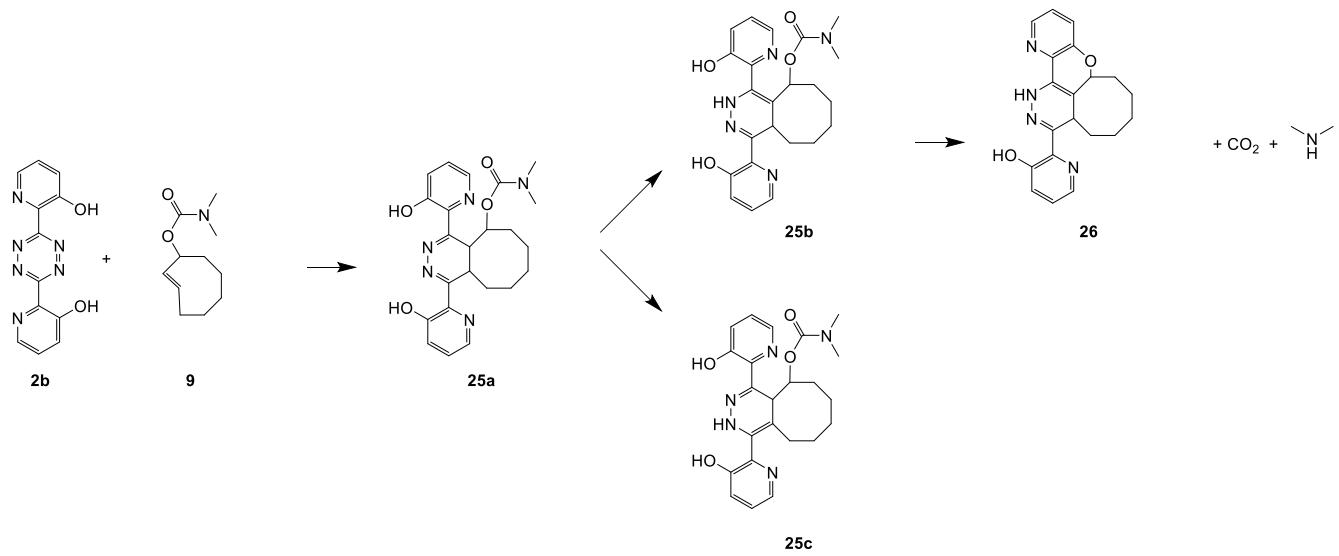

TCO **9** (3.4 mg, 1.7×10^{-5} mol) was dissolved in DMSO (0.200 mL), and the solution was diluted with water (0.630 mL) and 1 M phosphate buffer (pH=7.4) (0.070 mL). A solution of tetrazine **2b** (4.6 mg, 1.7×10^{-5} mol) dissolved in DMSO (0.100 mL) was added, and the mixture was stirred at 37°C for 2 h. The beige precipitate was isolated by centrifugation and washed with water (1 mL), to yield elimination product **26** as an off-white solid (3.8 mg). ^{1}H-NMR ($CDCl_3$): δ = 11.89 (s, 1H), 8.72 (s, 1H), 8.16 (dd, 1H), 8.05 (dd, 1H), 7.24 (d, 1H), 7.2 – 7.05 (m, 3H), 5.30 (d, 1H), 4.45 (dd, 1H), 2.21 (m, 2H), 2.03 (m, 1H), 1.77 (m, 4H), 1.57 (m, 3H) ppm. ^{13}C-NMR ($CDCl_3$): δ = 156.04, 150.23, 148.88, 140.85, 139.81, 136.16, 135.70, 128.89, 124.52, 123.97, 123.87, 122.44, 108.37, 75.89, 32.05, 30.97, 28.68, 25.38, 24.60, 22.87 ppm. ESI-MS: *m/z* Calc. for $C_{20}H_{20}N_4O_2$ 348.16; Obs. $[M+H]^+$ 349.25, λ_{max} = 332 nm.

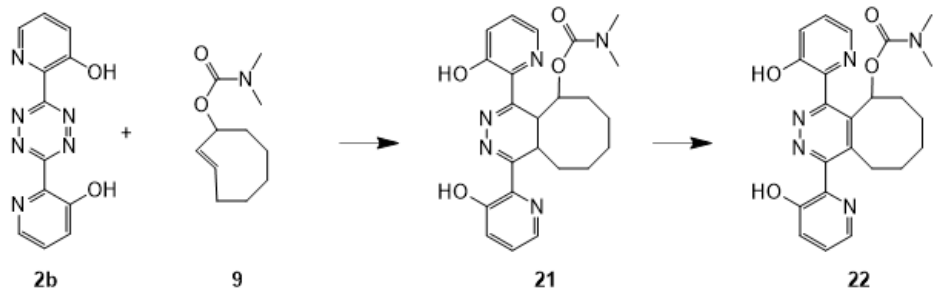

Reaction of TCO **9** and tetrazine **2b** as activator and in situ oxidation

Sodium nitrite (0.5 mg, 7.0×10^{-6} mol) was dissolved in water (0.700 mL), and acetonitrile (0.300 mL) was added, follow by a stock solution of TCO **9** (10 µL 25 mM in DMSO, 0.25×10^{-6} mol), a stock solution of tetrazine **2b** (10 µL 25 mM in DMSO, 0.25×10^{-6} mol), and formic acid (20 µL, 400×10^{-6} mol). The mixture was homogenized and stirred at 20°C for 15 min. Analysis by HPLC-MS/PDA demonstrated the formation of the oxidized IEDDA adduct **22**, which did not disappear in time. ESI-MS: *m/z* Calc. for $C_{23}H_{25}N_5O_4$ 435.19; Obs. $[M+H]^+$ 436.08, λ_{max} = 288 nm.

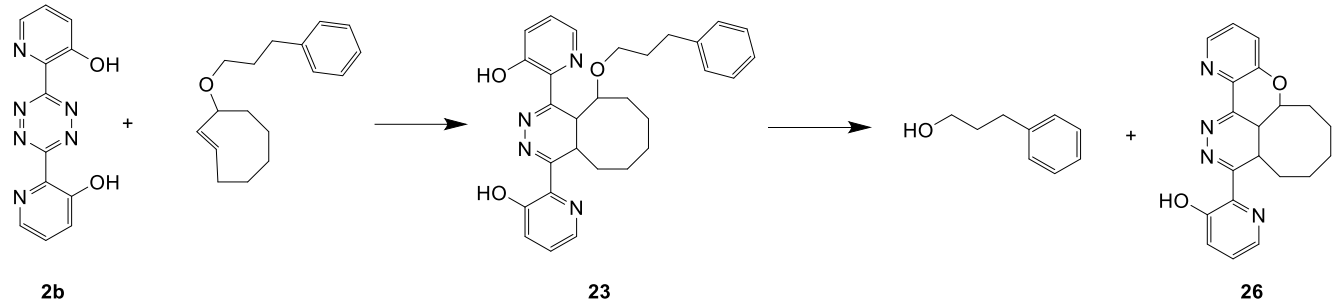

Reaction of ether-linked TCO **23** and tetrazine **2b** as activator

To a mixture of PBS (0.700 mL) and acetonitrile (0.300 mL) was added a stock solution of ether-linked TCO **23** [5] (10 µL 25 mM in DMSO, 0.25×10^{-6} mol), followed by a stock solution of tetrazine **2b** (10 µL 25 mM in DMSO, 0.25×10^{-6} mol). The mixture was homogenized and stirred at 20°C for 15 min. Analysis by HPLC-MS/PDA showed the near quantitative formation of elimination product **26**. ESI-MS: *m/z* Calc. for $C_{20}H_{20}N_4O_2$ 348.16; Obs. $[M+H]^+$ 349.25, λ_{max} = 332 nm.

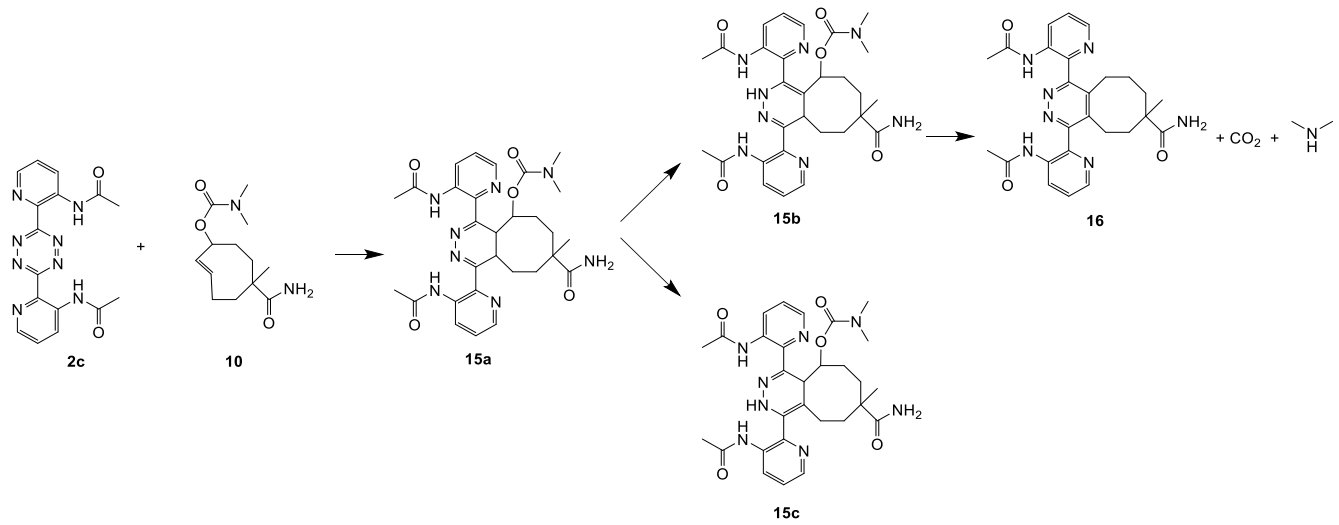

Reaction of TCO **10** and tetrazine **2c** as activator in a mixture of DMSO-d6 and D_2O-buffer (pD=7.4)

To a solution of TCO **10** in 50/50 DMSO-d6 / D_2O-buffer (0.300 mL 15 mM, 4.5×10^{-6} mol) was added a solution of tetrazine **2c** in 50/50 DMSO-d6 / D_2O-buffer (0.300 mL 15 mM, 4.5×10^{-6} mol). The orange solution was thoroughly mixed while the color fainted and turned yellowish and gas evolved. After 3 min, the mixture was transferred to an NMR tube and the progress of the reaction was monitored over time by ^{1}H-NMR and HPLC-MS/PDA (Supplementary Figure 16 – 18), showing the slow formation of elimination product **16** and N,N-dimethylamine, and 2,5-tautomer **15c.**

After 3 days, the mixture was acidified with formic acid (10 µL), and elimination product **16** and non-releasing 2,5-tautomer **15c** were isolated with preparative RP-HPLC (gradient of 20% to 50% acetonitrile / H_2O with 0.1 v/v% formic acid).

After freeze-drying, **16** was obtained as a colorless solid (1.0 mg, 45%). ^{1}H-NMR ($CDCl_3$): δ = 9.41 (s, 1H), 9.10 (s, 1H), 8.88 (d, 1H), 8.75 (d, 1H), 8.46 (m, 2H), 7.50 (m, 2H), 6.76 (br. s, 1H), 4.94 (br. s, 1H), 3.09 (m, 1H), 2.92 (m, 1H), 2.80 (m, 2H), 2.56 (m, 1H), 2.24 (m, 1H), 2.12 (s, 3H), 2.07 (s, 3H), 2.0 – 1.9 (m, 2H), 1.74 (m, 2H), 1.25 (s, 3H) ppm. ESI-MS: *m/z* Calc. for $C_{26}H_{29}N_7O_3$ 487.23; Obs. $[M+H]^+$ 488.42 and $[M-H]^+$ 486.50, λ_{max} ≈ 260 nm (shoulder).

After freeze-drying, **15c** was obtained as a beige solid (0.8 mg, 31%). ^{1}H-NMR (DMSO-d6): δ = 12.11 (s, 1H), 10.01 (s, 1H), 8.85 (d, 1H), 8.53 (s, 1H), 8.33 (s, 1H), 8.1 (br.s, 1H), 7.58 (dd, 1H), 7.34 (dd, 1H), 7.1 (br.s, 1H), 4.96 (s, 1H), 4.69 (s, 1H), 2.86 (s, 3H), 2.70 (s, 3H), 2.11 (s, 3H), 2.07 (s, 3H), 1.95 – 1.65 (m, 5H), 1.32 (m, 1H), 1.09 (s, 3H) ppm. ESI-MS: *m/z* Calc. for $C_{29}H_{36}N_8O_5$ 576.28; Obs. $[M+H]^+$ 577.25 and $[M-H]^+$ 575.42, λ_{max} = 359 nm.

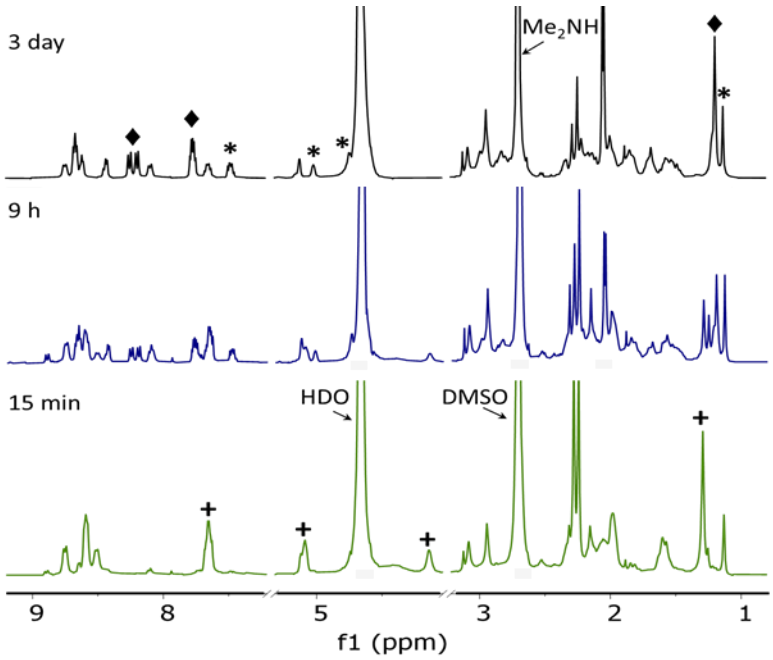

Supplementary Figure 16: ^{1}H-NMR spectra of the reaction mixture of TCO **10** and tetrazine **2c** in 50/50 DMSO-d6 / D_2O-buffer at different time points, showing release of *N*,*N*-dimethylamine (partially overlaps with DMSO peak), and formation of non-releasing 2,5-tautomer **15c** (legend: + **15a**; * **15c**; ♦ **16**).

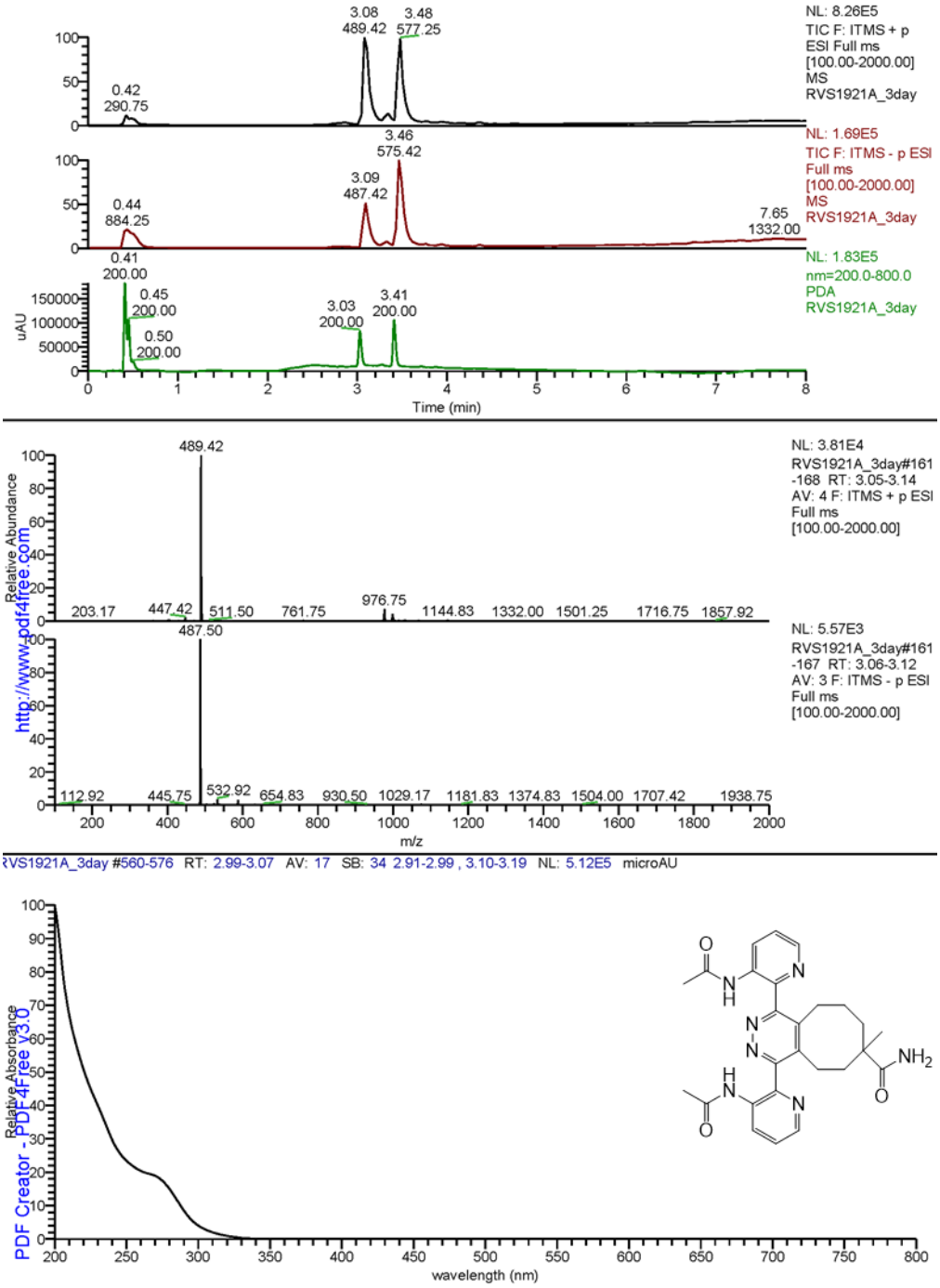

Supplementary Figure 17a: HPLC-MS/PDA analysis of the reaction mixture of TCO **10** and tetrazine **2c** in 50/50 DMSO-d6 / D_2O-buffer after 3 days, including MS and UV spectra of the elimination product **16** (MW=487.23), which elutes at 3.03 min.

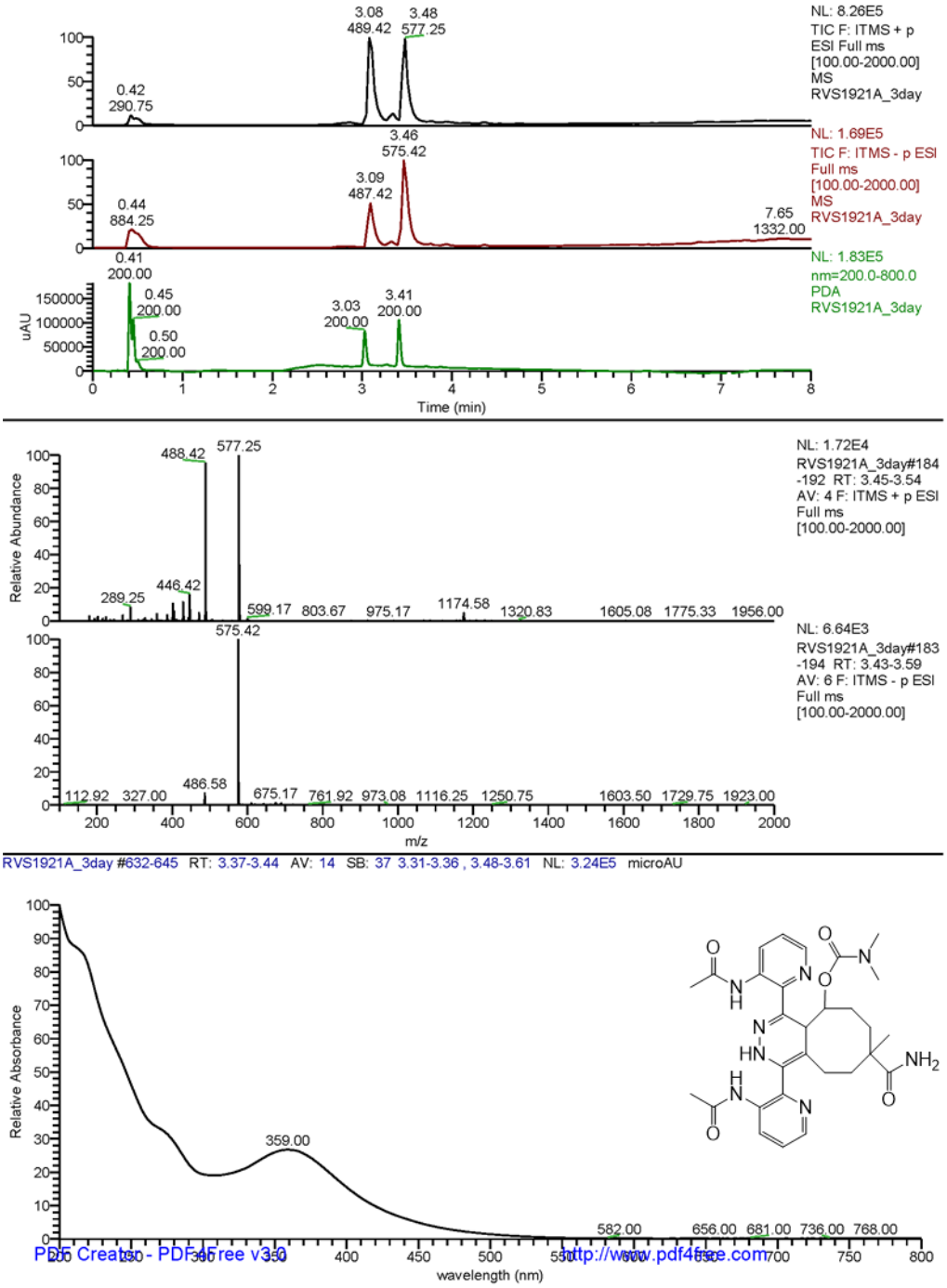

Supplementary Figure 17b: HPLC-MS/PDA analysis of the reaction mixture of TCO **10** and tetrazine **2c** in 50/50 DMSO-d6 / D_2O-buffer after 3 day, including MS and UV spectra of the 2,5-tautomer **15c** (MW=576.28), which elutes at 3.41 min.

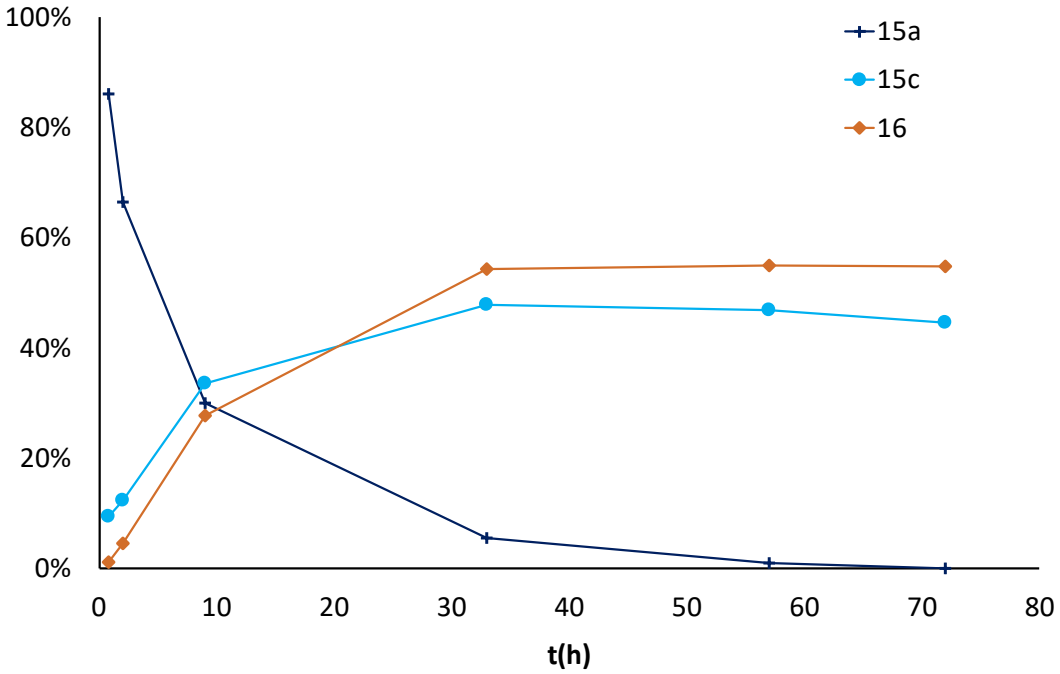

Supplementary Figure 18: Product distribution as a function of time for reaction of TCO **10** and tetrazine **2c** in 50/50 DMSO-d6 / D_2O-buffer. Legend: **15a** = 4,5-tautomer; **15c** = non-releasing 2,5-tautomer; **16** = elimination product. Data acquired by ^1H NMR monitoring.

Studies on the reaction of TCO 9 with tetrazine 2e

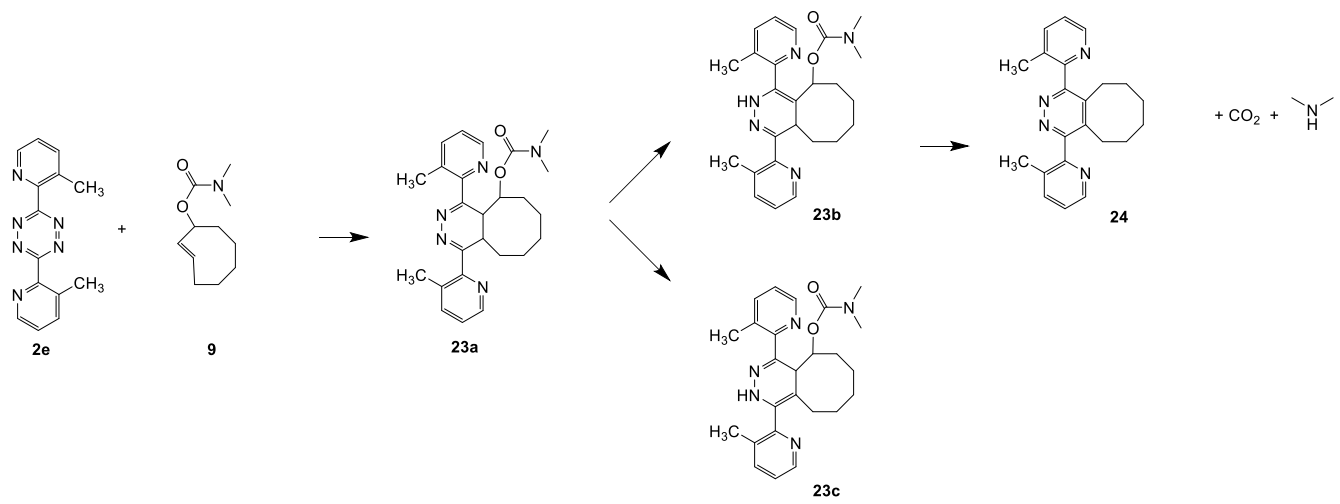

Reaction of TCO **9** and 3,6-bis(3-methylpyridin-2-yl)-1,2,4,5-tetrazine (**2e**) as activator in 20% acetonitrile in water

A stock solution of TCO **9** in DMSO (10 µL 25 mM, 2.5×10^{-7} mol) was diluted with acetonitrile (200 µL) and water (800 µL). A stock solution of **2e** in DMSO (10 µL 25 mM, 2.5×10^{-7} mol) was added, and the mixture was homogenized and incubated at 37°C. After 10 min, the sample was analyzed by HPLC-MS/PDA, and this was repeated after 23 h, but no formation of elimination product **24** was observed. Subsequently, formic acid (1 µL) was added, and the mixture was homogenized and incubated at 37°C. After 60 min and after 18 h the sample was analyzed by HPLC-MS/PDA, but still hardly any elimination product **24** was formed. Subsequently, potassium phosphate buffer (100 µL 1 M, pH=7.4) was added to neutralize the solution, and the mixture was homogenized and incubated at 37°C. After 10 min and after 18 h the sample was analyzed by HPLC-MS/PDA, showing predominately the presence of IEDDA adducts **23**, but hardly any formation of elimination product **24** (Supplementary Figure 19).

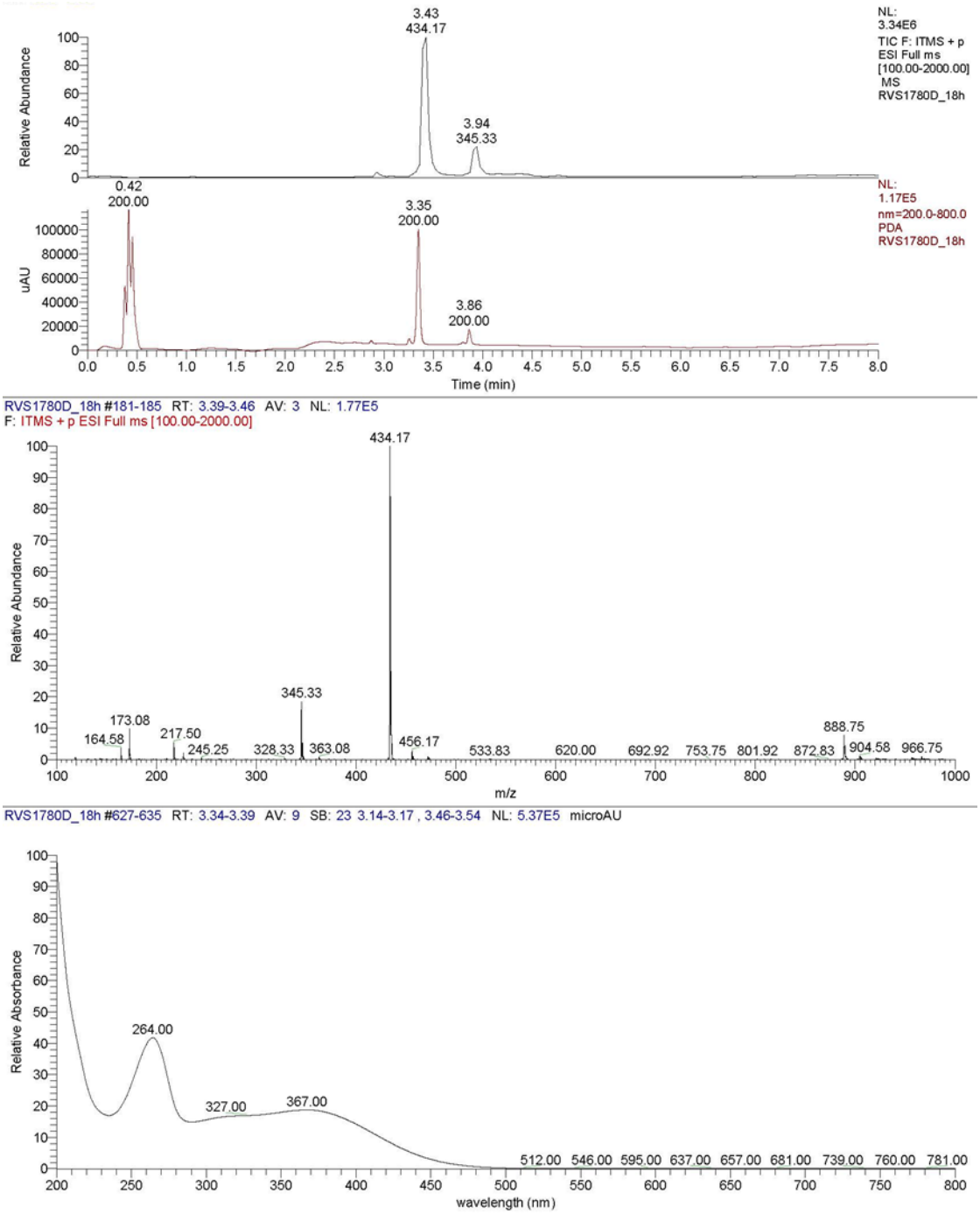

Supplementary Figure 19: HPLC-MS/PDA analysis of the reaction mixture of TCO **9** and tetrazine **2e** in 20% acetonitrile/water after addition of formic acid and neutralization with phosphate buffer, including MS and UV spectra of the IEDDA adduct **23** (MW=433.56) that elutes at 3.35 min.

MMAE release from ADC in vitro

In a 1.5 mL vial, the following was combined: 650 µL mouse plasma, 600 µL PBS, 20 µL ADC (1.62 µg/µL in PBS) and 7.5 µL d8-MMAE solution (0.167 µg/µL, internal standard). Next, aliquots of 20 µL were prepared to which 5.2 µL of a tetrazine solution (0.25 mM in DMSO:H_2O = 1:1) was added and the solution was incubated at 37°C. At various times, 100 µL of cold MeCN was added to the aliquot and the mixture was vortexed, stored at 4°C for 30 min. and centrifuged. Supernatant (20 µL) was taken and combined with 100 µL of 1% formic acid (aq) solution. This sample was analysed with HPLC-SIM-MS to quantify the ratio of free MMAE and d8-MMAE, which is a measure of the release yield.

Section S7: Cell proliferation assays and animal studies

Cell culture and proliferation assay

The human colon carcinoma LS174T cell line was obtained from the American Type Culture Collection and cultured in RPMI-1640 medium supplemented with 2 mM glutamine and 10% heat inactivated fetal calf serum. Twenty-four hours prior to the experiment, the cells were plated in 96-well plates at a 5000 cells/well density. The cells were then incubated with serial dilutions (10 µM – 1 µM; n=6) of activators **1a,b,d**, **2a,b,d** or 3,6-dimethyl tetrazine in culture medium for 72 h at 37°C. The % cell proliferation was assessed by an MTT assay, in comparison to cells incubated in culture medium without activator.

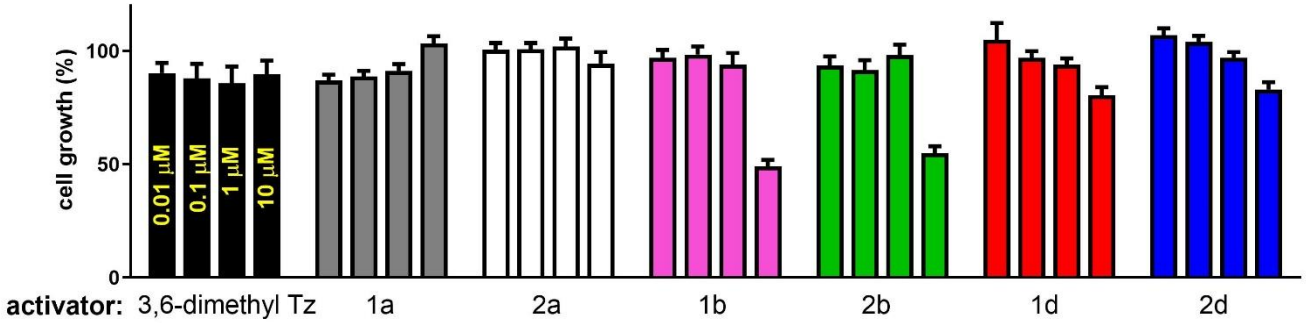

Supplementary Figure 20. Cell proliferation assay: LS174T cell growth after 72 h incubation at 37°C in the presence of activators **1a,b,d**, **2a,b,d** or 3,6-dimethyl tetrazine. Data are the mean with SEM (n=6).

Animal studies

The animal studies were performed in accordance with the principles established by the revised Dutch Act on Animal Experimentation (1997) and were approved by the institutional Animal Welfare Committee of the Radboud University Nijmegen. To determine the appropriate group sizes for the different experiments, the Java Applet for Power and Sample Size was used (http://www.stat.uiowa.edu/~rlenth/Power). Upon arrival, female BALB/c nude mice (BALB/cAnN-Fox1$^{nu/nu}$/Rj; 6-8 week old; 18-22 g body weight; Janvier Labs) were acclimatized for one week before any experimental procedure. The mice had unlimited access to food and water and were maintained in a controlled environment (22±1°C, 55±10% humidity, 12 h dark/light cycles, 5-6 animals per cage, cage and nesting material change once per week or every 2-3 days during therapy administration). The mice were subcutaneously inoculated ca. 1×10^6 LS174T cells in 100 µL culture medium in the hind limb. Tumor size was determined by caliper measurements in 3 dimensions (tumor volume = ½ × l × w × h) 2 times per week and mouse welfare was assessed daily. Animals were allocated to treatments groups using a random sequence generator and the biotechnician performing the experiments were blinded to the group allocation. Biodistribution studies started when the tumors reached 0.1-0.2 cm^3 size. Therapy studies started when the tumors became palpable (5-11 days after tumor cell inoculation).

In vivo reaction between ADC and activator: tumor blocking study

The complete evaluation of ADC biodistribution, blood circulation and binding in normal mice and mice bearing (TAG72 +) LS174T xenografts was presented previously [3]. In this present study we performed tumor blocking experiments [2, 3] to evaluate the in vivo reactivity between the TCO linker on the ADC and activators **1b**, **1d**, **2b** and **2d** in LS174T xenografts. The activators were administered at a 20- to 100-lower dose than that used in previous tumor blocking and therapy studies (ca. 0.335 mmol/kg [3]). As previously, a highly reactive ^{111}In-labeled tetrazine-DOTA probe was used as a reporter to show the presence of residual (unreacted) TCO moieties in the tumors of mice treated with ADC followed by the activators, in comparison to mice that did not receive the activator [2, 3].

Groups of tumor bearing mice (n=4) were injected with ^{125}I-labeled ADC (2 mg/kg, ca. 0.35 MBq/100 µL saline per mouse) followed 48 h later by the activators (dose 1x: 3.3 µmol/kg; dose 5x: 16.7 µmol/kg; 100 µL PBS containing 5% DMSO) and, after 1 h, by [^{111}In]In-DOTA-tetrazine probe (0.33 µmol/kg, ca. 1 MBq/100 µL saline per mouse).

One group of mice was injected with the same amount of ^{125}I-labeled ADC followed only by ^{111}In-labeled probe 49 h later. One last group of mice was injected only with the probe (non-specific probe binding). All mice were euthanized 23 h post-probe injection and the ^{125}I and ^{111}In uptakes in tumors were measured by γ-counting (dual-isotope protocol with cross contamination correction), together with standards to determine the % injected dose per gram (%ID/g). The on-tumor reaction yield between ADC and activator was calculated as previously reported [2, 3] with minor modifications. Briefly, the ^{111}In uptake in the tumors (%ID/g) was corrected for mean non-specific probe binding (Supplementary Table 4, mean ^{111}In %ID/g for probe alone) and divided by the ^{125}I uptake (%ID/g), to account for different ADC uptake in different sized tumors. The obtained ratios were normalized for the mean value obtained in mice not treated with an activator (mean In-111/I-125 ratio for the "no activator" group in Supplementary Table 4). In this group, the max probe binding was achieved, signifying 0% reaction yield between ADC and activator.

Supplementary Table 4. ^{125}I-ADC and ^{111}In-probe tumor uptakes in mice used for in vivo activator reactivity (tumor blocking) studies.

group	^{125}I (%ID/g)	^{111}In (%ID/g)	tumor size (gr)	reaction yield (%)
probe alone	NA	0.09 0.10 0.09 0.11	0.141 0.238 0.377 0.255	NA
no activator	23.29 18.46 16.54 18.41	5.59 4.28 2.98 3.95	0.175 0.157 0.436 0.334	0
1b, dose 1x	16.09 19.59 17.60 19.24	2.41 2.93 4.17 3.23	0.509 0.365 0.314 0.339	32.1 24.5 -9.3 23.1
2b, dose 1x	17.85 20.58 12.89	2.73 2.61 1.68	0.552 0.490 0.480	30.1 42.2 42.0

	12.78	1.79	0.592	37.5
1d, dose 1x	12.78	1.85	0.176	35.3
	20.94	3.14	0.154	31.3
	14.18	1.88	0.265	40.5
	12.36	1.05	0.153	63.3
2d, dose 1x	22.71	2.09	0.209	58.5
	14.49	1.24	0.254	62.8
	15.39	0.99	0.335	72.4
	10.22	0.82	0.361	66.4
1d, dose 5x	18.20	0.85	0.311	80.3
	12.22	0.67	0.300	77.9
	15.44	0.72	0.337	81.0
	18.37	0.83	0.274	81.2
2d, dose 5x	14.35	0.18	0.361	97.1
	10.27	0.26	0.246	92.3
	21.30	0.54	0.108	90.1
	19.46	0.21	0.294	97.3

Supplementary Table 5: ^{125}I-ADC and ^{111}In-probe distribution in other organs and tissues in mice used for in vivo activator reactivity (in vivo competition) studies. Data presented as the mean ± SD (n=4).

ADC	2 mg/kg	2 mg/kg	2 mg/kg	2 mg/kg	4 mg/kg	2 mg/kg	--
activator	**1b**, dose 1x	**2b**, dose 1x	**1d**, dose 1x	**2d**, dose 1x	**1d**, dose 5x	--	--
				%ID/g ^{125}I-ADC			
blood	0.17±0.08	0.10±0.02	0.15±0.07	0.13±0.07	0.18±0.09	0.18±0.06	--
heart	0.07±0.02	0.04±0.01	0.05±0.02	0.06±0.03	0.06±0.02	0.08±0.02	--
lung	0.19±0.06	0.14±0.03	0.17±0.06	0.17±0.06	0.18±0.07	0.23±0.05	--
liver	0.61±0.42	1.91±0.98	0.41±0.23	0.37±0.09	0.22±0.16	0.68±0.38	--
spleen	0.24±0.12	0.58±0.24	0.24±0.08	0.17±0.01	0.16±0.03	0.34±0.17	--
kidney L	0.36±0.11	0.24±0.04	0.26±0.08	0.33±0.07	0.28±0.05	0.34±0.07	--
muscle	0.03±0.01	0.02±0.00	0.02±0.01	0.02±0.01	0.02±0.01	0.03±0.01	--
bone	0.05±0.01	0.05±0.02	0.04±0.01	0.04±0.01	0.04±0.01	0.06±0.00	--
				%ID/g ^{111}In-probe			
blood	0.06±0.02	0.05±0.01	0.06±0.03	0.04±0.01	0.03±0.01	0.12±0.04	0.02±0.01
heart	0.06±0.01	0.05±0.00	0.05±0.01	0.04±0.01	0.03±0.01	0.10±0.03	0.03±0.01
lung	0.14±0.02	0.11±0.01	0.13±0.04	0.10±0.02	0.09±0.02	0.23±0.04	0.07±0.01
liver	0.29±0.04	0.38±0.06	0.20±0.01	0.17±0.01	0.12±0.01	0.46±0.12	0.44±0.44
spleen	0.16±0.03	0.20±0.02	0.14±0.02	0.10±0.01	0.10±0.01	0.29±0.06	0.27±0.26
kidney L	1.20±0.25	1.06±0.09	1.06±0.11	1.09±0.10	1.13±0.08	1.39±0.22	1.00±0.21
muscle	0.02±0.01	0.02±0.00	0.02±0.01	0.02±0.01	0.02±0.00	0.04±0.01	0.01±0.00
bone	0.07±0.00	0.06±0.00	0.06±0.01	0.04±0.01	0.06±0.01	0.11±0.01	0.05±0.03

MMAE measurement in tumors

The concentration of released free MMAE was measured in the tumors of selected groups used for tumor blocking experiments and in those from one more group of mice (n=4) treated with 4 mg/kg ADC and 33.5 µmol/kg (dose 10x) activator **1d** using the same protocol.

After γ-counting, tumors samples (0.1-0.2 gr) were transferred into MagNA Lyser green beads tubes (Roche) together with 1 mL methanol and a weighed amount of a d8-MMAE solution as internal standard. The tissues were homogenized (4×30 sec cycles, 6.5k rpm, with 1 min cooling in between cycles) and the debris was removed by centrifugation (13k rpm, 5 min). The methanol was evaporated under a stream of N_2, the residue was reconstituted in PBS (containing BSA digest and 10% MeCN). After overnight standing at -20°C the solutions were filtered through a 0.22 µm filter. The d0/d8-MMAE metabolites of interest were separated on a C_{18} RP column (2.1×100 mm, 3 µm particle size) with a linear 10 – 80% acetonitrile (containing 0.1% formic acid) gradient (gradient length 2 to 10 min; flow rate 250 µL/min; injection volume 5 µl). The eluent from 3 to 6 min was introduced into the mass spectrometer. The collision energy for Xevo-TQS micro system (Waters) using nitrogen collision gas was 25 eV and the cell pressure was 0.35 Pa. The source temperature was set at 150°C and the capillary voltage was maintained at 0.40 kV.

The specific m/z transitions of 718.5 to 506.4 and 718.5 to 321.2 for d0-MMAE and 726.6 to 506.3 and 726.6 to 321.2 for d8-MMAE were detected and the d0/d8 peak area ratio was used for quantitation.

Supplementary Table 6. Free MMAE concentration in tumor.

group	MMAE (nM)
1d, dose 1x	45.3 88.9 68.0 50.6
2d, dose 1x	87.5 84.5 85.6 90.3
1d, dose 5x	236.5 180.9 295.0 190.8
2d, dose 5x	161.6 98.6 110.1 141.3
1d, dose 10x[a]	456.0 235.7 321.6 343.2

[a] Mice treated with a ca 4 mg/kg ADC dose

Therapy studies

One group of LS174T xenograft bearing mice (n=10) was administered four cycles of ADC (4 mg/kg) followed by activator **1d** (33.5 µmol/kg) 48 later, following the injection scheme in Supplementary Figure 21. Control groups (n=10) received ADC alone, activator alone, or vehicle. The animals were monitored daily by experienced biotechnicians and were removed from the study in case of poor physical conditions (mainly discomfort due to tumor skin ulceration due to rapid growth), in case of excessive body weight loss (>20% with respect to baseline) or when tumors reached a 1.5 cm^3 tumor size (Supplementary Table 7). If none of these conditions occurred the mice were maintained in the study for up to 2 months.

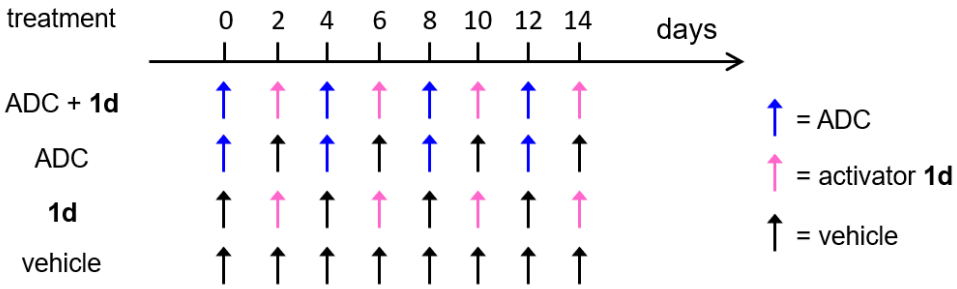

Supplementary Figure 21. Injection scheme for therapy study.

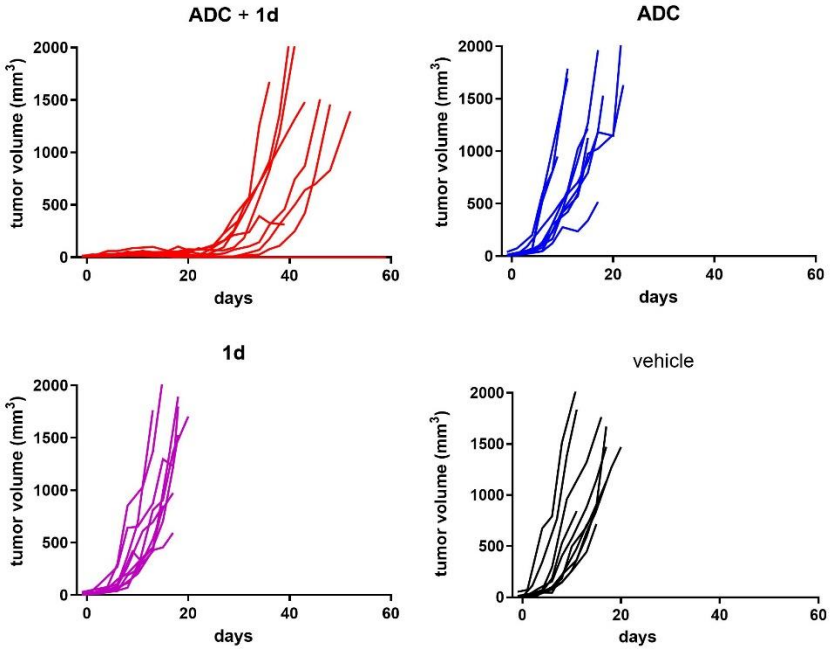

Supplementary Figure 22. Single-mouse LS174T tumor growth curves in mice that within two weeks received i.v. four cycles of the combination of ADC (ca. 4 mg/kg) and activator **1d** (ca. 33.5 µmol/kg, 48 h post-ADC), the ADC alone, **1d** alone or vehicle.

Supplementary Table 7. Number of tumor bearing mice removed from the therapy study (based on pre-defined criteria) and median survival.

	Tumor >1.5cm^3	Body weight loss	Poor physical condition	Median survival (days)
ADC + 1d	7/10	0/10	2/10	42.0
ADC	6/10	0/10	3/10	16.5
1d	6/10	0/10	4/10	17.5
vehicle	6/10	1/10	3/10	15.5

Blood samples (ca. 150 µL) was withdrawn from 4 mice randomly selected within each therapy group before treatment (day -1), immediately after treatment (day 15) and, when possible, approximately two weeks after treatment to assess hematological toxicity. The levels of leukocytes, thrombocytes and hemoglobin detected in blood before and after treatment were in a normal range and similar for all 4 groups (Supplementary Figure 23) signifying lack of treatment related toxicity.

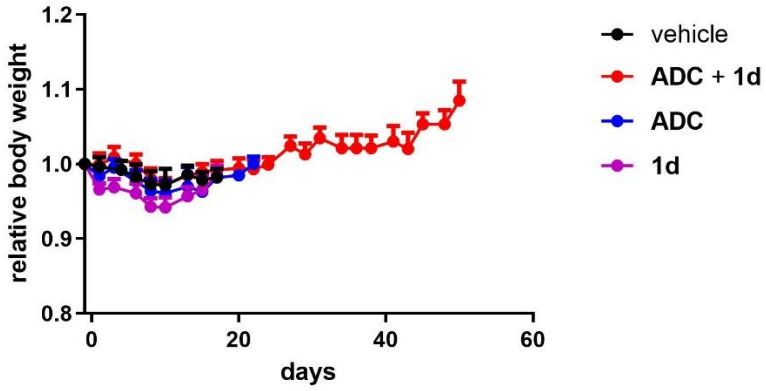

Supplementary Figure 23a. Relative body weights of mice bearing LS174T xenografts used in therapy study.

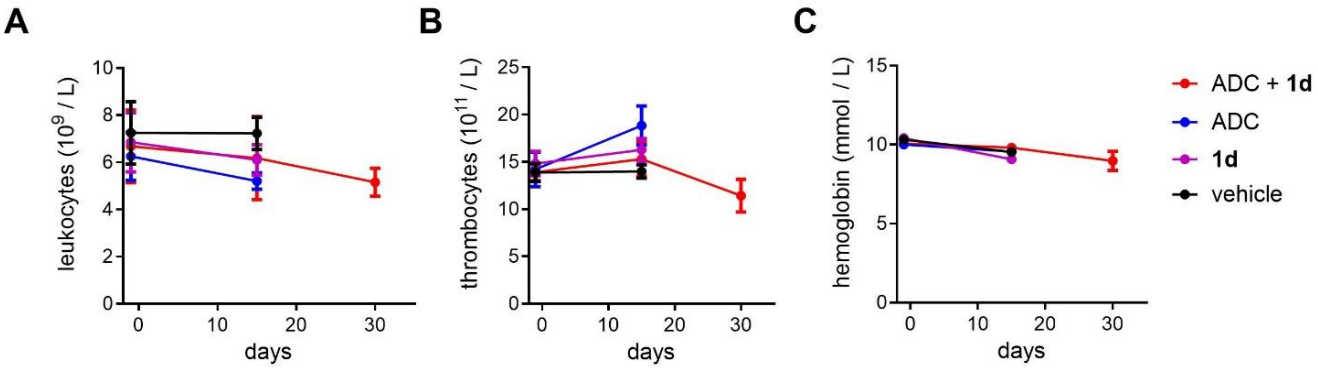

Supplementary Figure 23b. Hematologic toxicity: (A) leukocytes, (B) thrombocytes and (C) hemoglobin values in tumor bearing mice that within two weeks received i.v. four cycles of the combination of ADC (ca. 4 mg/kg)

and activator **1d** (ca. 33.5 µmol/kg, 48h post-ADC), the ADC alone, **1d** alone or vehicle. Data represent the mean with SEM (n=4).

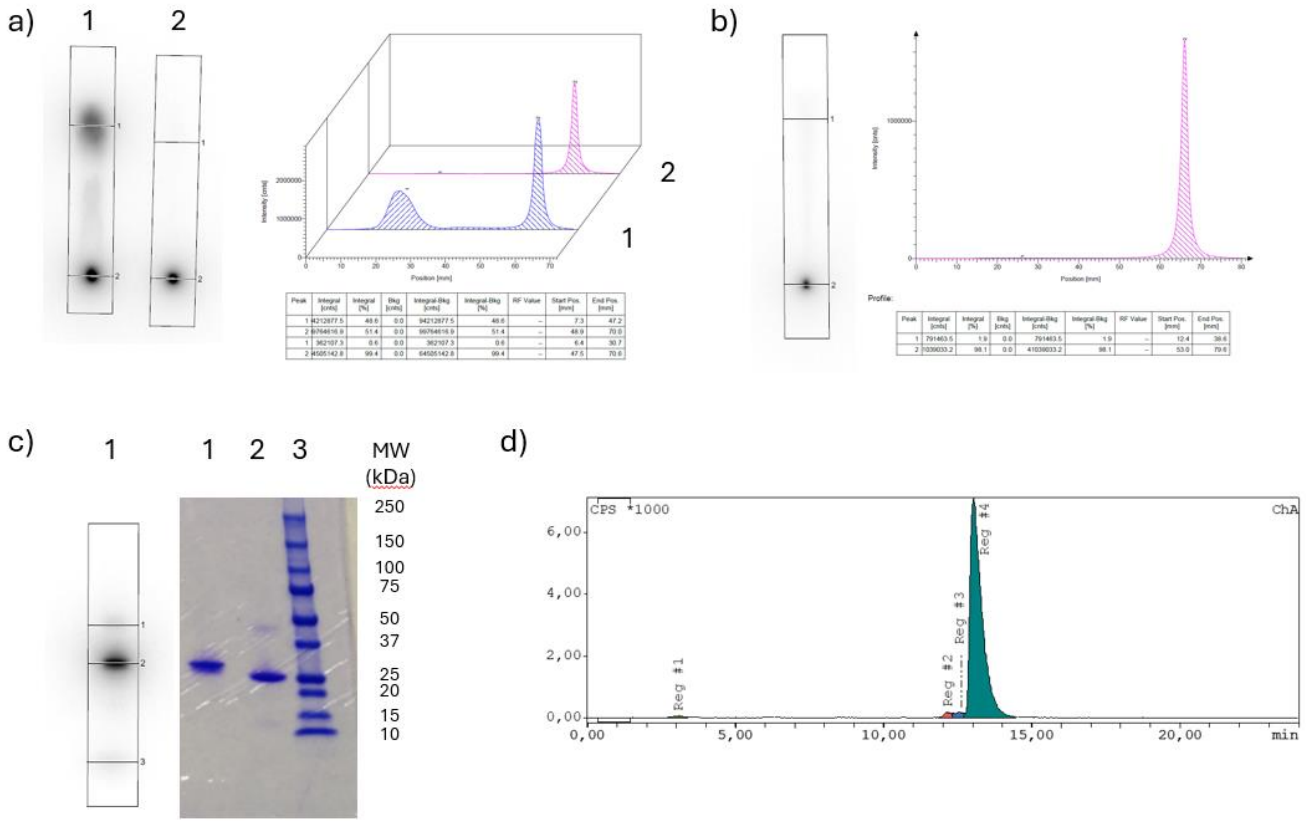

Supplementary Figure 24. Representative radiograms of the radiolabeled species used for animal studies in this work. a) Radio-ITLC of (1) crude and (2) purified ^{125}I-ADC. b) Radio-ITLC of ^{111}In-labeled probe. c) SDS-PAGE analysis (radiogram and Coomassie blue protein staining, 4-15% gradient gel) showing the monomeric form of (1) ^{125}I-labeled ADC (RCP = 95.4 %) and (2) native diabody (lane 3: protein MW marker). d) Radio-RP-HPLC of ^{111}In-labeled probe (R_t = 13.05 min, RCP = 96.1%).

Section S8: Computational modeling

DFT computational settings

The Amsterdam Density Functional (ADF) program was employed for performing the DFT calculations [6]. The B3LYP exchange-correlation functional in conjunction with a triple-ζ (TZP) Slater-type basis set was used in all calculations [7-10]. Implicit solvation effects were considered by employing the COSMO model with parameters for water [11]. Please note that these calculations are performed with an implicit solvent and thus should be treated in a qualitative fashion. Internal hydrogen bonding and steric hindrance can be reliably evaluated using implicit solvation as these correspond to intramolecular properties.

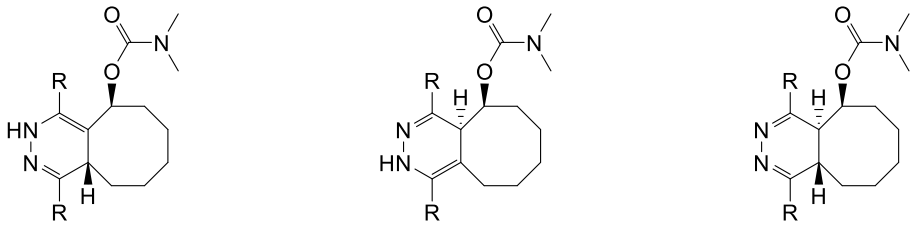

R =

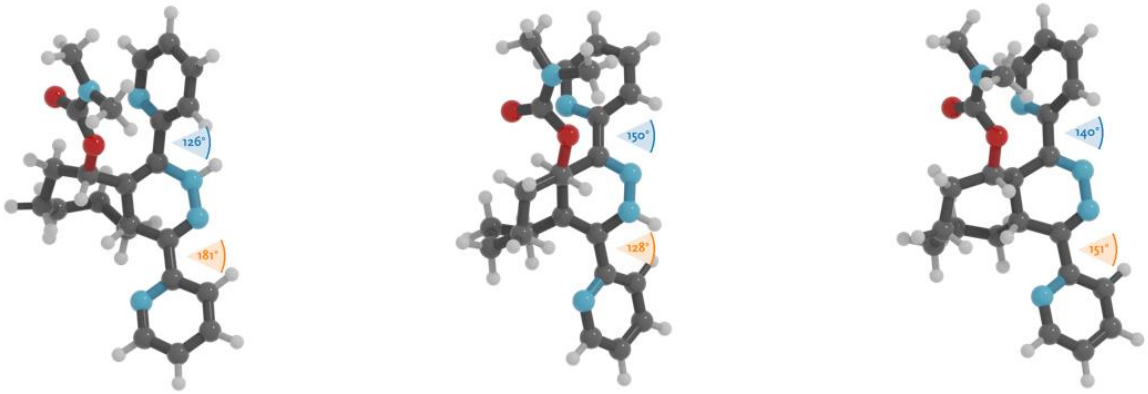

Supplementary Figure 25a. Lowest energy structures of the three tautomers of IEDDA adducts of TCO **9** and tetrazine **2a**. Left: 1,4-tautomer, middle 2,5-tautomer, right 4,5-tautomer. The dihedral angles between the central rings and the top or bottom rings are shown in blue and orange, respectively.

R = 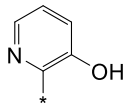

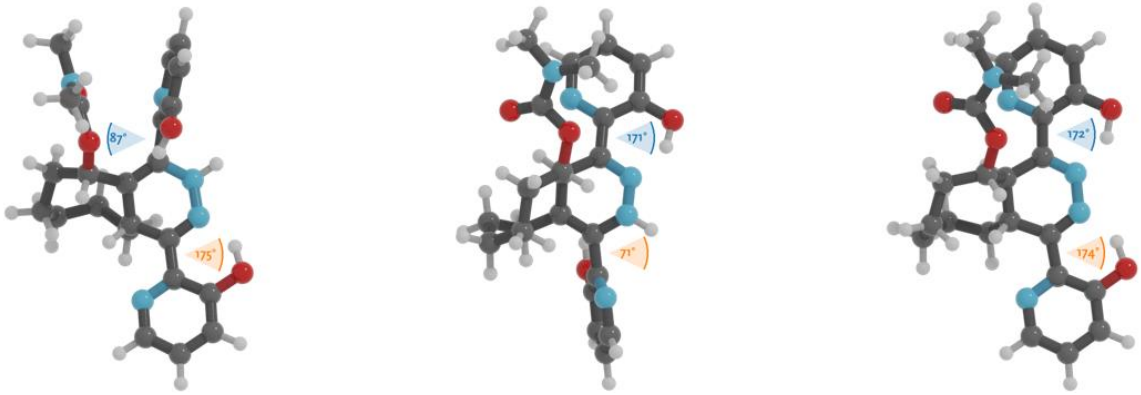

Supplementary Figure 25b. Lowest energy structures of the three tautomers of IEDDA adducts of TCO **9** and tetrazine **2b**. Left: 1,4-tautomer, middle 2,5-tautomer, right 4,5-tautomer. The dihedral angles between the central rings and the top or bottom rings are shown in blue and orange, respectively.

R = 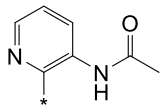

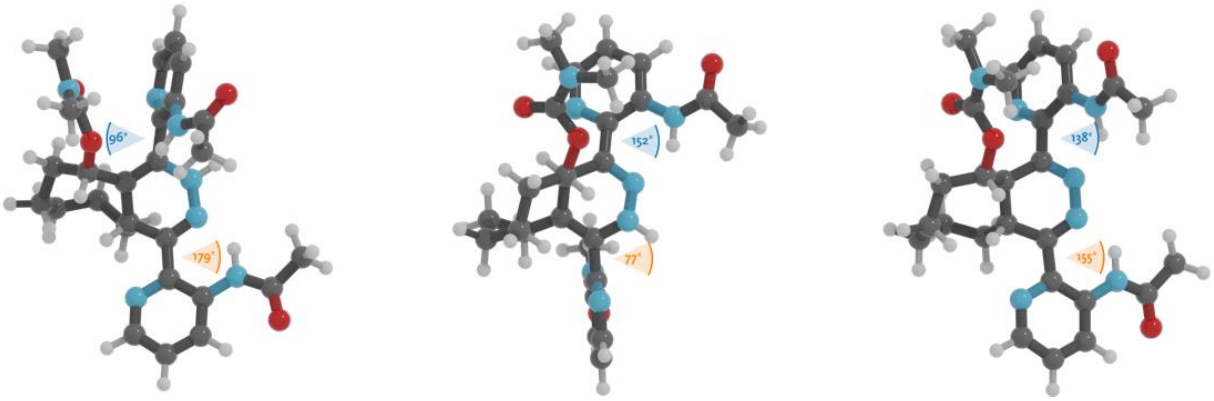

Supplementary Figure 25c. Lowest energy structures of the three tautomers of IEDDA adducts of TCO **9** and tetrazine **2c**. Left: 1,4-tautomer, middle 2,5-tautomer, right 4,5-tautomer. The dihedral angles between the central rings and the top or bottom rings are shown in blue and orange, respectively.

R = 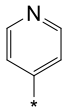

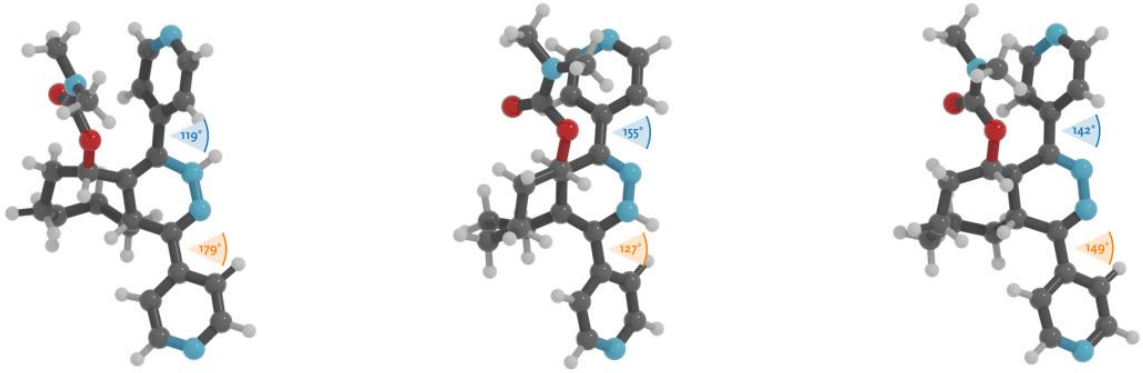

Supplementary Figure 25d. Lowest energy structures of the three tautomers of IEDDA adducts of TCO **9** and tetrazine **1a**. Left: 1,4-tautomer, middle 2,5-tautomer, right 4,5-tautomer. The dihedral angles between the central rings and the top or bottom rings are shown in blue and orange, respectively.

R = 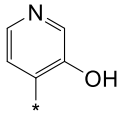

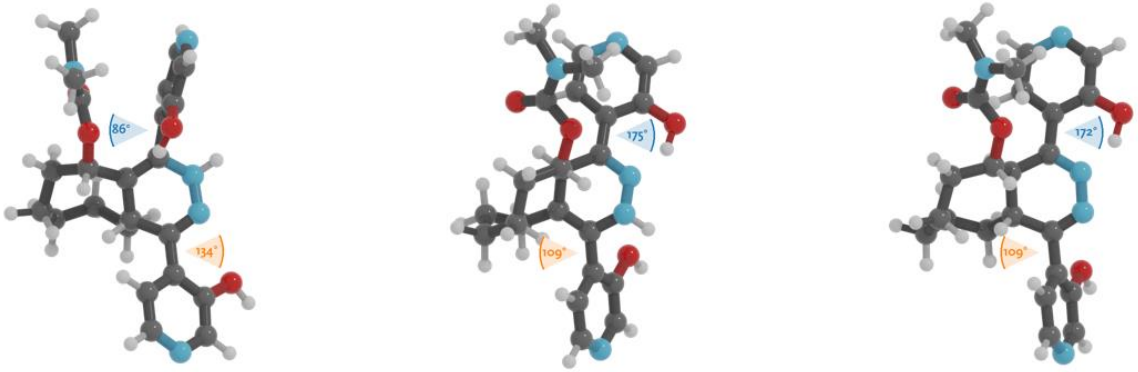

Supplementary Figure 25e. Lowest energy structures of the three tautomers of IEDDA adducts of TCO **9** and tetrazine **1b**. Left: 1,4-tautomer, middle 2,5-tautomer, right 4,5-tautomer. The dihedral angles between the central rings and the top or bottom rings are shown in blue and orange, respectively.

R = 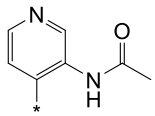

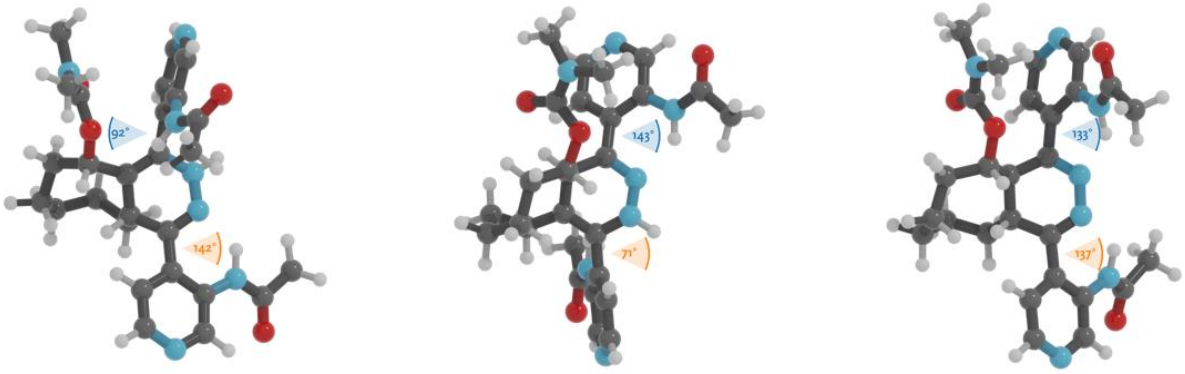

Supplementary Figure 25f. Lowest energy structures of the three tautomers of IEDDA adducts of TCO **9** and tetrazine **1c**. Left: 1,4-tautomer, middle 2,5-tautomer, right 4,5-tautomer. The dihedral angles between the central rings and the top or bottom rings are shown in blue and orange, respectively.

Supplementary Table 8. Dihedral angles between the central dihydropyridazine ring and the top and bottom pyridinyl rings, of the three tautomers of IEDDA adducts of TCO **9** and a selection of tetrazines. “Top ring”: same side as the carbamate; “bottom ring”: opposite side vs. the carbamate.

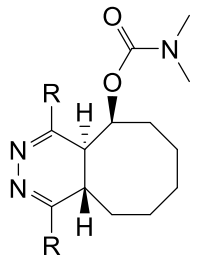

4,5-tautomer

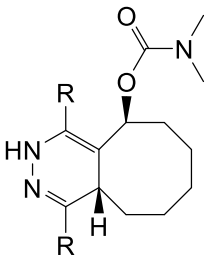

1,4-tautomer

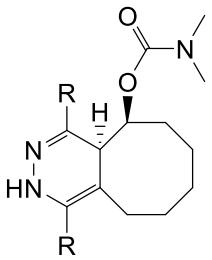

2,5-tautomer

Structure R-group	Tautomer	Dihedral angle Top [degrees]	Dihedral angle Bottom [degrees]
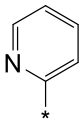	1,4	126.4	181.1
	2,5	150.5	128.4
	4,5	140.0	151.9
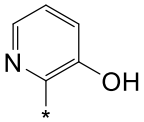	1,4	87.7	175.1
	2,5	171.8	71.0
	4,5	173.0	174.9
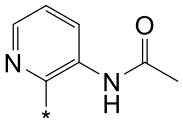	1,4	96.9	179.2
	2,5	152.5	77.5
	4,5	138.7	155.3
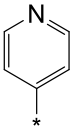	1,4	119.2	179.8
	2,5	155.6	127.1
	4,5	142.1	149.7
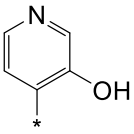	1,4	86.5	134.3
	2,5	175.8	109.6
	4,5	172.3	109.9
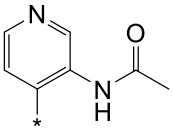	1,4	92.4	142.6
	2,5	143.7	71.7
	4,5	133.6	137.9

Section S9: Spectra

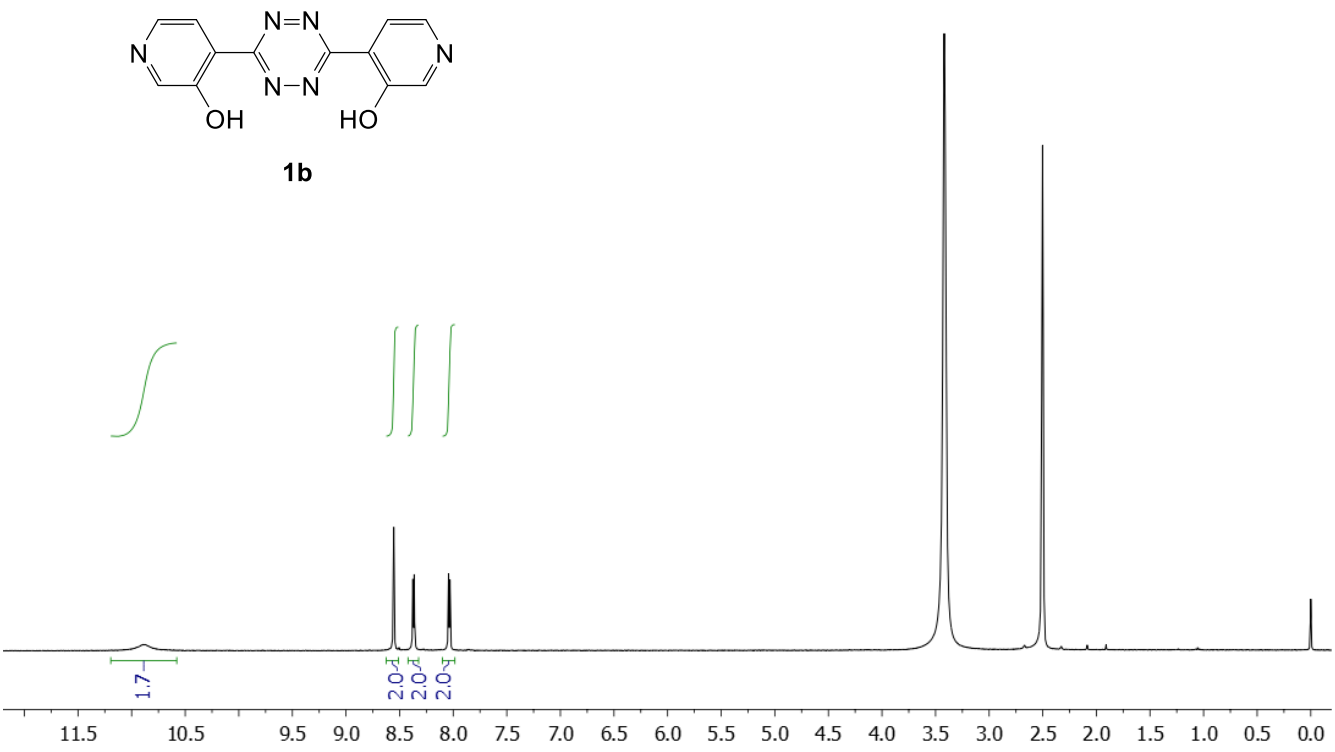

^{1}H-NMR spectrum ($CDCl_3$) of 4,4'-(1,2,4,5-Tetrazine-3,6-diyl)bis(pyridin-3-ol) (**1b**).

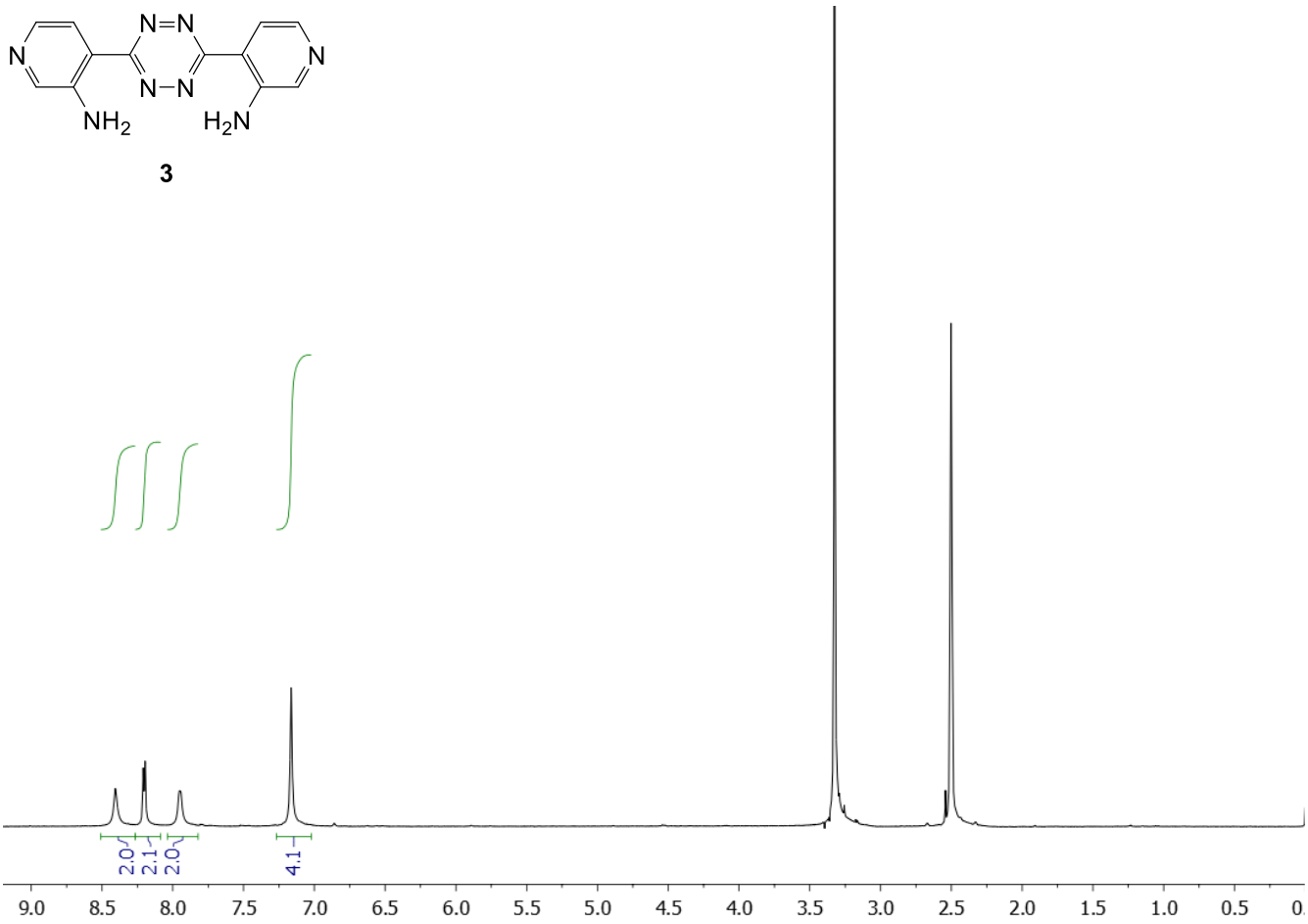

^{1}H-NMR spectrum (DMSO-d_6) of 4,4'-(1,2,4,5-Tetrazine-3,6-diyl)bis(pyridin-3-amine) (**3**).

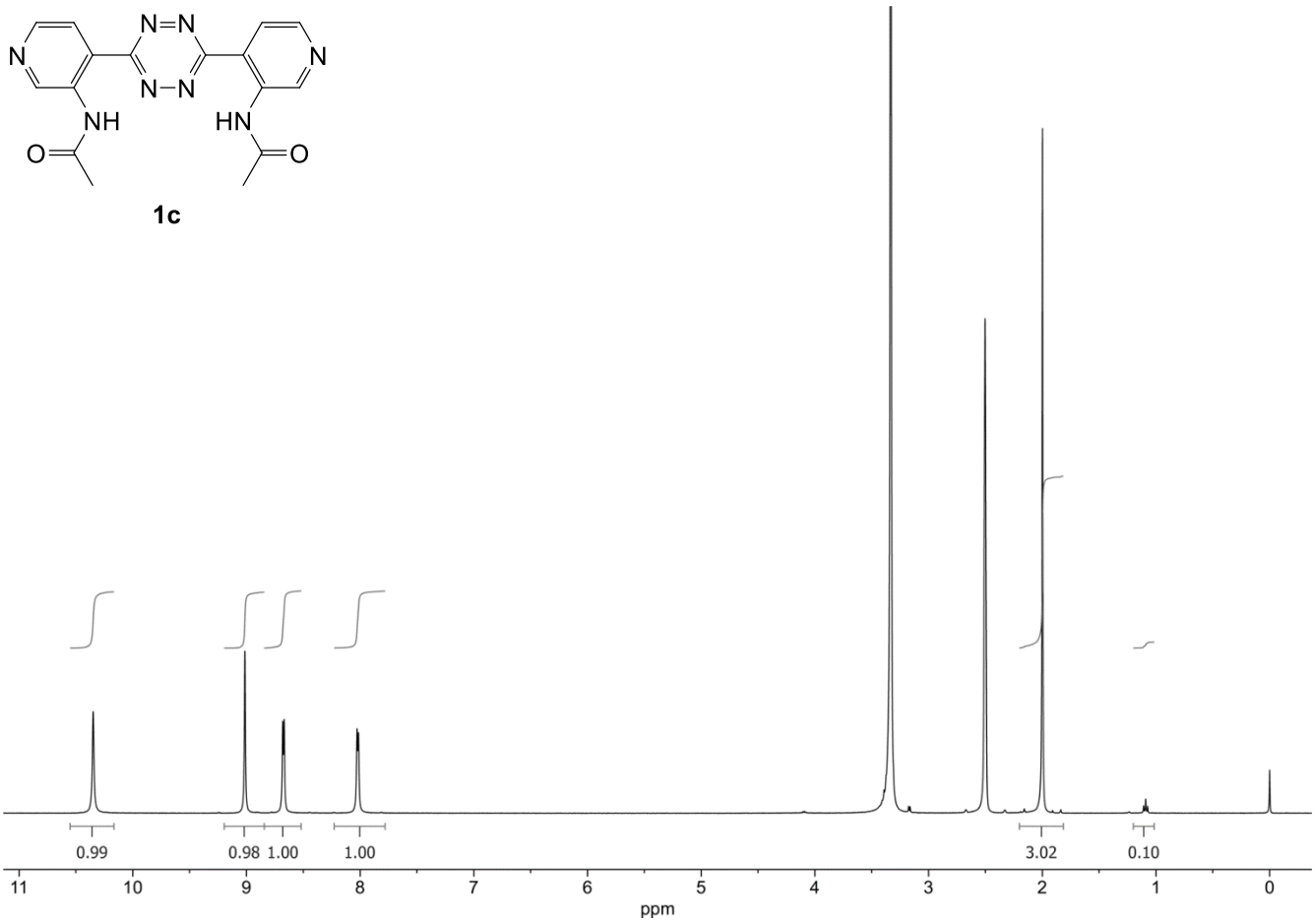

^{1}H-NMR spectrum (DMSO-d_6) of *N*,*N*'-(4,4'-(1,2,4,5-Tetrazine-3,6-diyl)bis(pyridine-4,3-diyl)) diacetamide (**1c**).

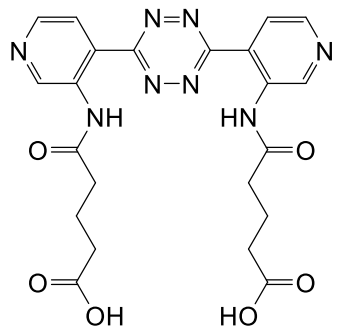

5

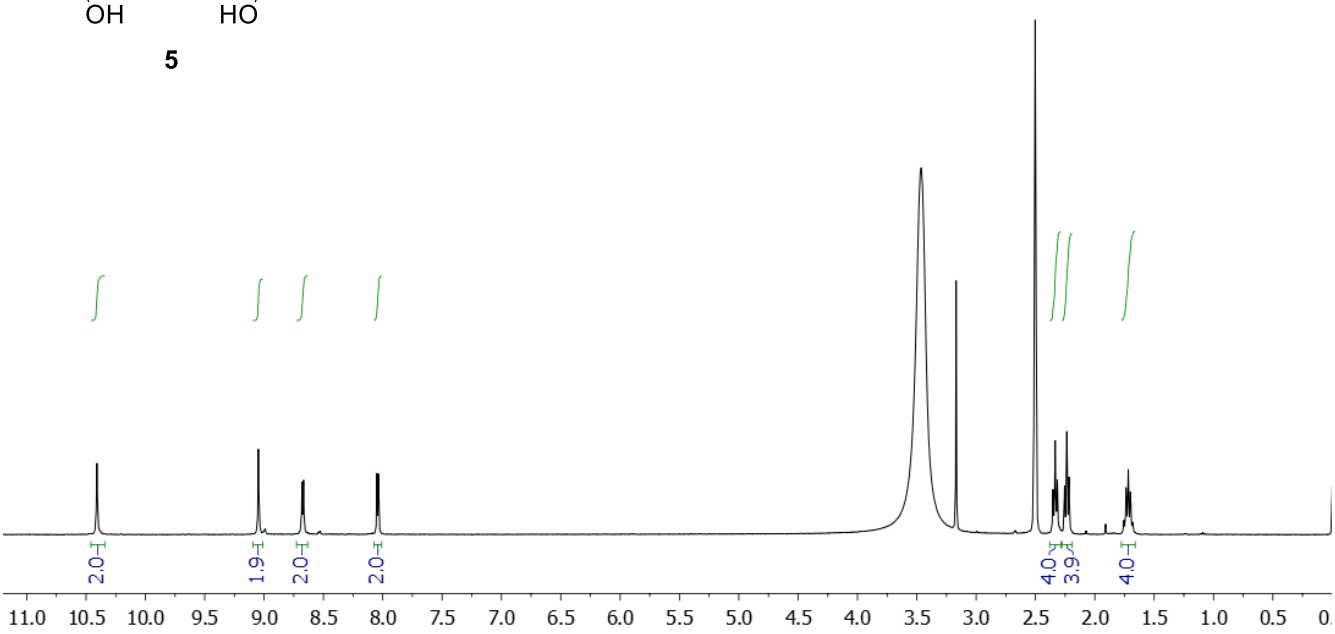

^{1}H-NMR spectrum (DMSO-d_6) of 5,5'-((4,4'-(1,2,4,5-Tetrazine-3,6-diyl)bis(pyridine-4,3-diyl))bis(azanediyl))bis(5-oxopentanoic acid) (**5**).

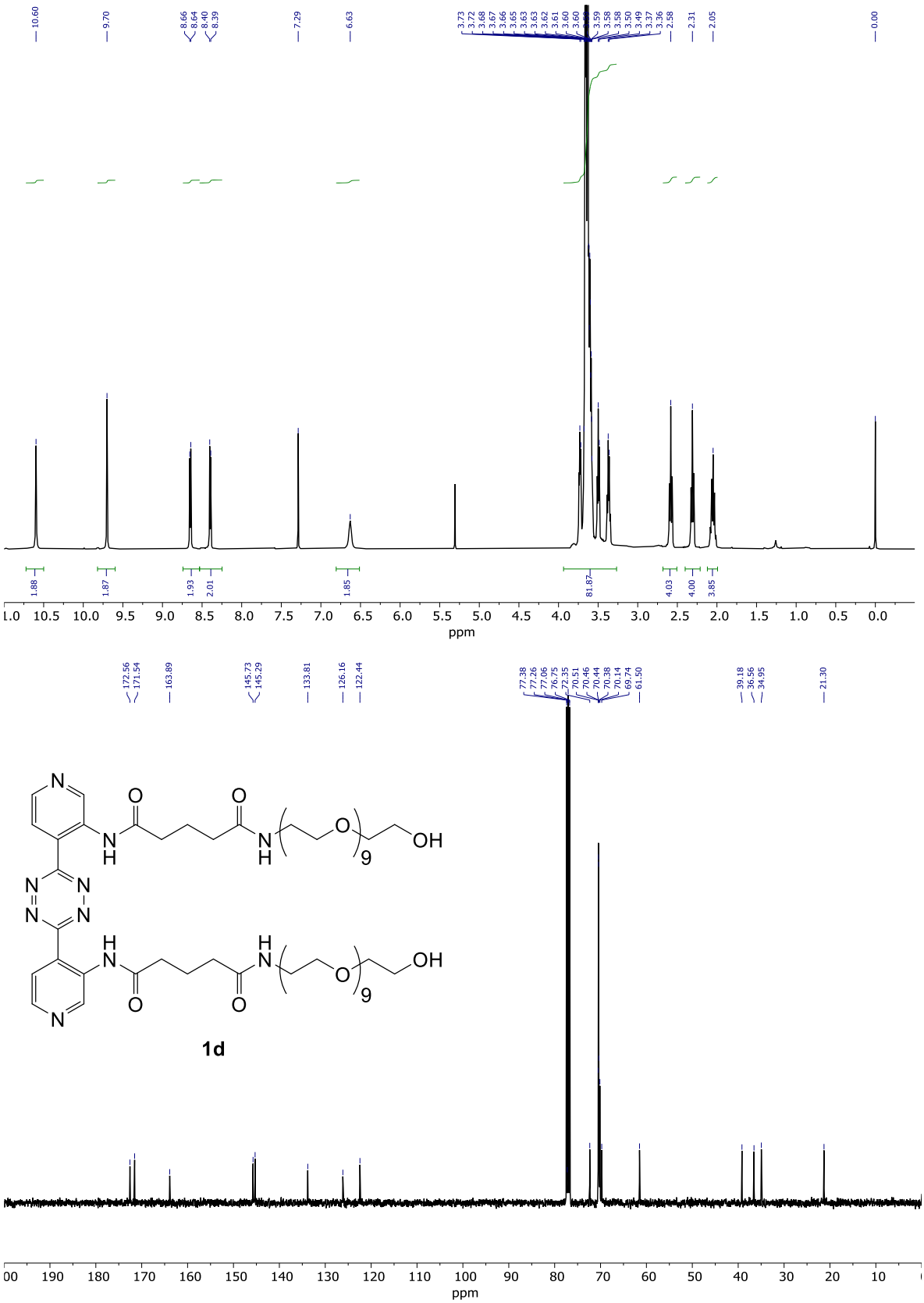

^{1}H (top) and ^{13}C (bottom) NMR spectra ($CDCl_3$) of N^1,$N^{1'}$-(4,4'-(1,2,4,5-Tetrazine-3,6-diyl)bis(pyridine-4,3-diyl))bis(N^5-(29-hydroxy-3,6,9,12,15,18,21,24,27-nonaoxanonacosyl) glutaramide) (**1d**).

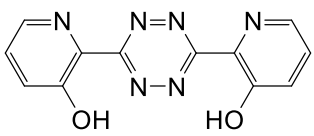

2b

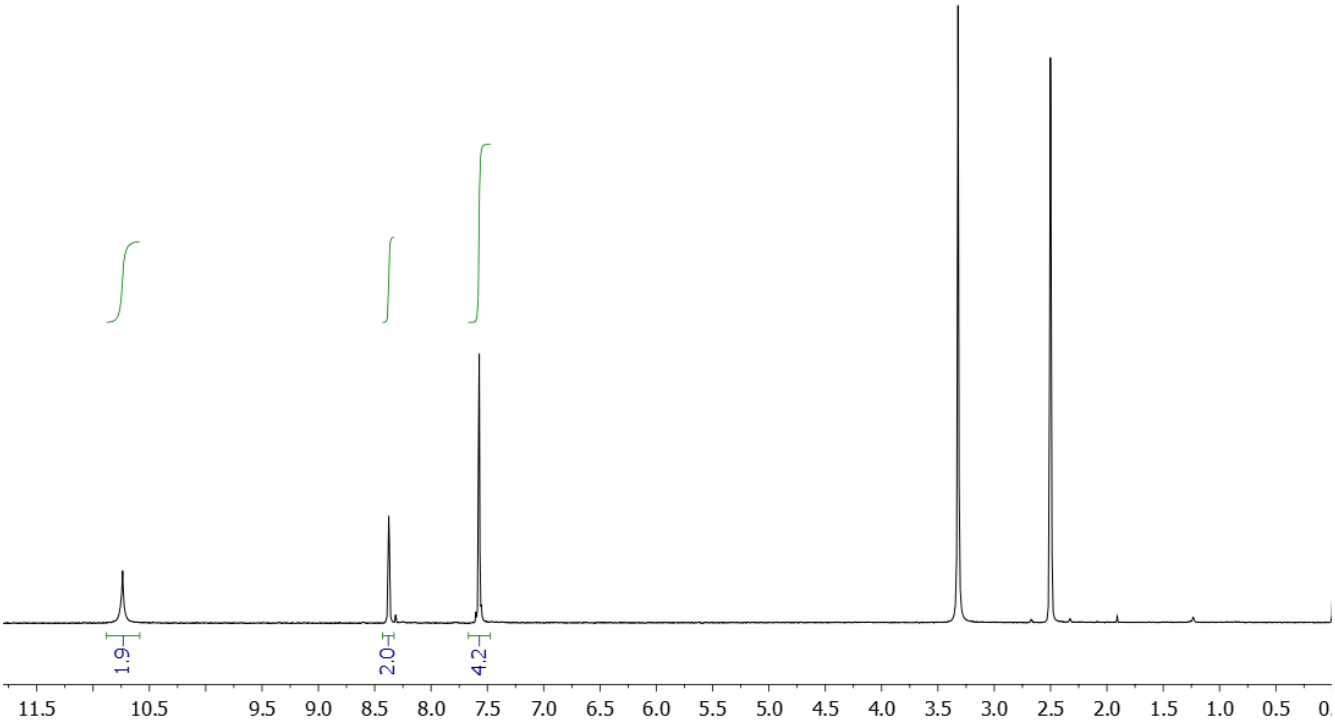

^{1}H-NMR spectrum (DMSO-d_6) of 2,2'-(1,2,4,5-Tetrazine-3,6-diyl)bis(pyridin-3-ol) (**2b**).

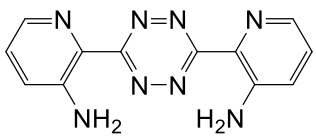

7

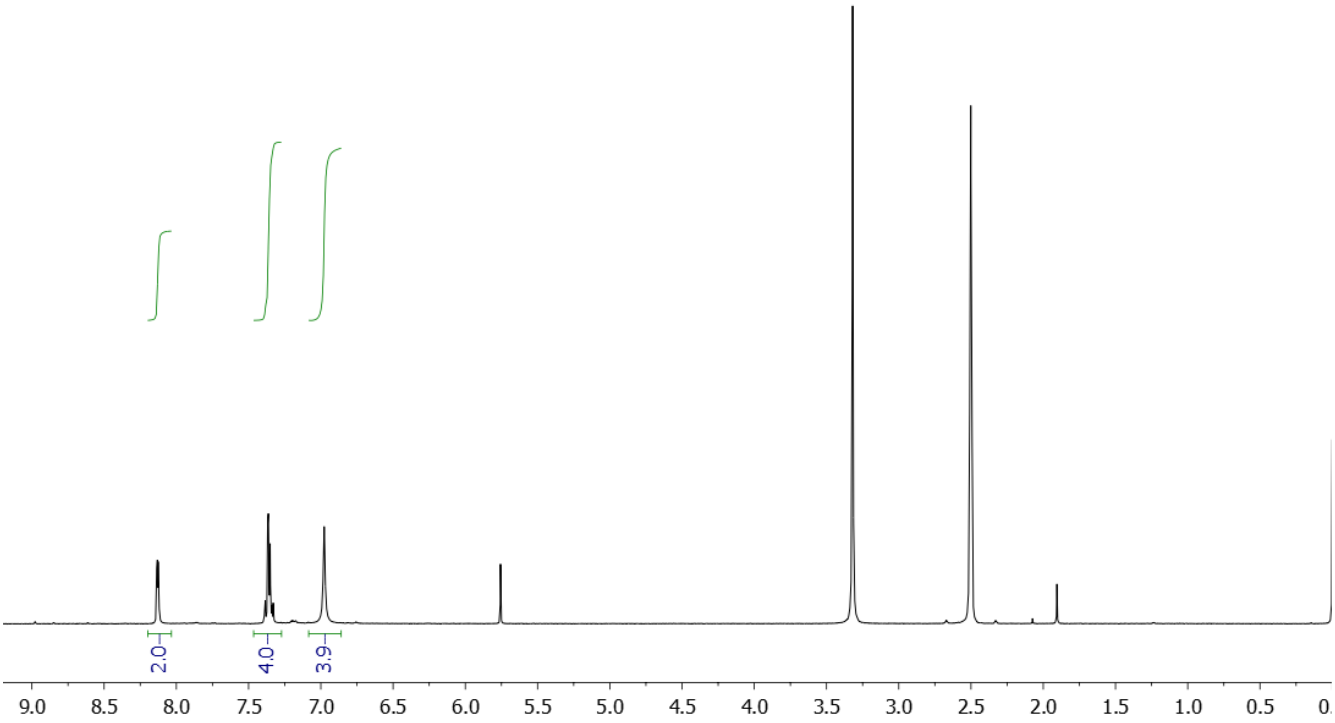

^{1}H-NMR spectrum (DMSO-d_6) of 2,2'-(1,2,4,5-Tetrazine-3,6-diyl)bis(pyridin-3-amine) (**7**).

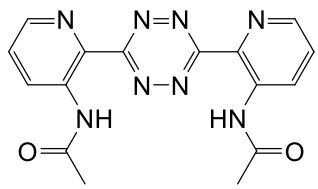

2c

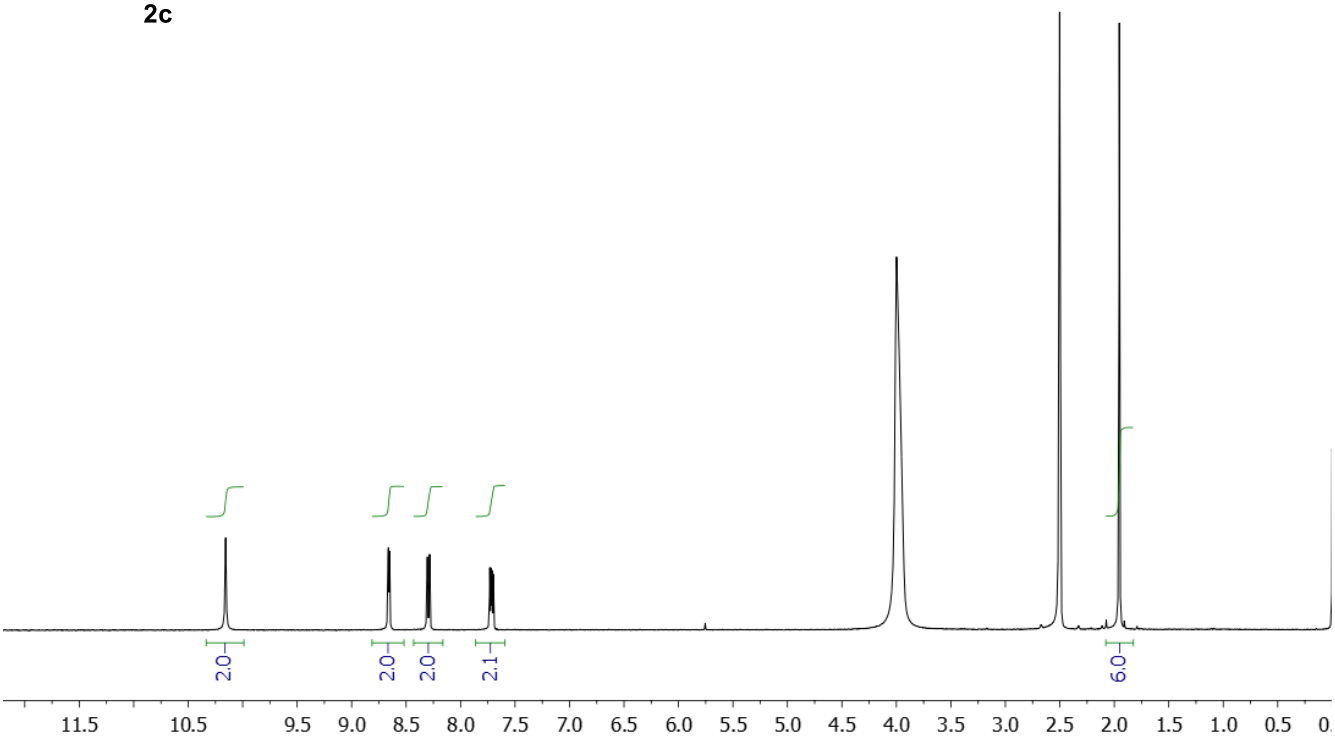

^{1}H-NMR spectrum (DMSO-d_6) of *N*,*N*'-(2,2'-(1,2,4,5-Tetrazine-3,6-diyl)bis(pyridine-3,2-diyl))diacetamide (**2c**).

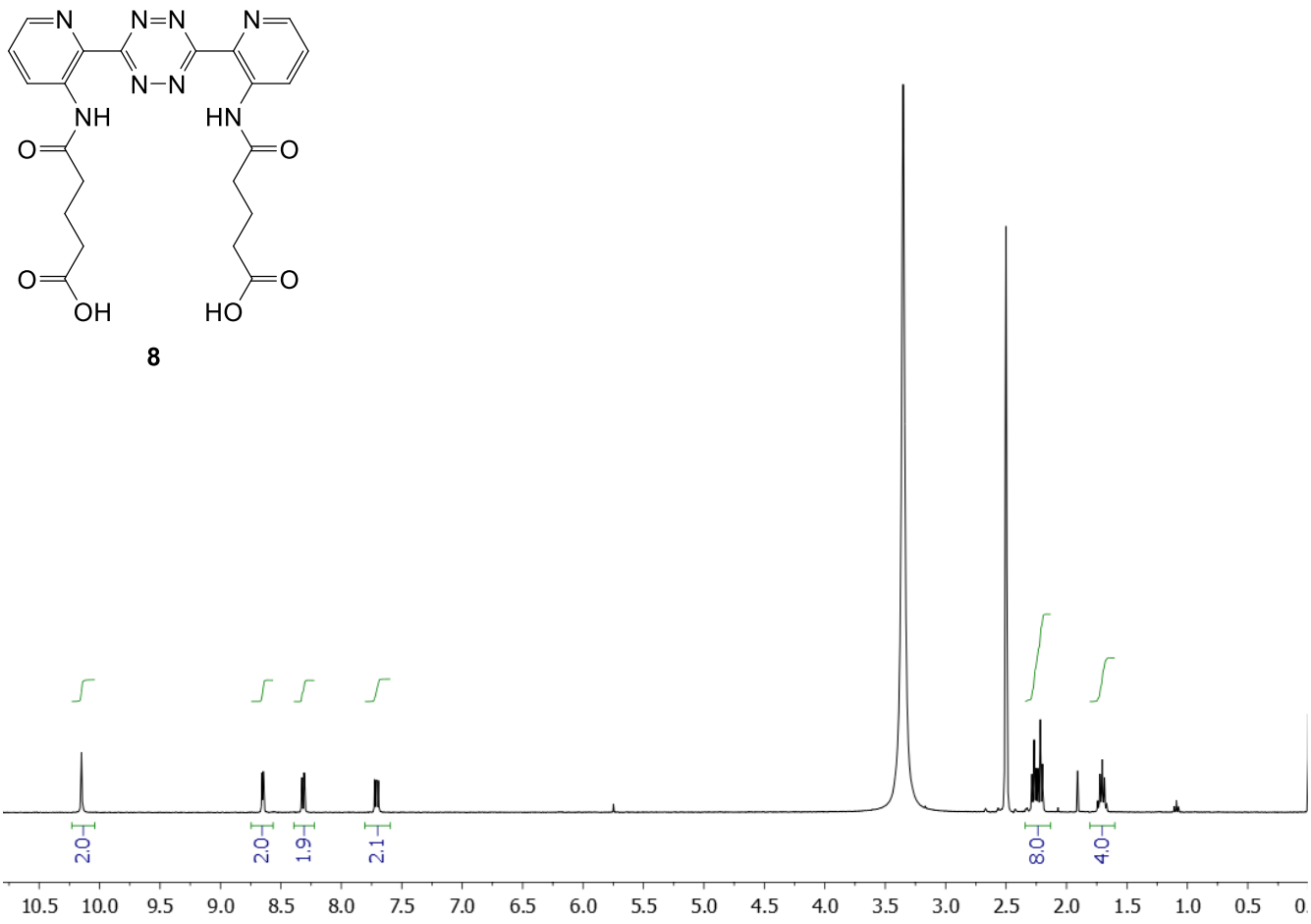

^{1}H-NMR spectrum (DMSO-d_6) of 5,5'-((2,2'-(1,2,4,5-Tetrazine-3,6-diyl)bis(pyridine-3,2-diyl))bis(azanediyl))bis(5-oxopentanoic acid) (**8**).

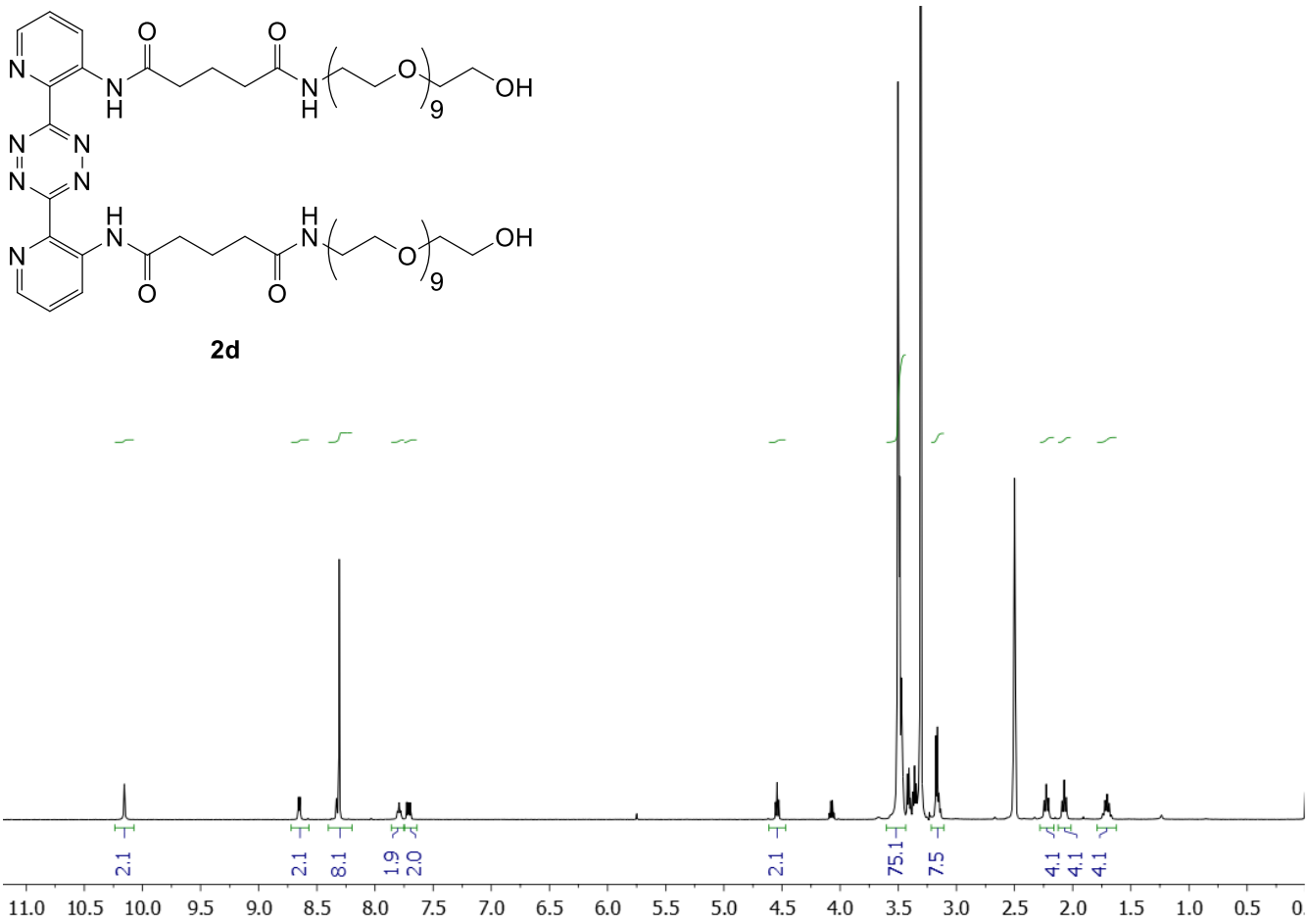

^{1}H-NMR spectrum (DMSO-d_6) of N^1,$N^{1'}$-(2,2'-(1,2,4,5-Tetrazine-3,6-diyl)bis(pyridine-3,2-diyl))bis(N^5-(29-hydroxy-3,6,9,12,15,18,21,24,27-nonaoxanonacosyl)glutaramide) (**2d**).

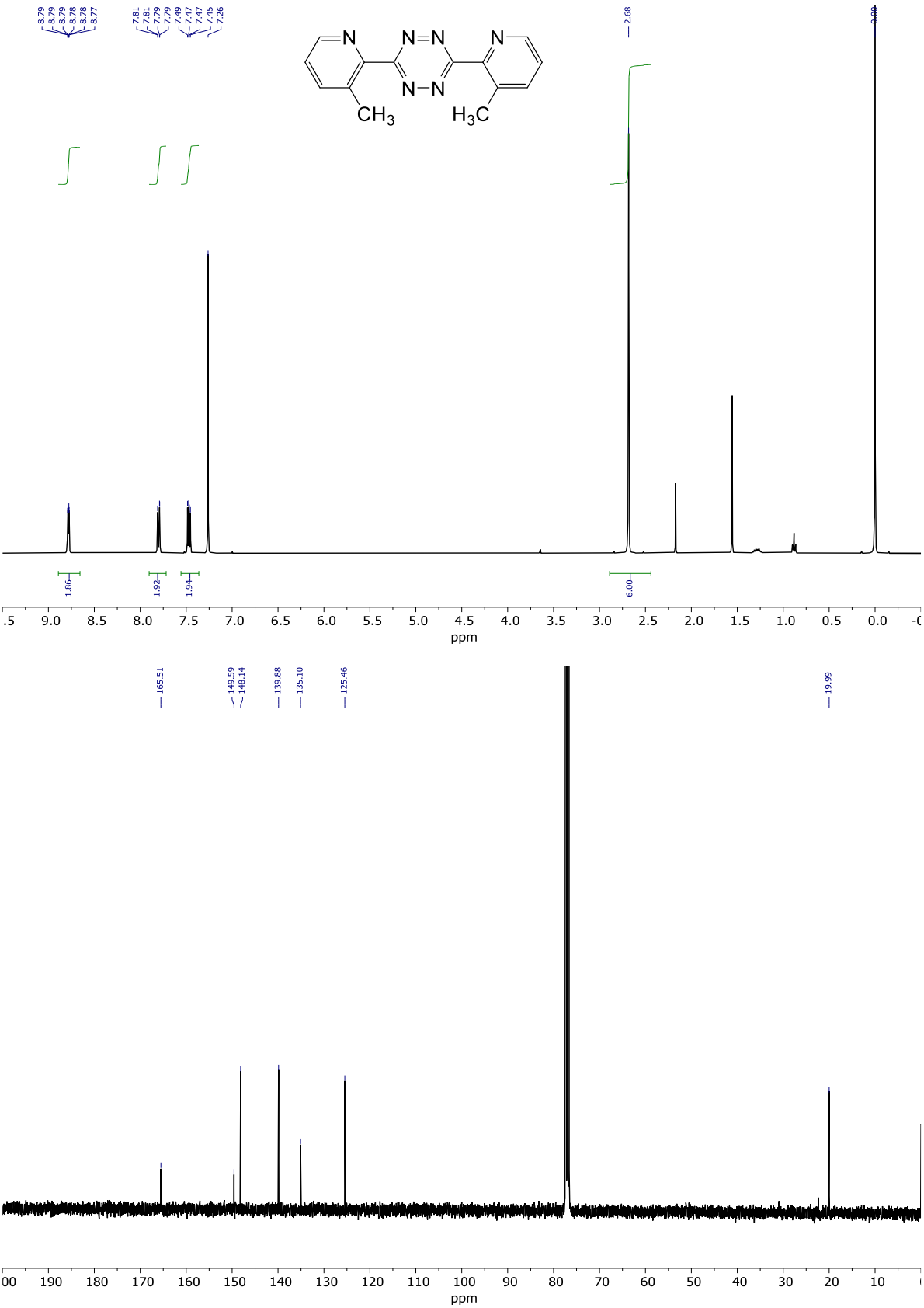

^{1}H (top) and ^{13}C (bottom) NMR spectra ($CDCl_3$) of 3,6-bis(3-methylpyridin-2-yl)-1,2,4,5-tetrazine (**2e**).

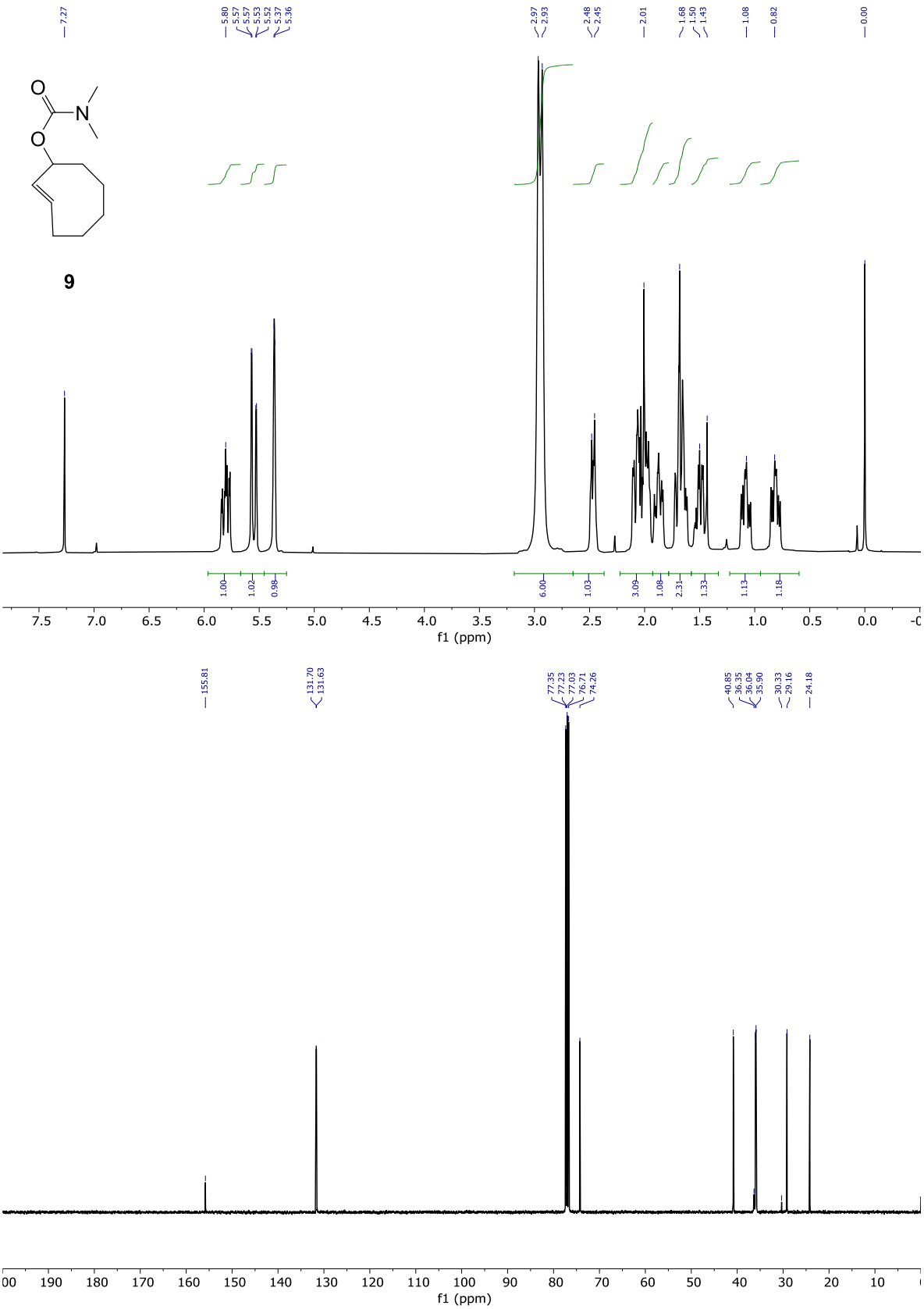

^{1}H (top) and ^{13}C (bottom) NMR spectra ($CDCl_3$) of (*E*)-cyclooct-2-en-1-yl dimethylcarbamate (axial isomer) (**9**).

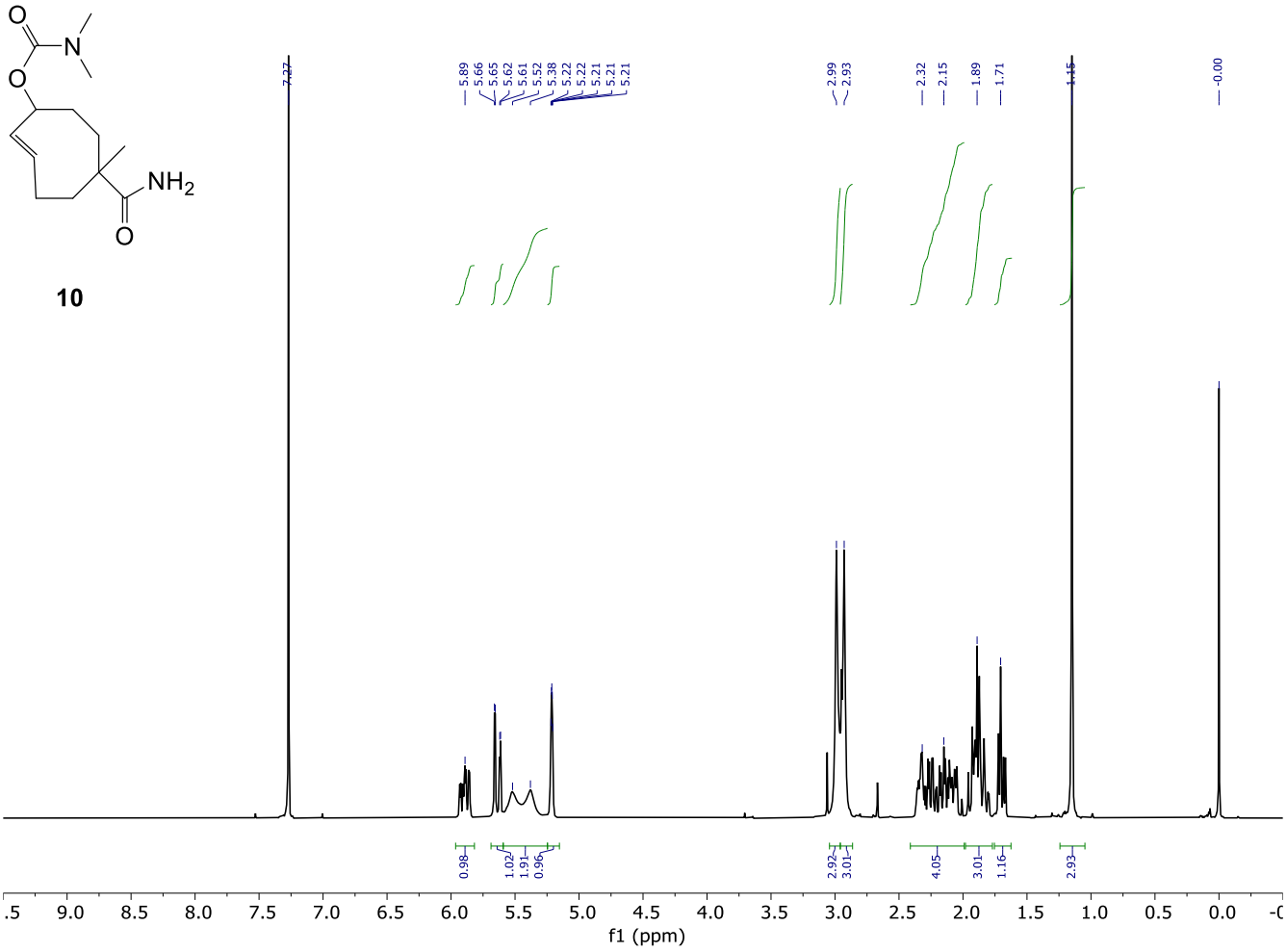

^{1}H-NMR spectrum ($CDCl_3$) of *rel*-(1*S*,6*S*,*E*,*pS*)-6-carbamoyl-6-methylcyclooct-2-en-1-yl dimethylcarbamate (**10**).

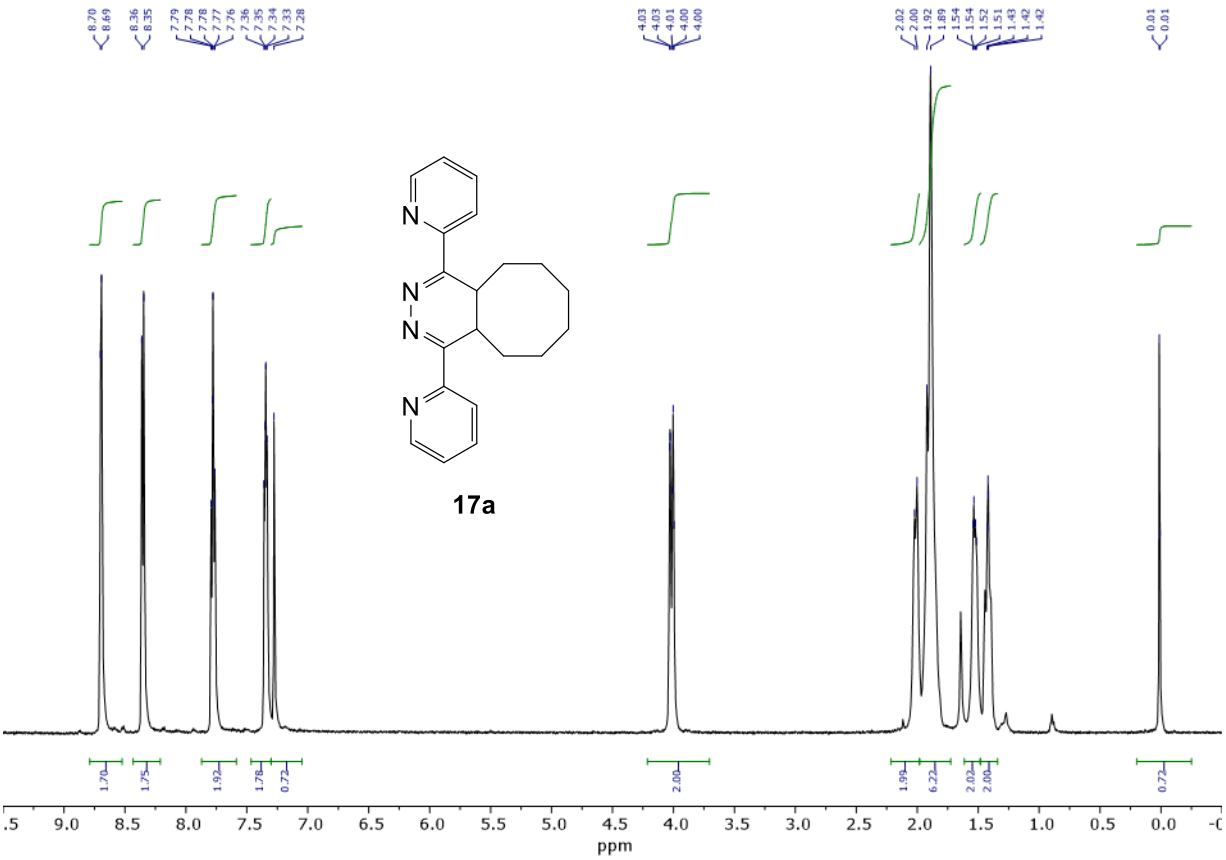

^{1}H-NMR spectrum ($CDCl_3$) of 4,5-tautomer **17a**.

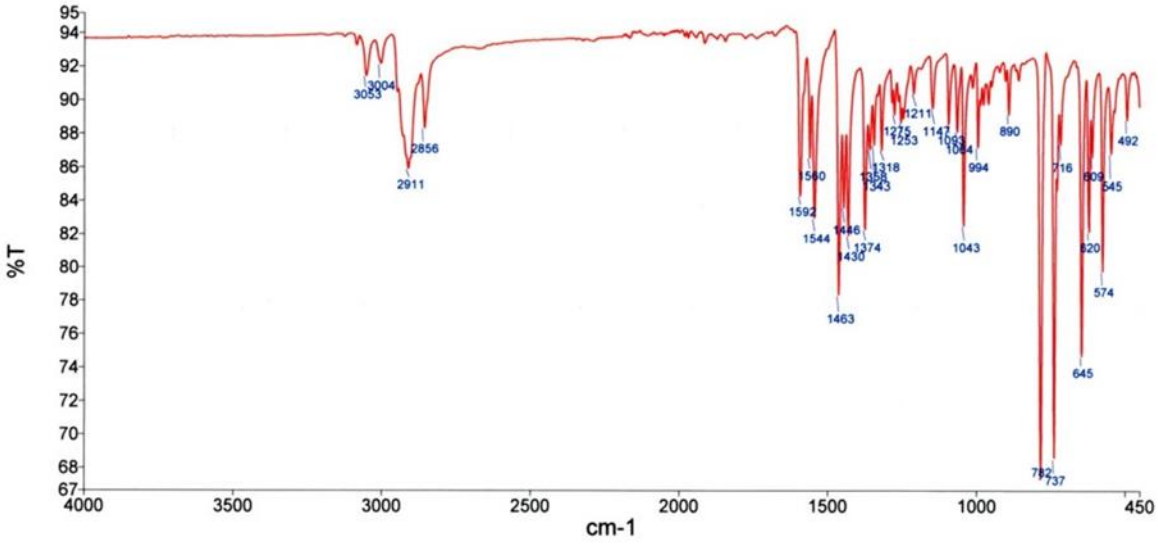

FT-IR spectrum of 4,5-tautomer **17a**, showing the absence of a NH stretch band around 3250 cm^{-1}.

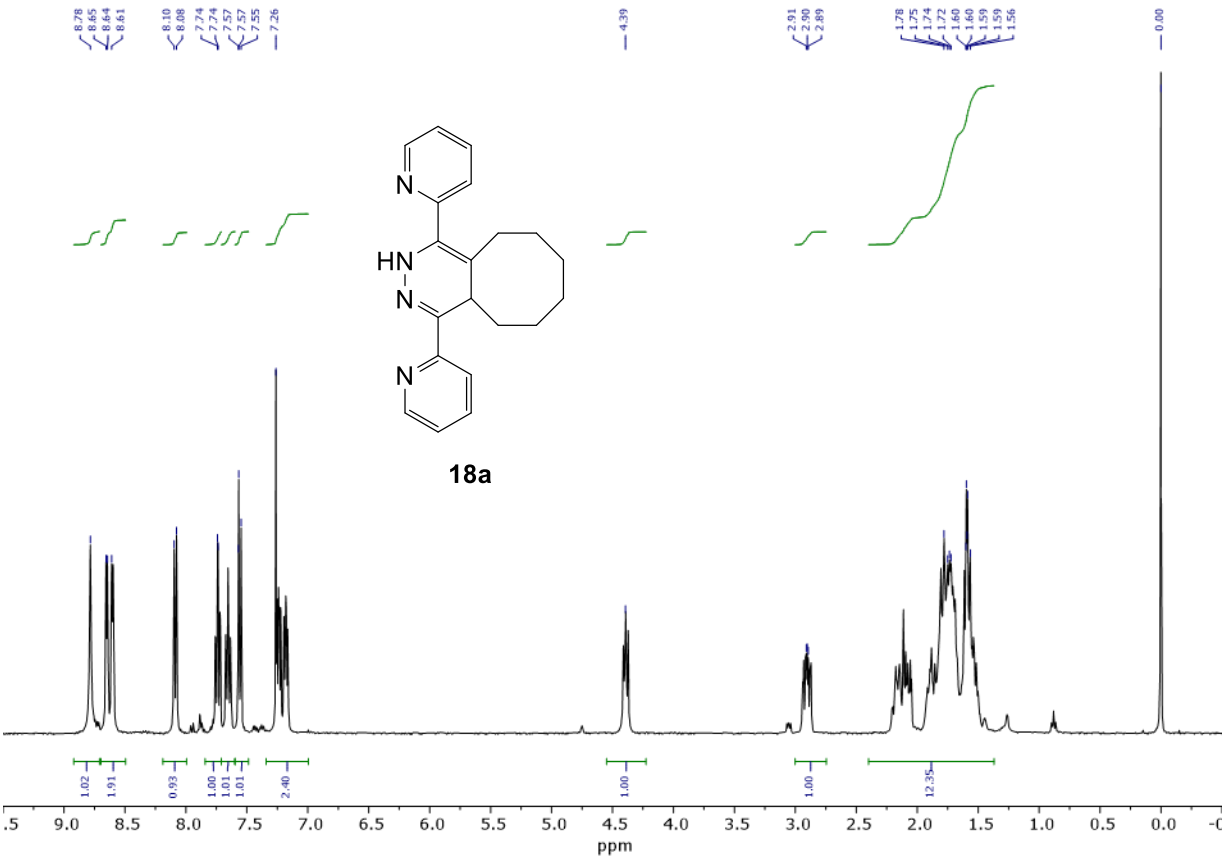

^{1}H-NMR spectrum ($CDCl_3$) of 1,4-tautomer **18a**.

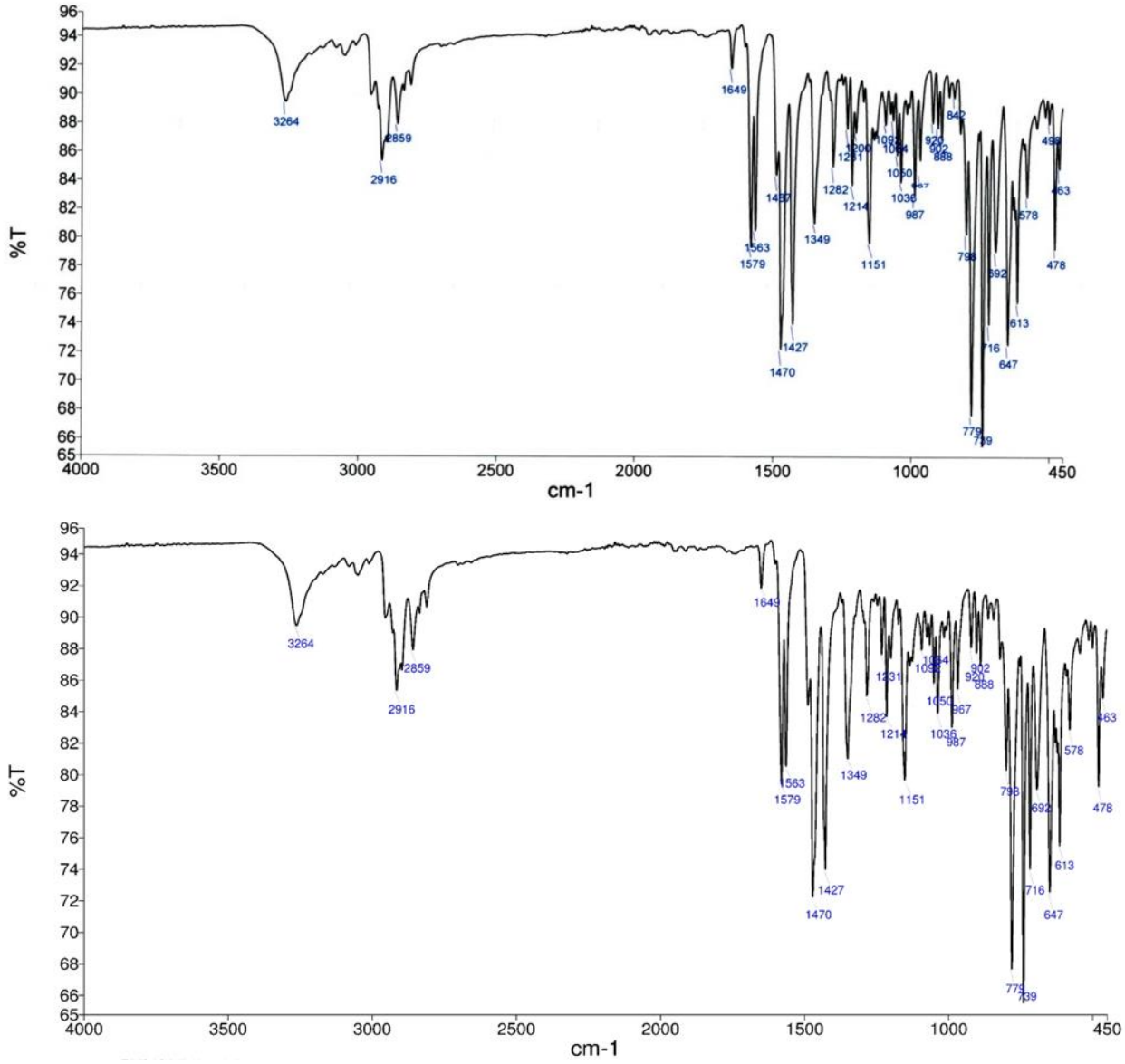

FT-IR (ATR) spectrum of 1,4-tautomer **18a**, showing the presence of a NH stretch band at 3264 cm^{-1}.

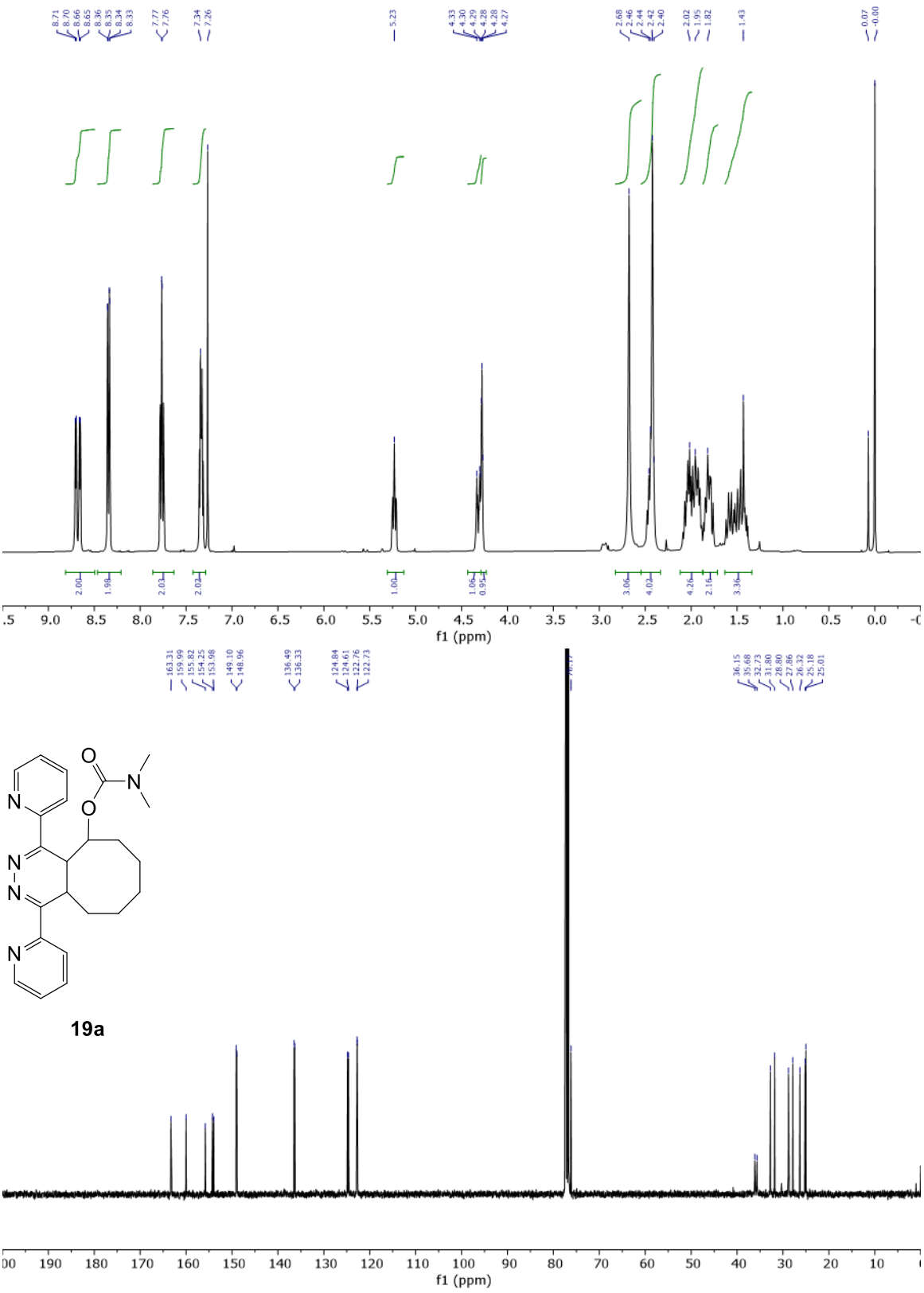

^{1}H (top) and ^{13}C (bottom) NMR spectra of the IEDDA-adduct of TCO **9** and 3,6-di(pyridin-2-yl)-1,2,4,5-tetrazine **2a** in $CDCl_3$, demonstrating the exclusive formation of the 4,5-tautomer **19a**.

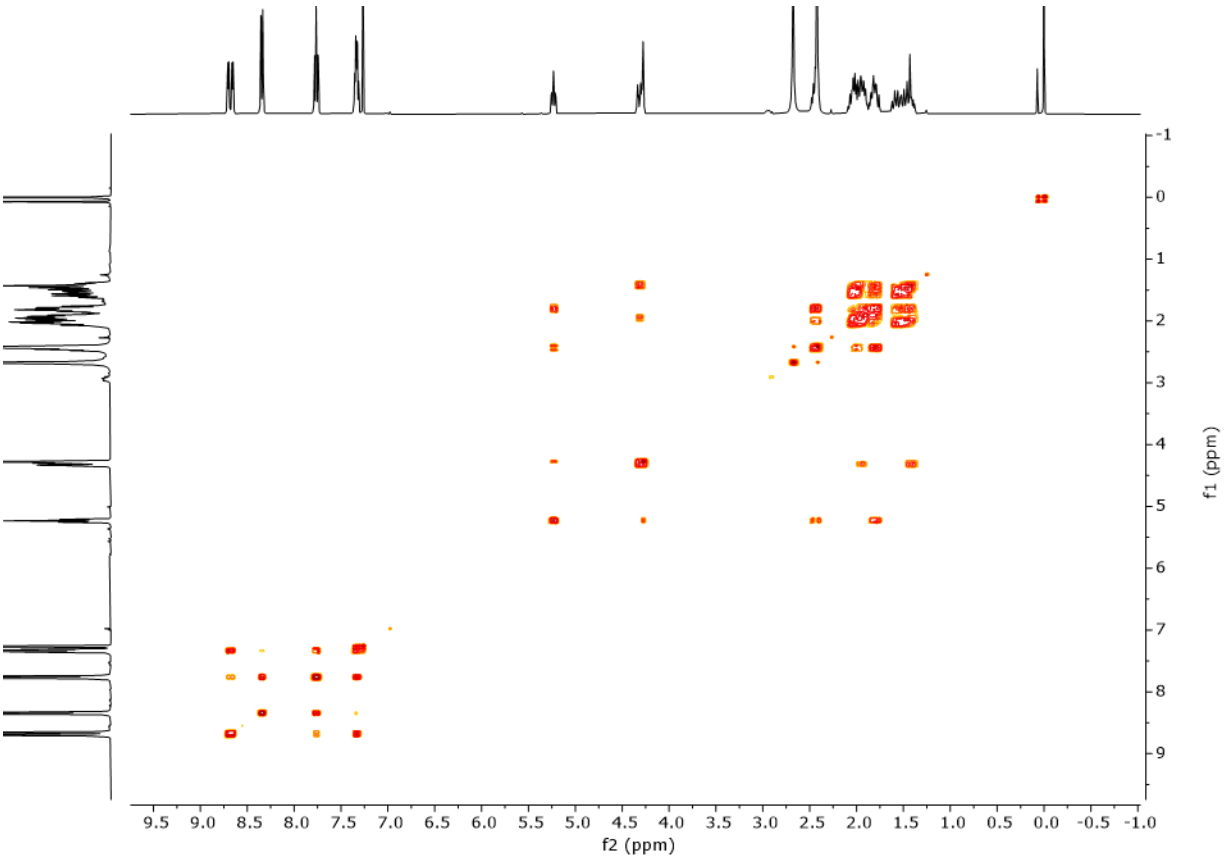

COSY NMR spectrum of **19a**, the IEDDA-adduct of TCO **9** and 3,6-di(pyridin-2-yl)-1,2,4,5-tetrazine **2a** in $CDCl_3$.

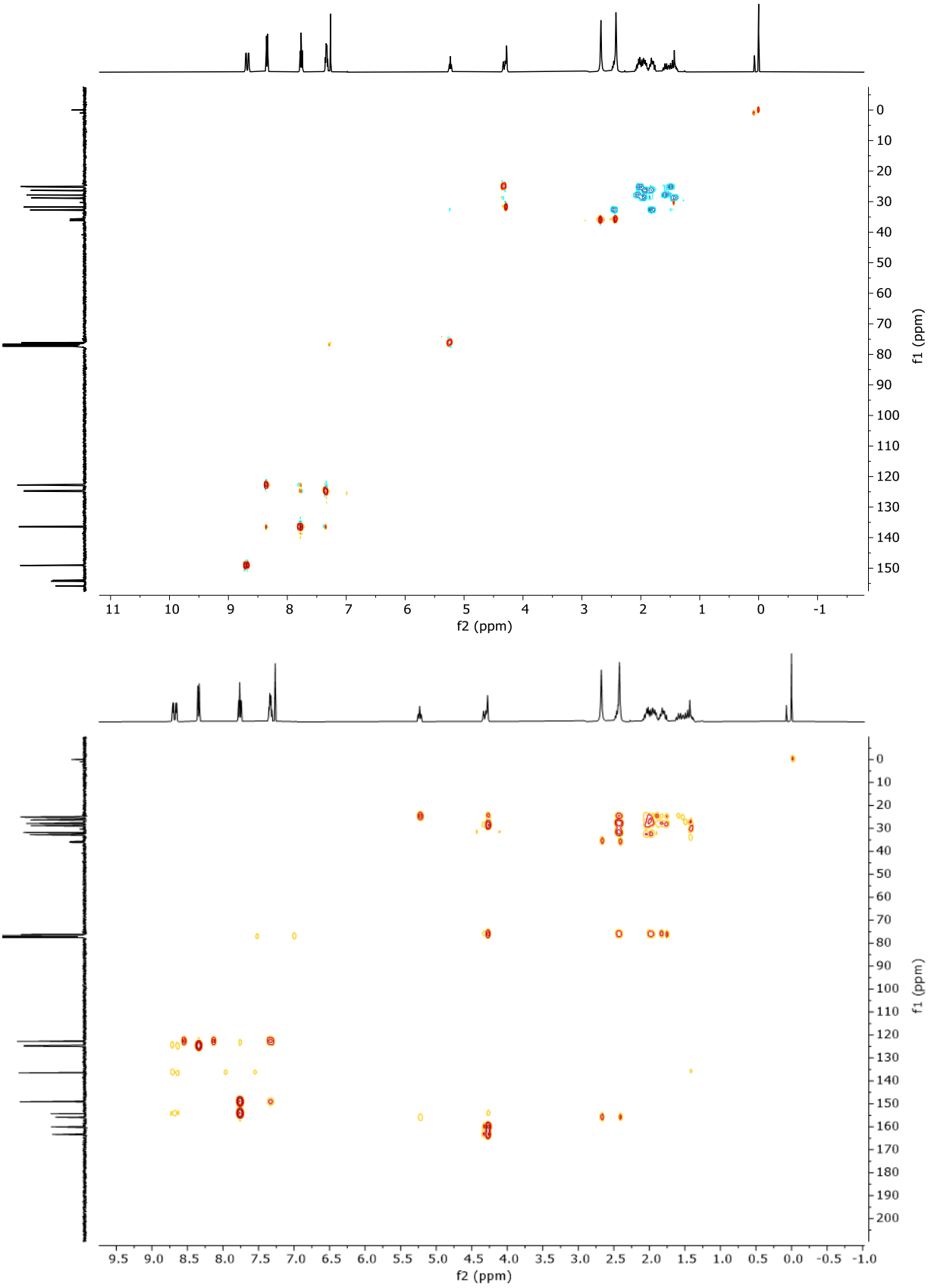

HSQC (top) and HMBC (bottom) NMR spectra of **19a**, the IEDDA-adduct of TCO **9** and 3,6-di(pyridin-2-yl)-1,2,4,5-tetrazine **2a** in $CDCl_3$.

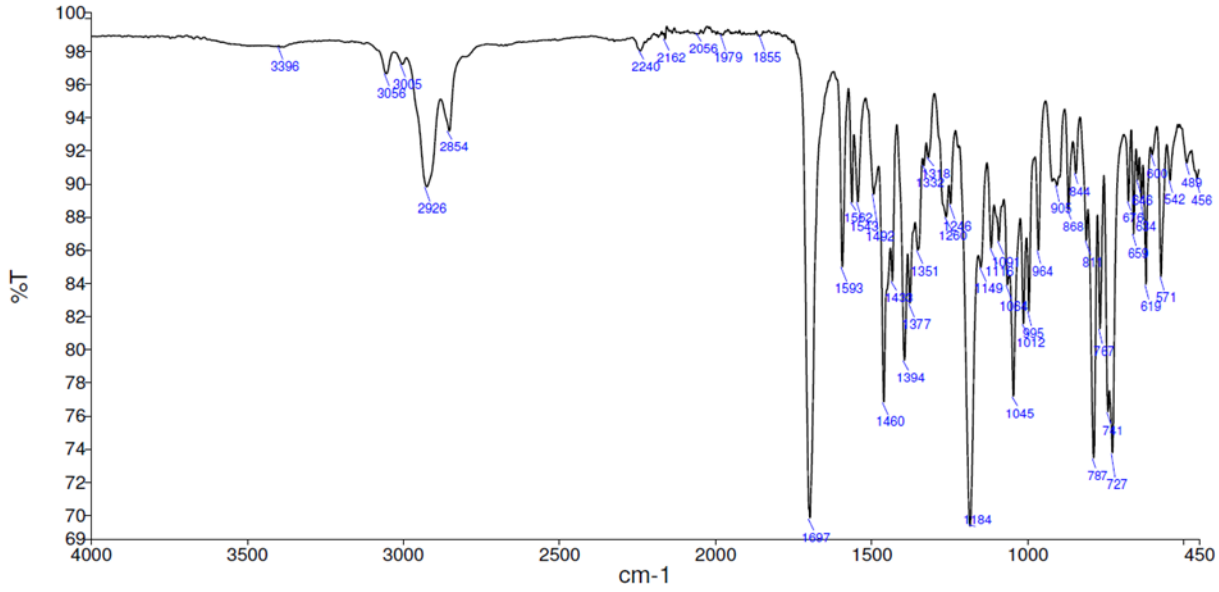

FT-IR (ATR) spectrum of **19a**, the IEDDA-adduct of TCO **9** and 3,6-di(pyridin-2-yl)-1,2,4,5-tetrazine **2a**, showing the absence of a NH stretch band around 3300 cm^{-1}.

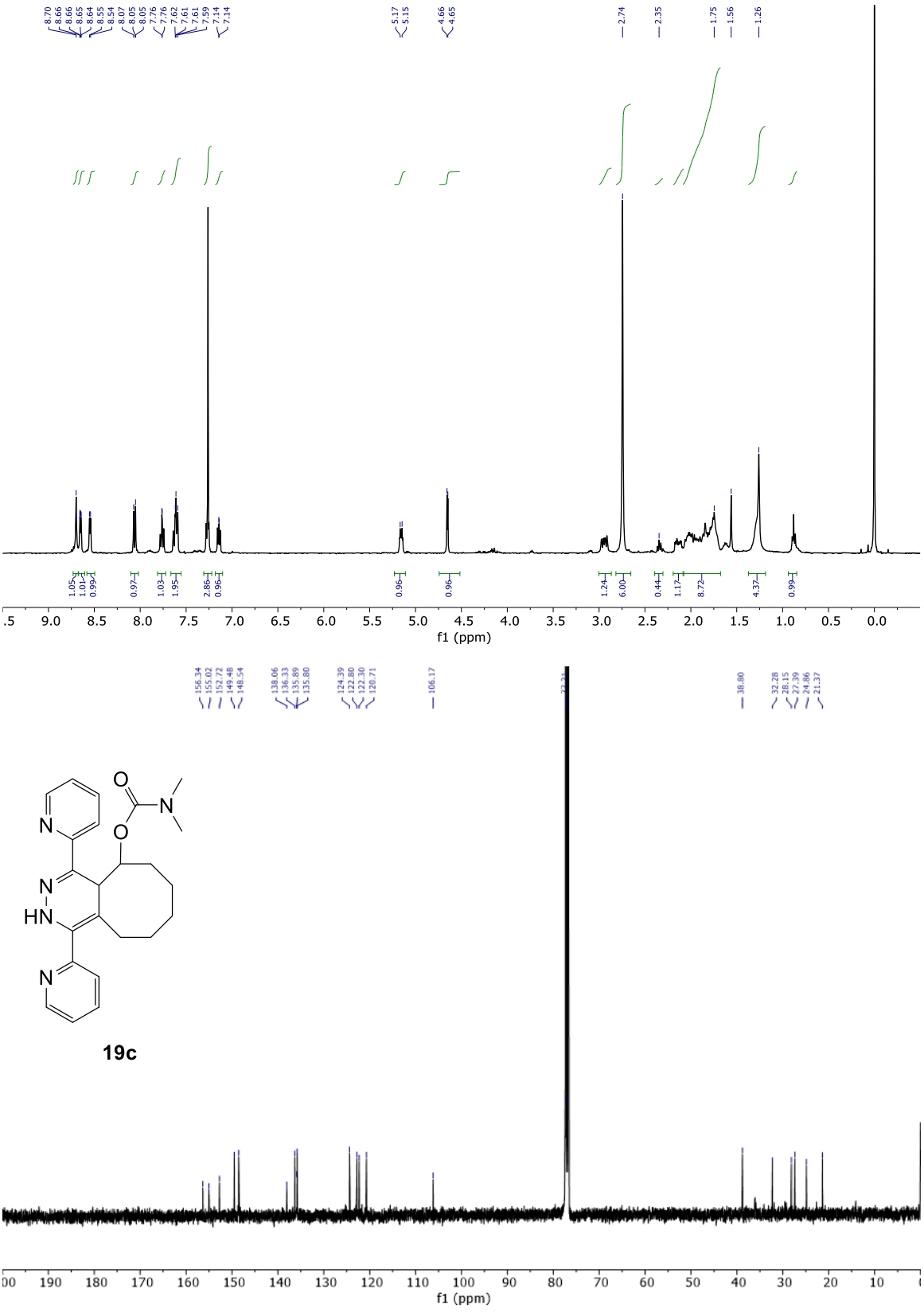

^{1}H (top) and ^{13}C (bottom) NMR spectra of 2,5-tautomer **19c** of the IEDDA-adduct of TCO **9** and 3,6-di(pyridin-2-yl)-1,2,4,5-tetrazine **2a** in $CDCl_3$.

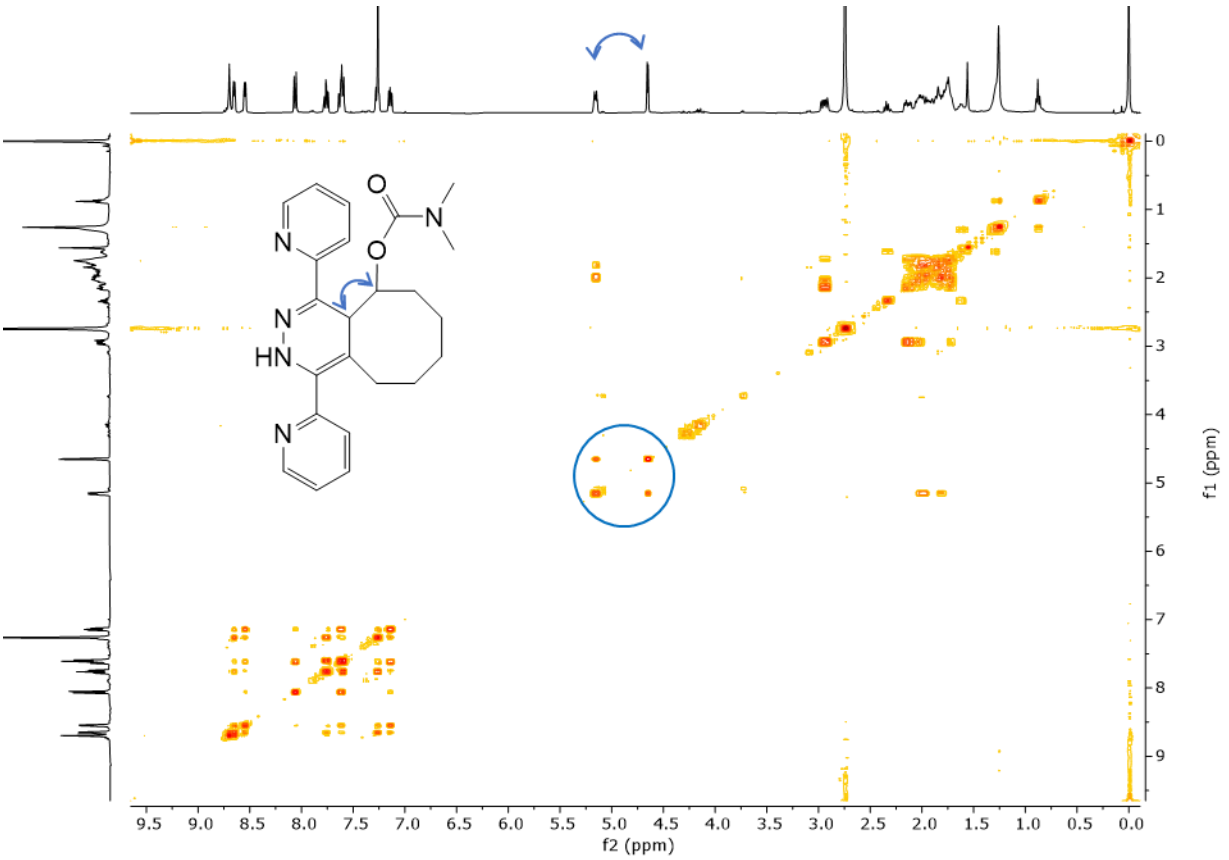

COSY NMR spectrum of 2,5-tautomer **19c** of the IEDDA-adduct of TCO **9** and 3,6-di(pyridin-2-yl)-1,2,4,5-tetrazine **2a** in $CDCl_3$, showing the cross peak between CHO (5.16 ppm) and H5 (4.65 ppm).

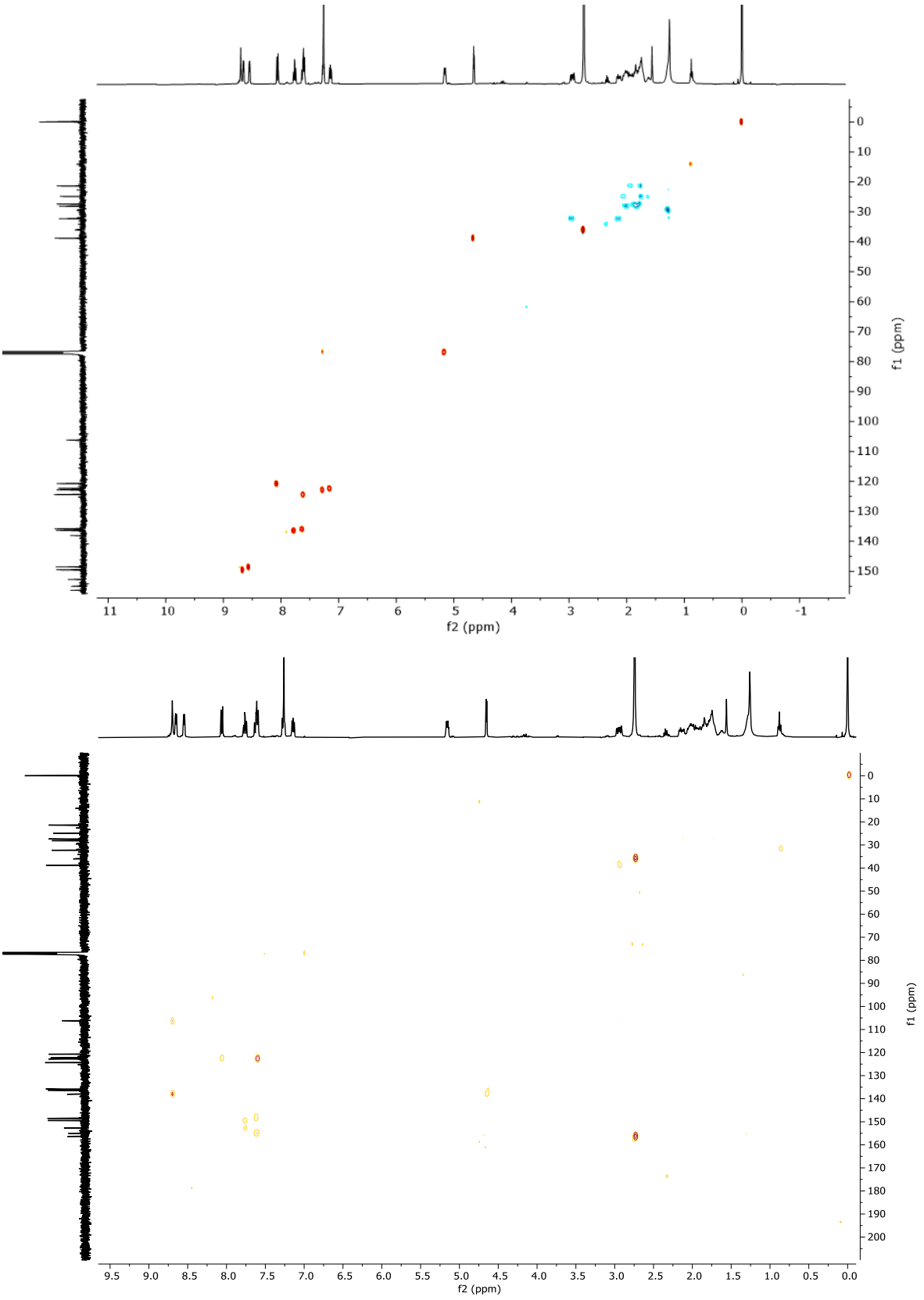

HSQC (top) and HMBC (bottom) NMR spectra of 2,5-tautomer **19c** of the IEDDA-adduct of TCO **9** and 3,6-di(pyridin-2-yl)-1,2,4,5-tetrazine **2a** in $CDCl_3$.

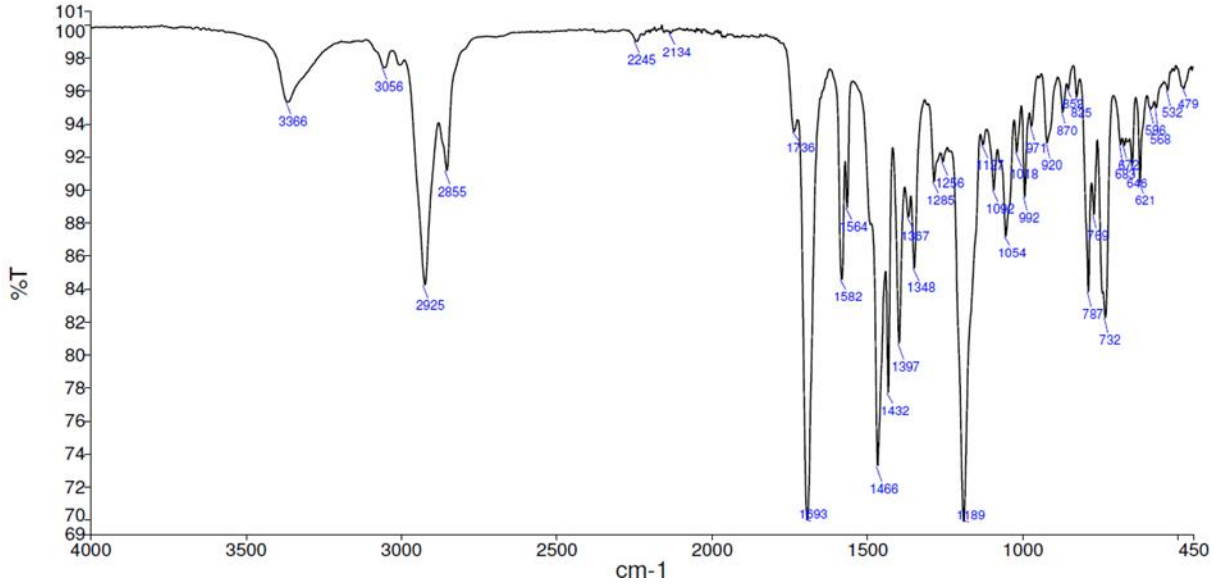

FT-IR (ATR) spectrum of 2,5-tautomer **19c** of the IEDDA-adduct of TCO **9** and 3,6-di(pyridin-2-yl)-1,2,4,5-tetrazine **2a**, showing the presence of a NH stretch band at 3366 cm^{-1}.

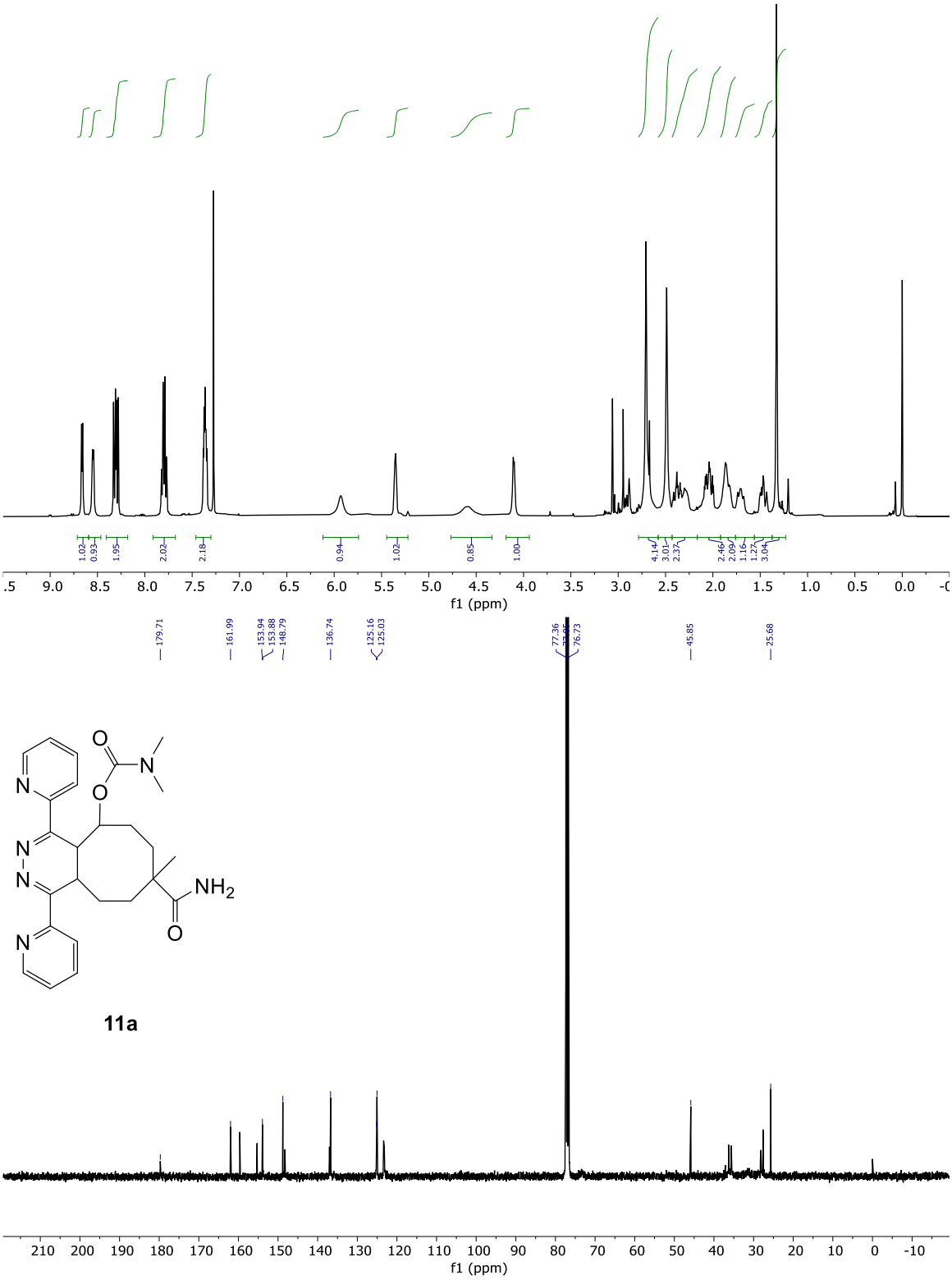

^{1}H (top) and ^{13}C (bottom) NMR spectra of the IEDDA-adduct of TCO **10** and 3,6-di(pyridin-2-yl)-1,2,4,5-tetrazine **2a** in $CDCl_3$ after 5 h, demonstrating the exclusive formation of the 4,5-tautomer **11a**.

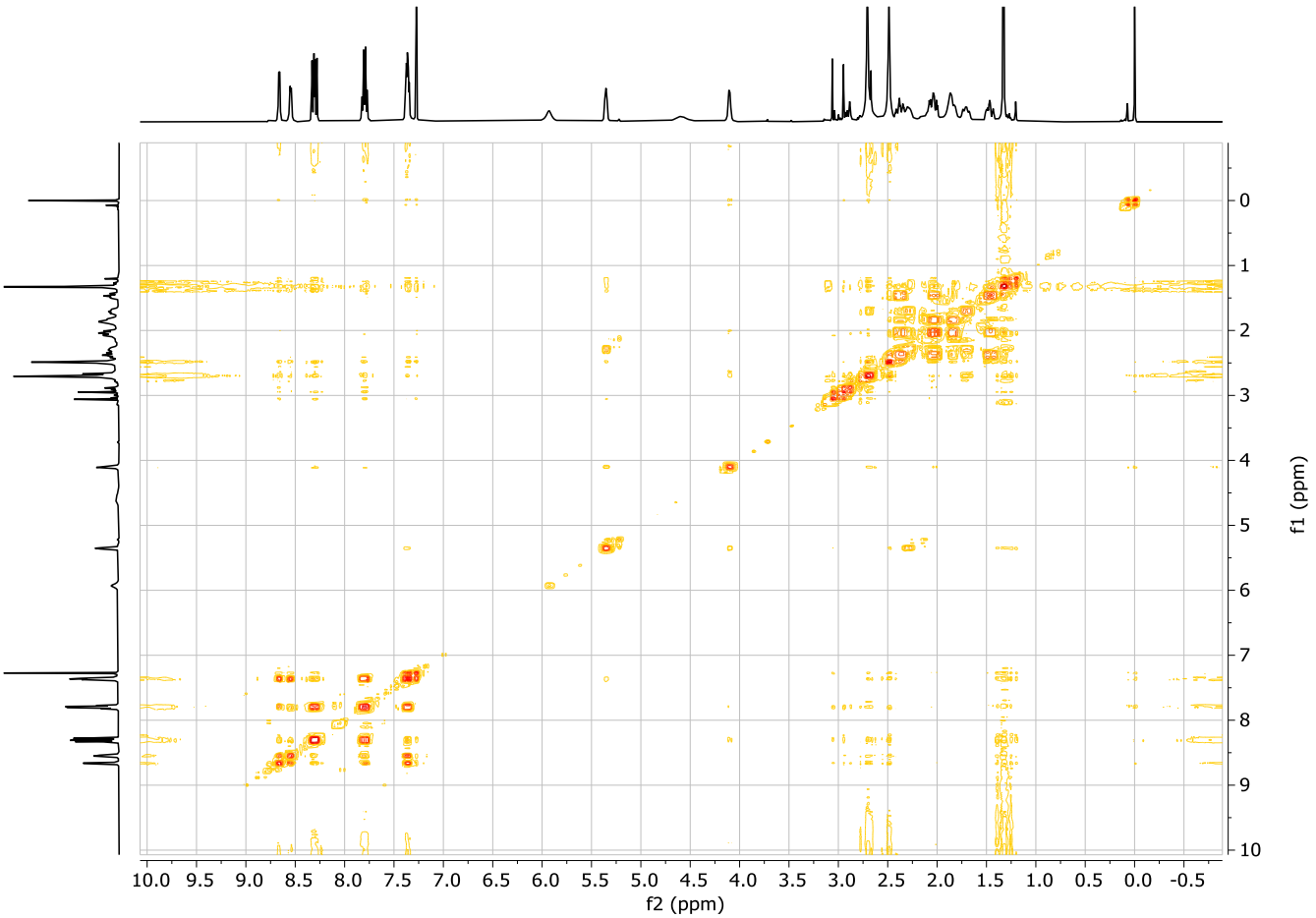

COSY-NMR spectrum of the IEDDA-adduct of TCO **10** and 3,6-di(pyridin-2-yl)-1,2,4,5-tetrazine **2a** in $CDCl_3$ after 10 min, indicating the cross-coupling between H5 and C<u>H</u>O in 4,5-tautomer **11a**.

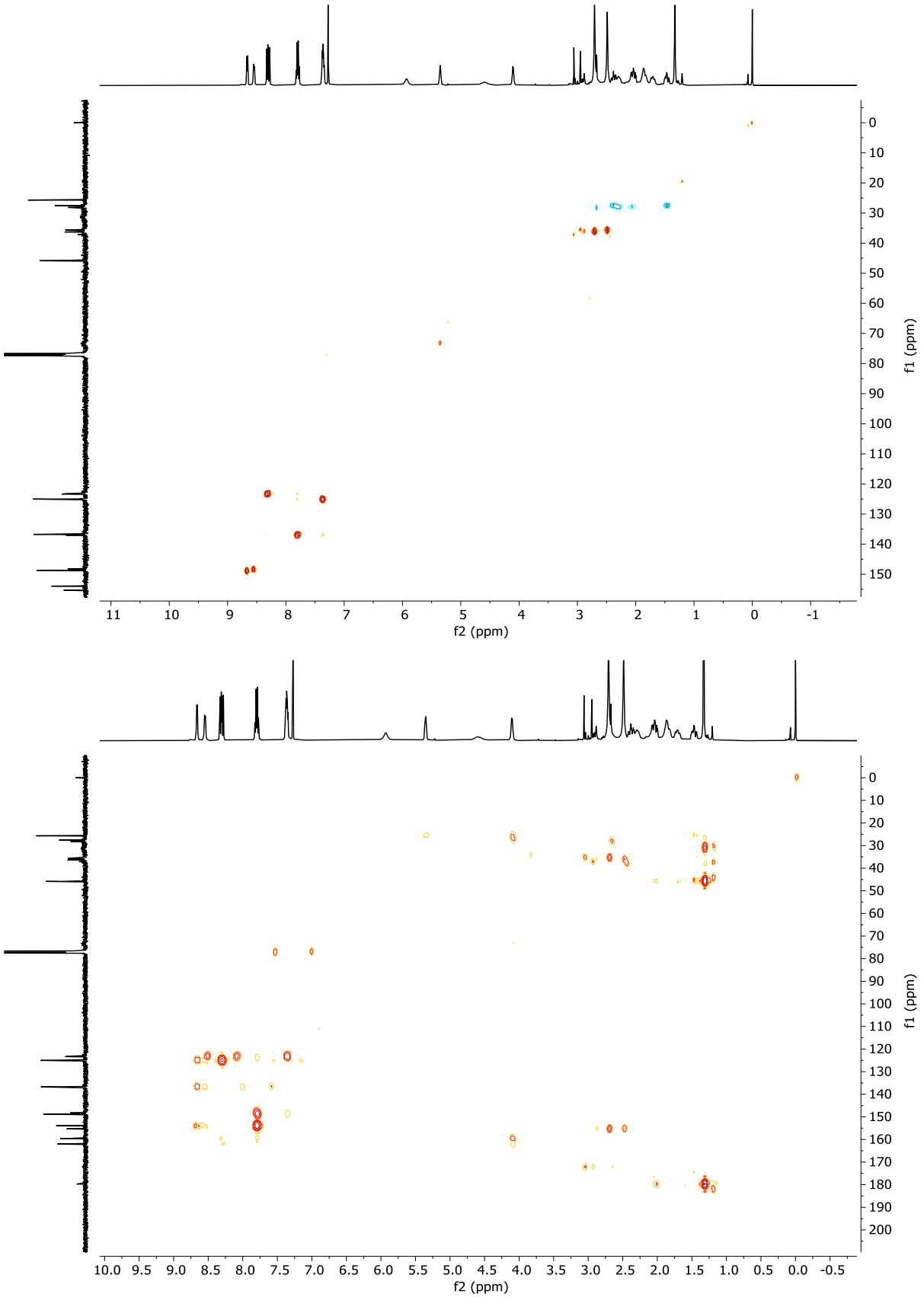

HSQC (top) and HMBC (bottom) NMR spectra of the IEDDA-adduct **11a** of TCO **10** and 3,6-di(pyridin-2-yl)-1,2,4,5-tetrazine **2a** in $CDCl_3$ after 10 h.

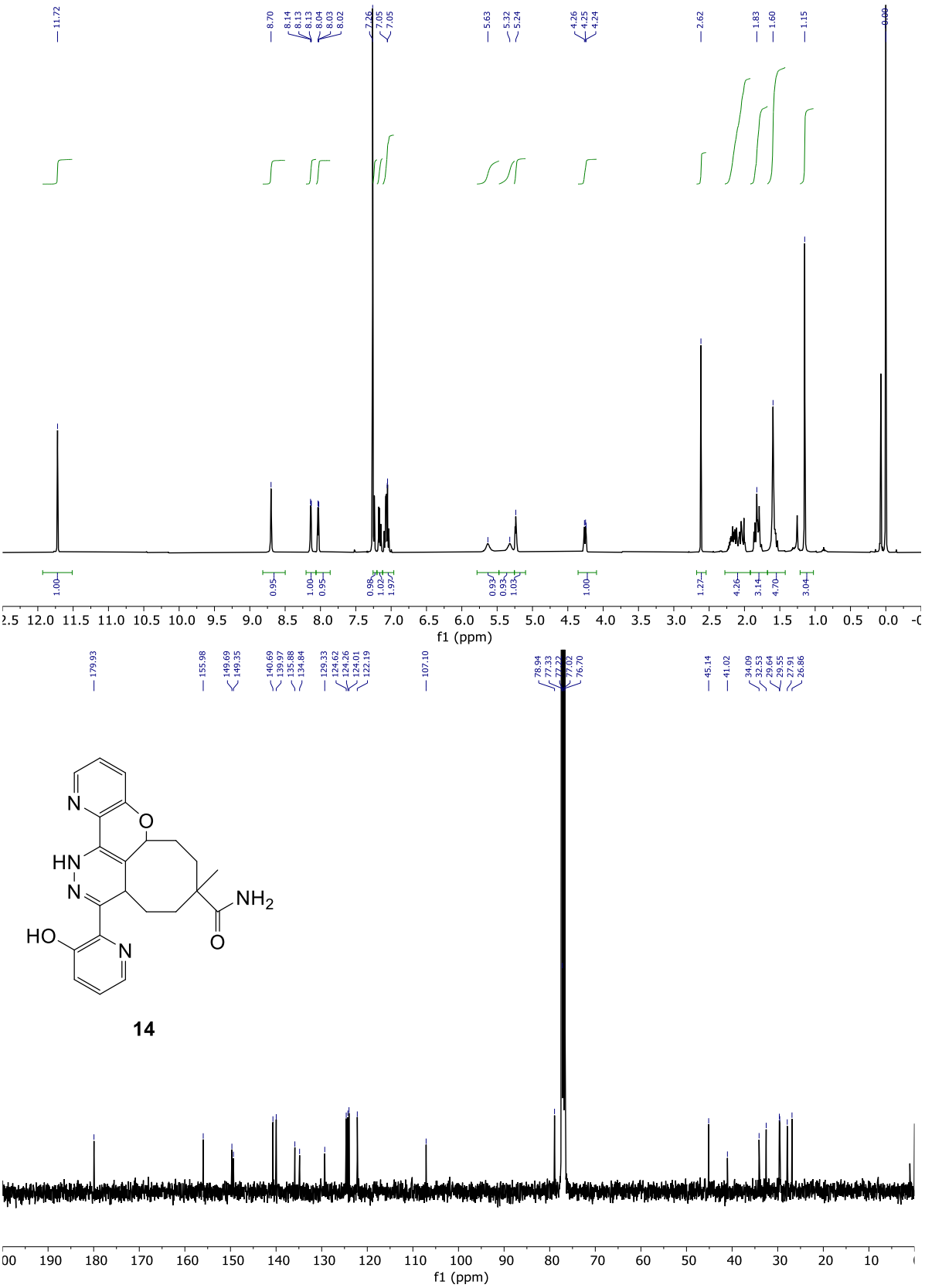

14

^{1}H-NMR spectrum (top) and ^{13}C-NMR spectrum (bottom) (in $CDCl_3$) of elimination product **14**. Singlet at 2.62 ppm (^{1}H) and 41.0 ppm (^{13}C) originate from residual DMSO.

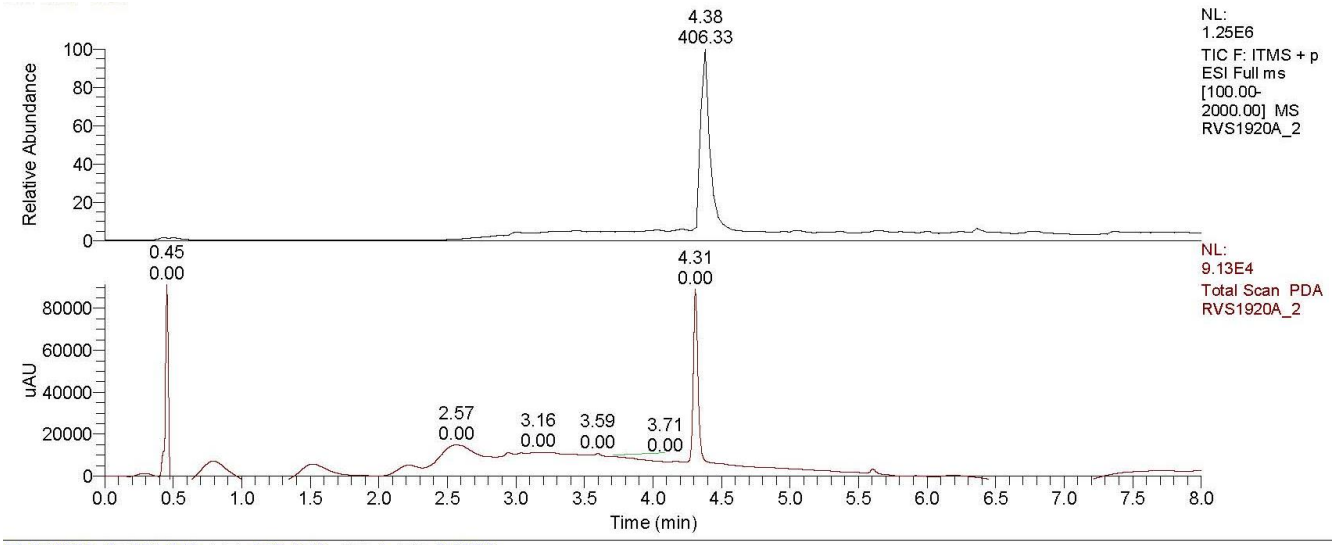

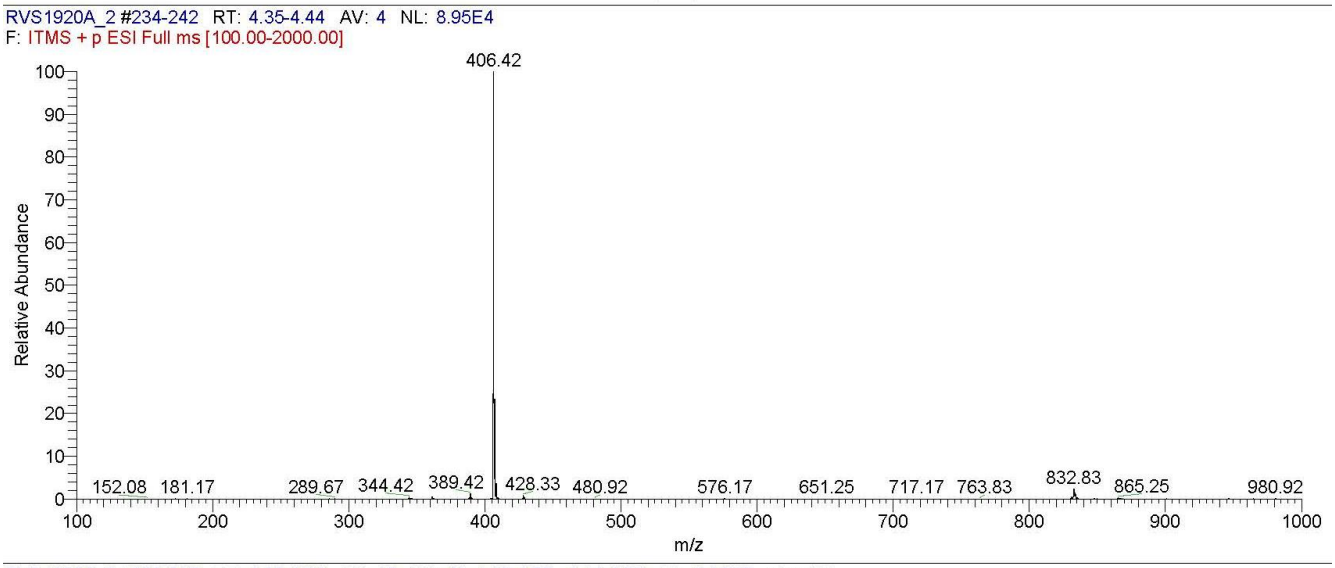

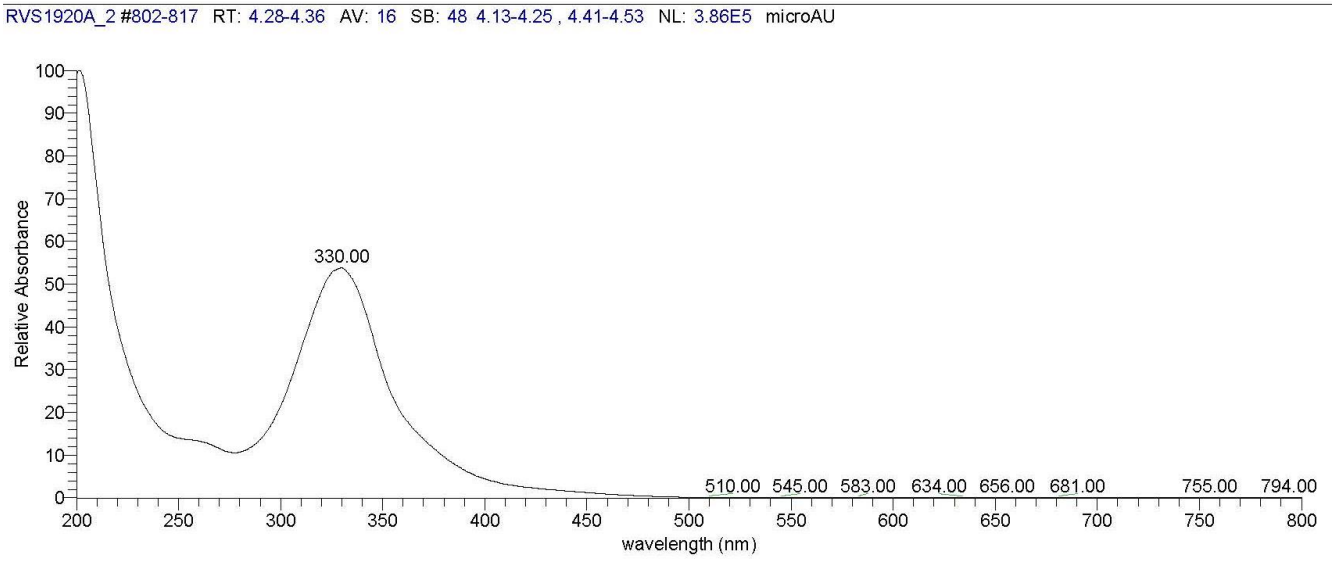

HPLC-MS/PDA analysis of elimination product **14** (MW=405)

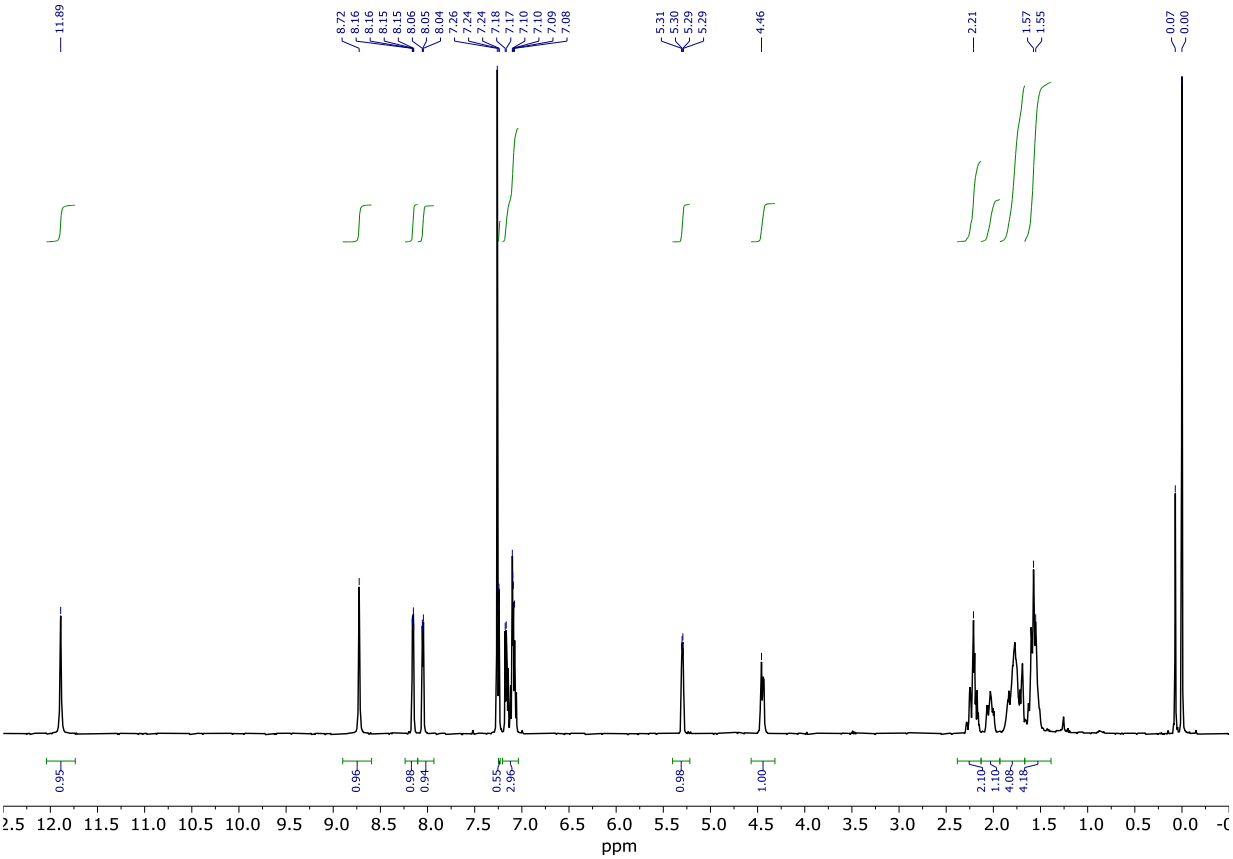

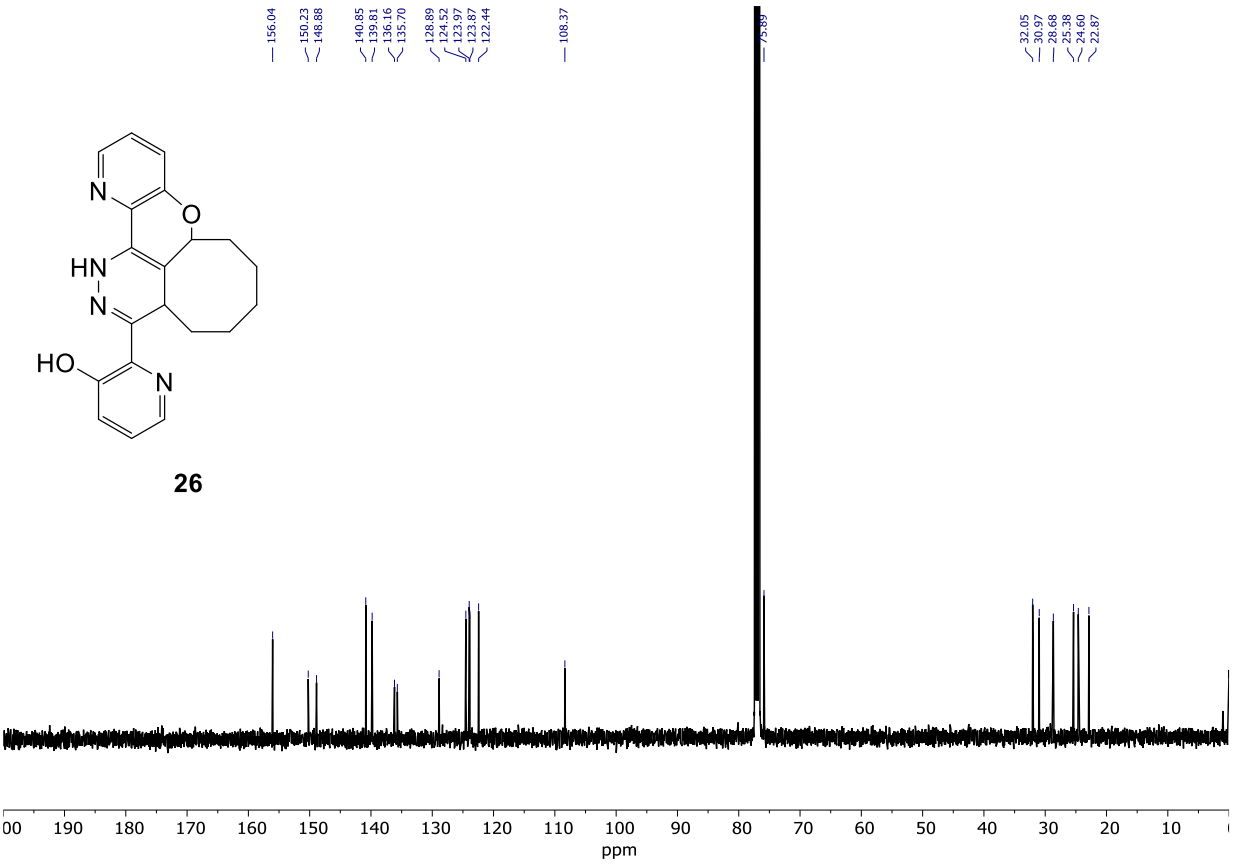

26

^{1}H-NMR spectrum (top) and ^{13}C-NMR spectrum (bottom) (in $CDCl_3$) of elimination product **26**.

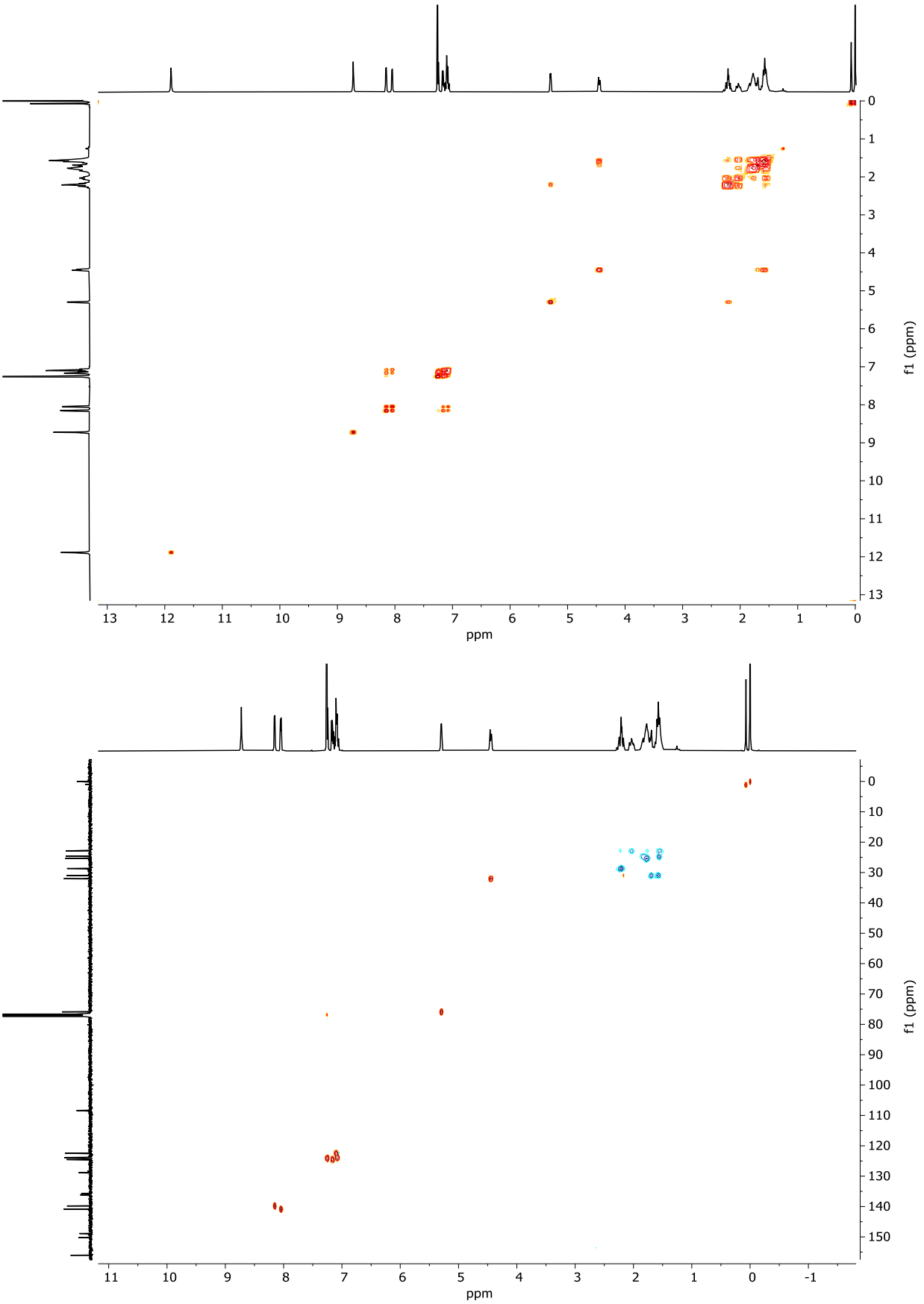

COSY (top) and HSQC (bottom) spectra (in $CDCl_3$) of elimination product **26**.

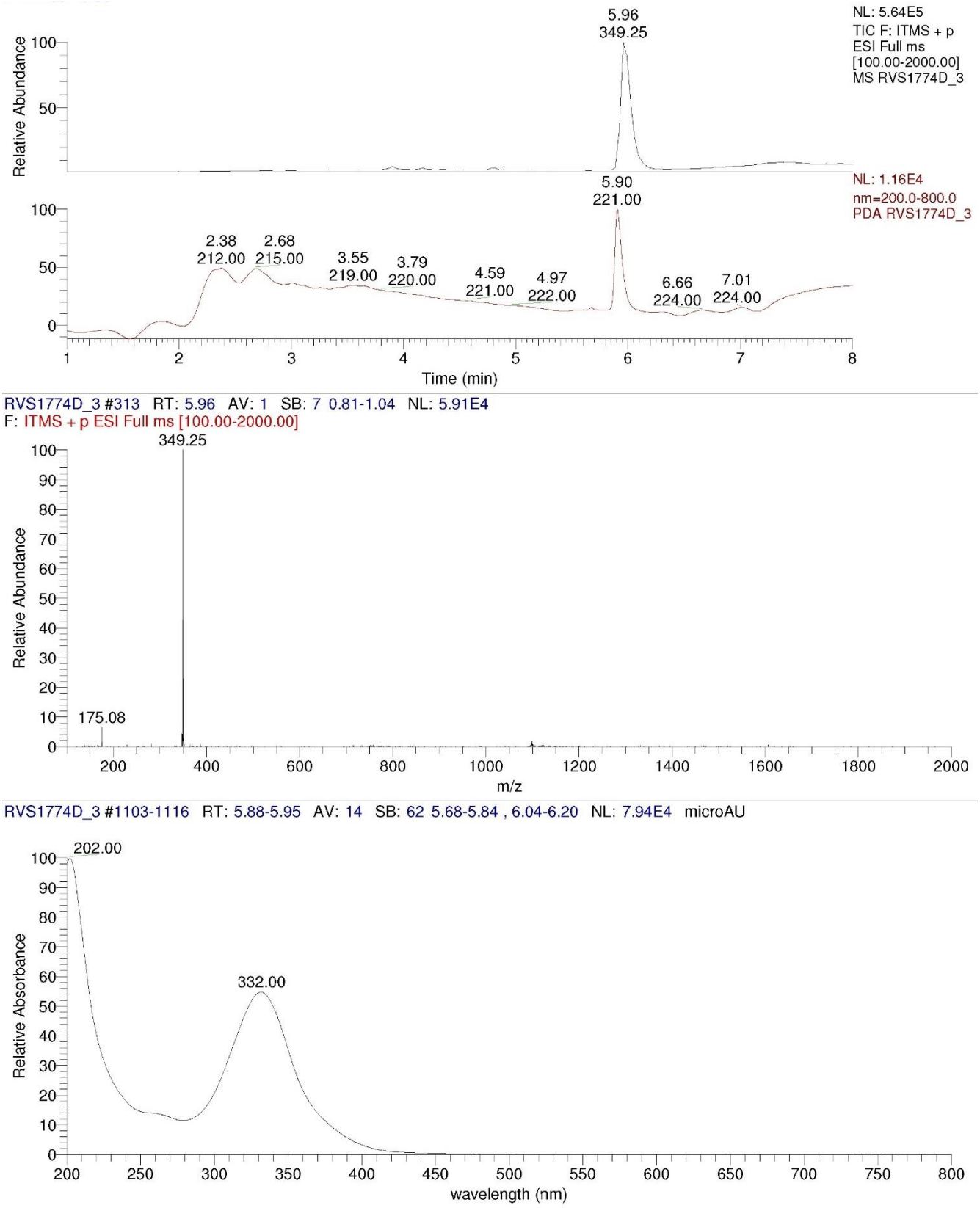

HPLC-MS/PDA analysis of elimination product **26** (MW=348)

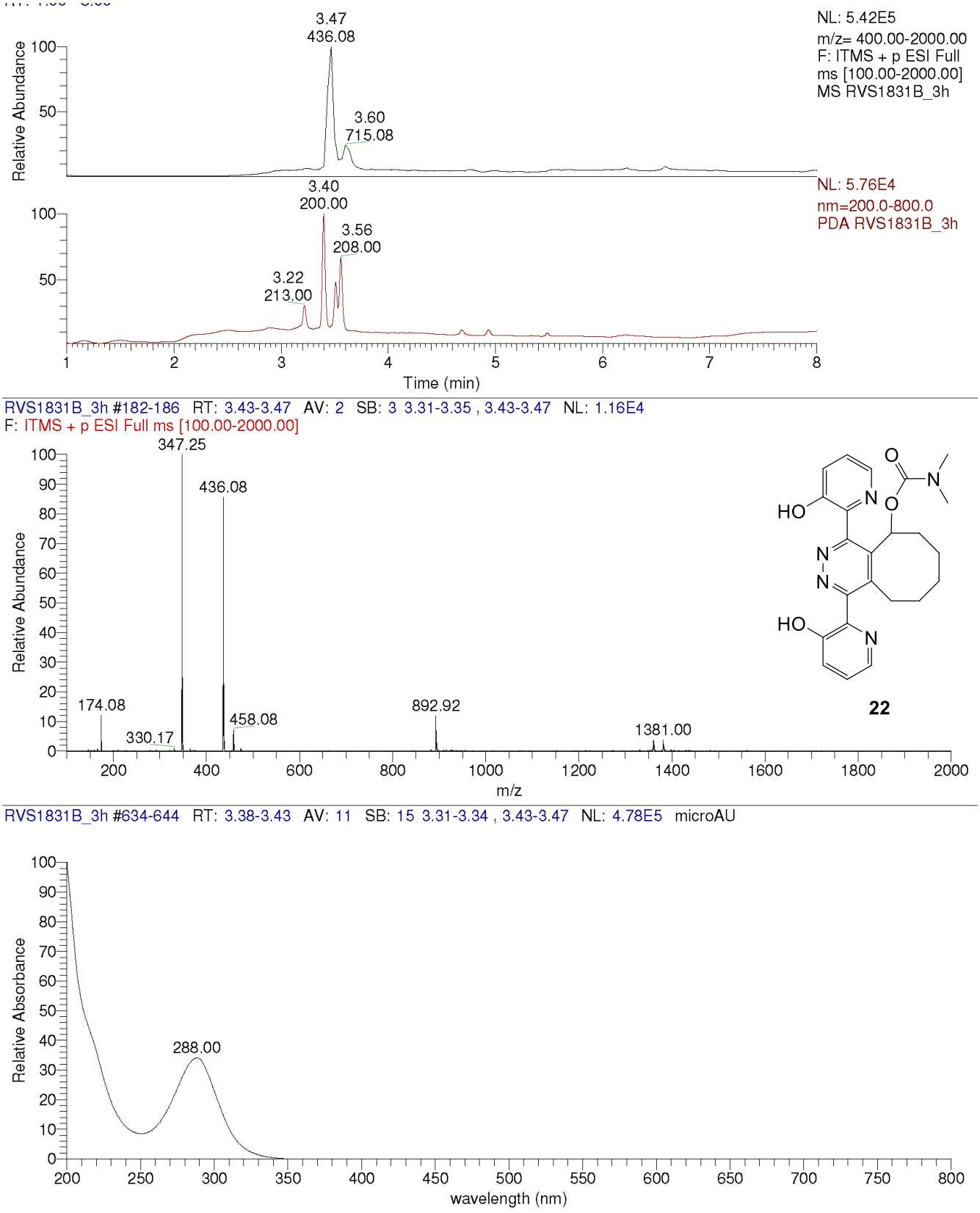

HPLC-MS/PDA analysis of the reaction mixture of TCO **9** and tetrazine **2b** in 30/70 ACN/water with $NaNO_2$ after 3 h, demonstrating the formation of oxidized IEDDA adduct **22** at 3.4 min (MW=435).

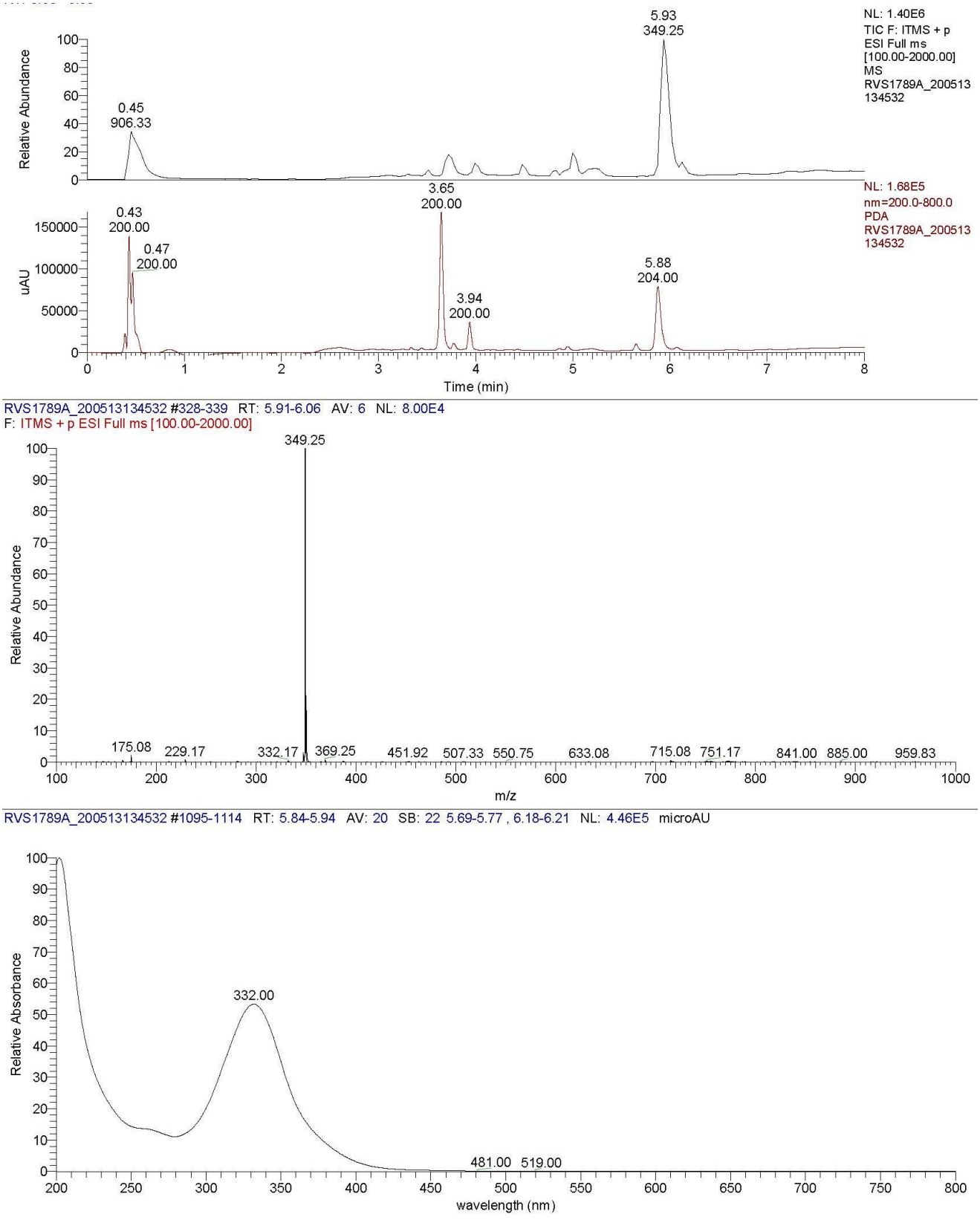

HPLC-MS/PDA analysis of the reaction mixture of ether-linked TCO **23** and tetrazine **2b** in 30/70 ACN/PBS, demonstrating the formation of elimination product **26** at 5.9 min (MW=348). Peaks at 3.65 and 3.94 min originate from excess tetrazine, and hydrolyzed tetrazine, respectively.

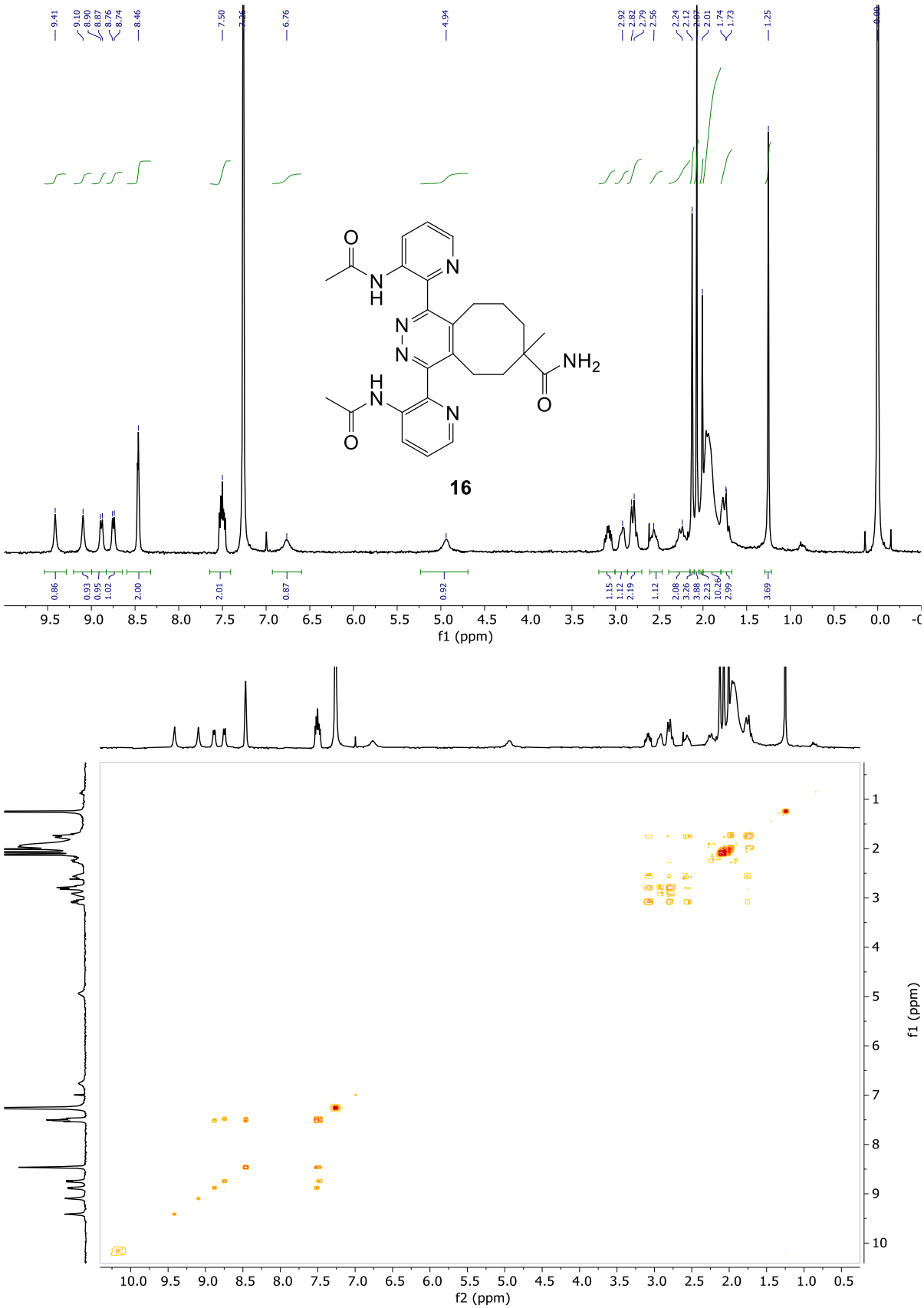

^{1}H (top) and COSY (bottom) NMR spectra (in $CDCl_3$) of elimination product **16**.

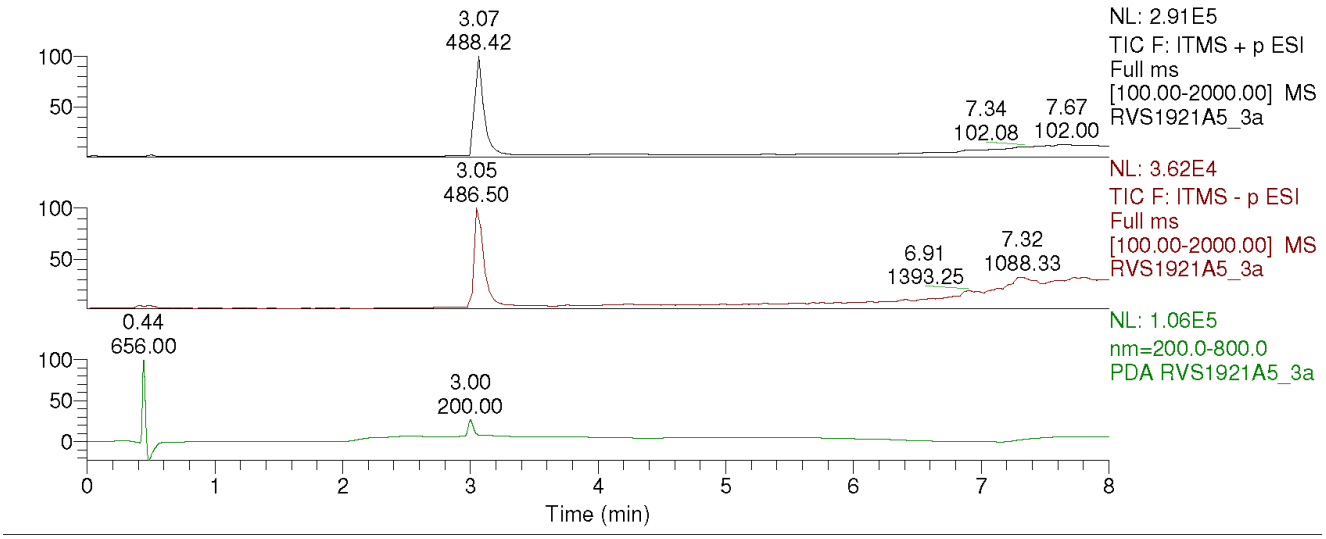

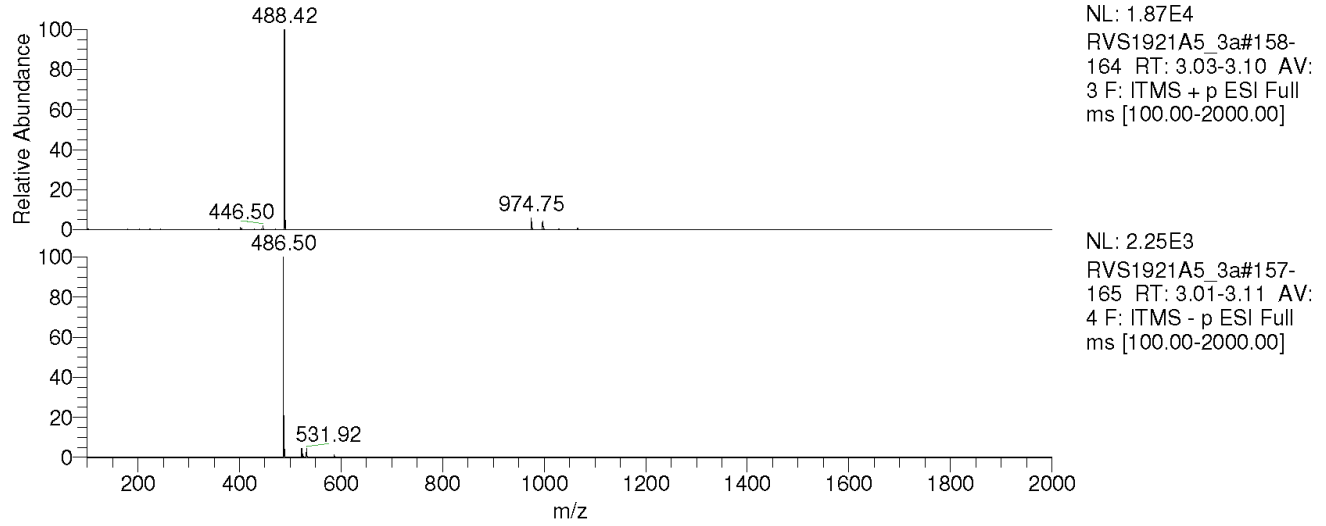

RVS1921A5_3a #555-571 RT: 2.96-3.05 AV: 17 SB: 73 2.85-2.94 , 3.06-3.34 NL: 1.78E5 microAU

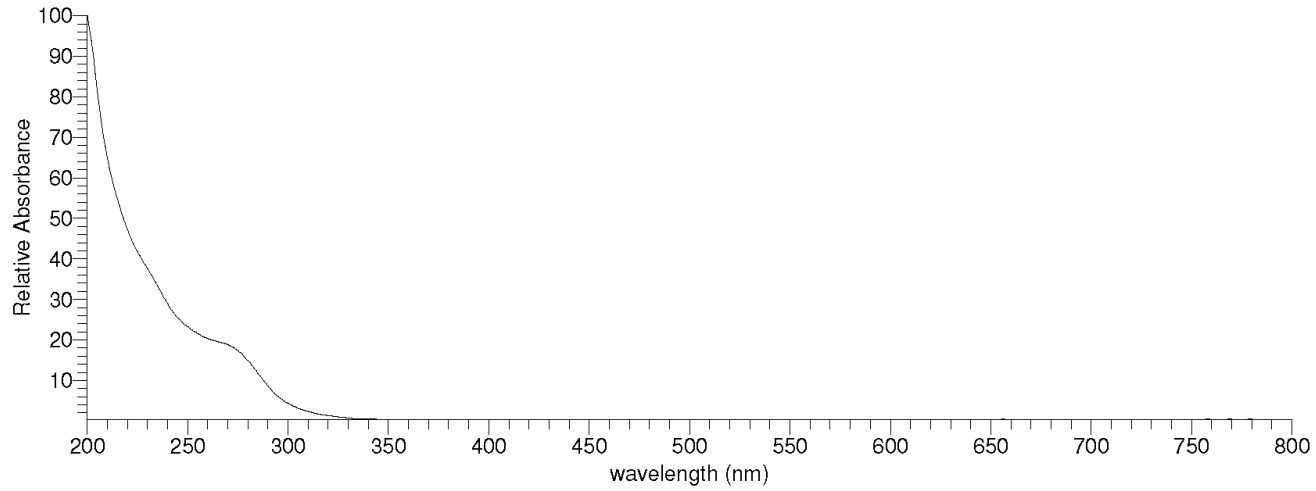

HPLC-MS/PDA analysis of elimination product **16** (MW=487)

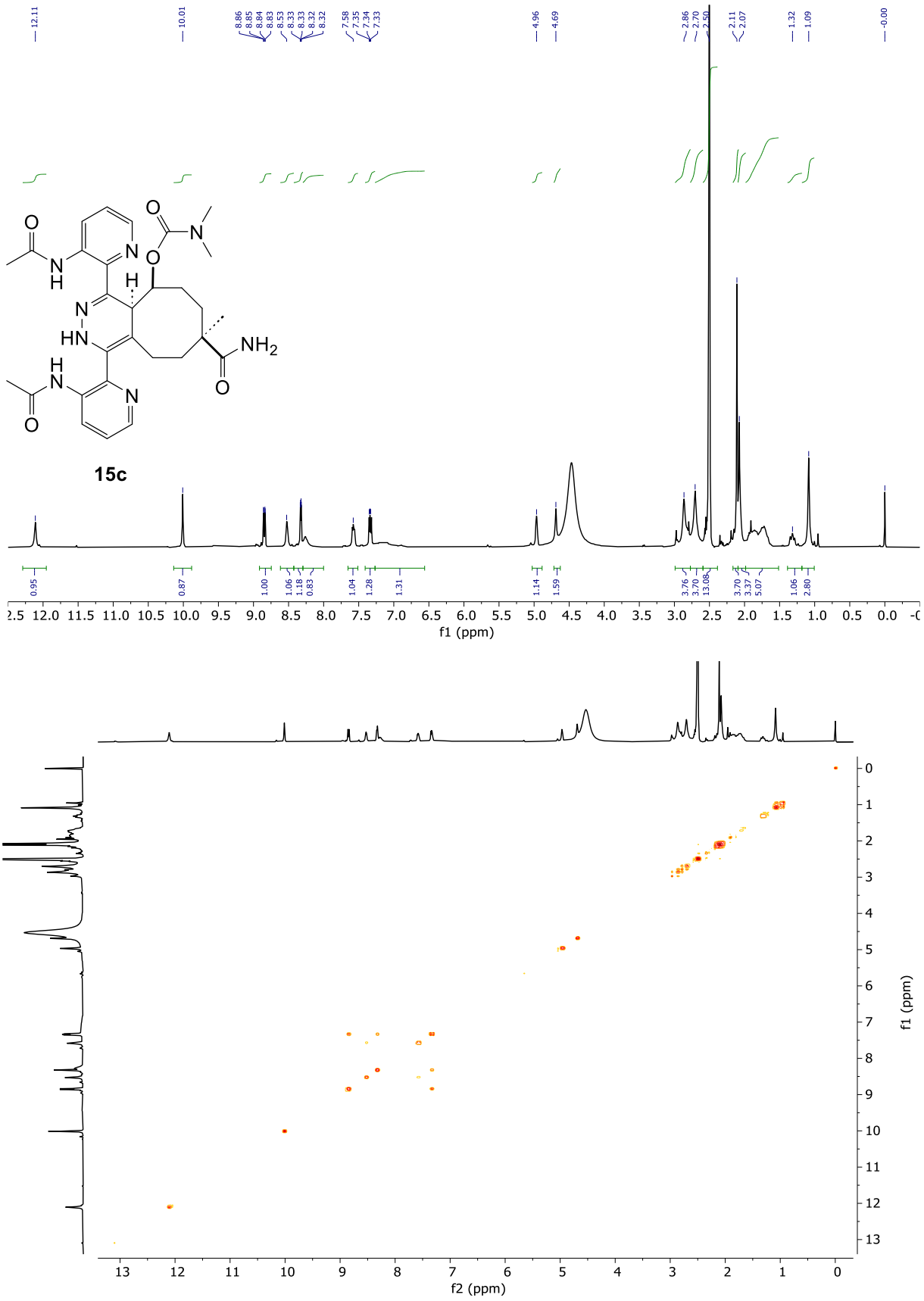

^{1}H (top) and COSY (bottom) NMR spectra (in DMSO-d_6) of non-releasing 2,5-tautomer **15c**, showing the cross peak between CHO (4.96 ppm) and H5 (4.66 ppm).

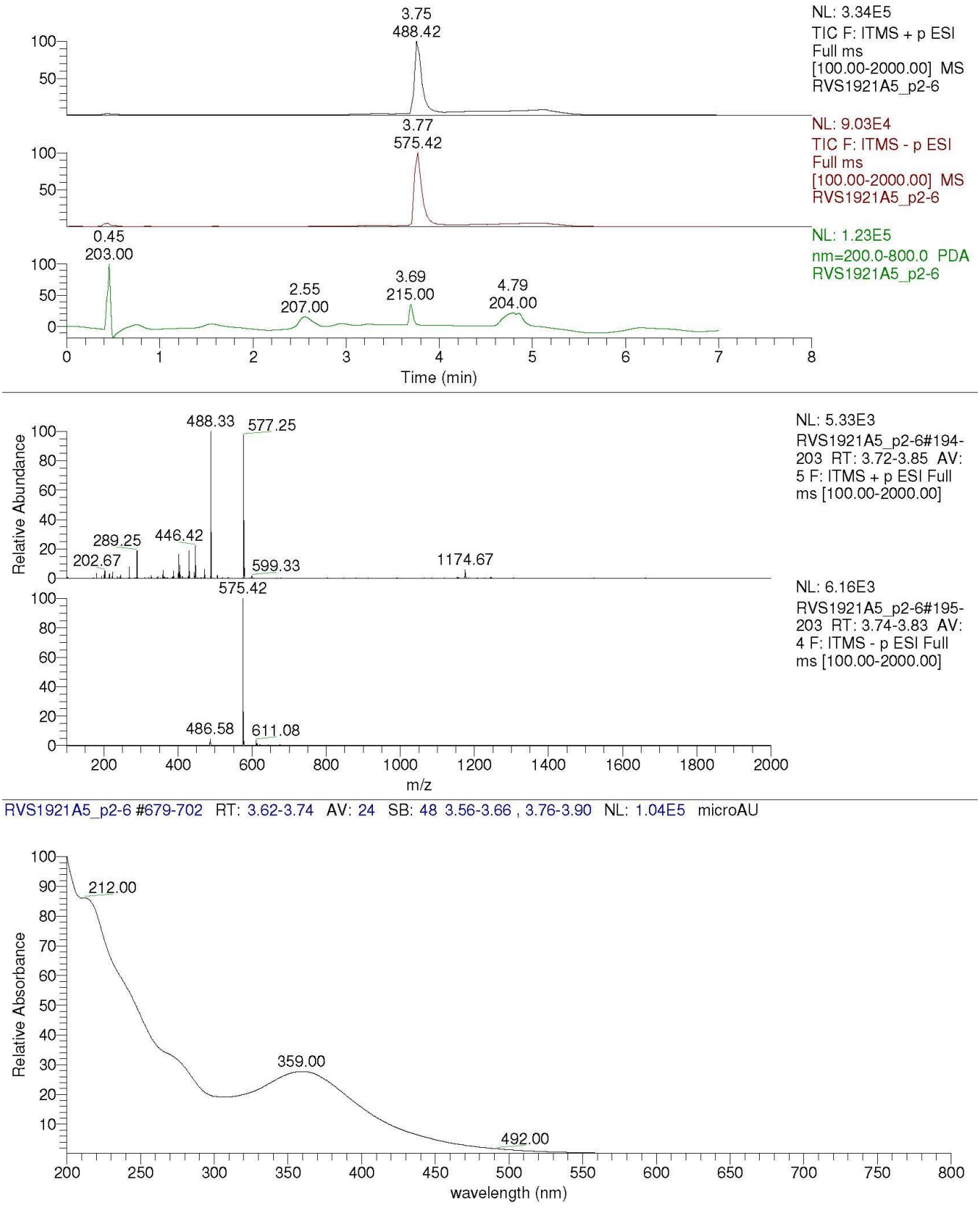

HPLC-MS/PDA analysis of non-releasing 2,5-tautomer **15c** (MW=576)

Section S10: Supplementary References

1. Versteegen, R.M., Rossin, R., ten Hoeve, W., Janssen, H.M. & Robillard, M.S. Click to Release: Instantaneous Doxorubicin Elimination upon Tetrazine Ligation. *Angewandte Chemie International Edition* **52**, 14112-14116 (2013).
2. Rossin, R. et al. Triggered Drug Release from an Antibody–Drug Conjugate Using Fast "Click-to-Release" Chemistry in Mice. *Bioconjugate Chemistry* **27**, 1697-1706 (2016).
3. Rossin, R. et al. Chemically triggered drug release from an antibody-drug conjugate leads to potent antitumour activity in mice. *Nature Communications* **9**, 1484 (2018).
4. Rossin, R. et al. Highly Reactive trans-Cyclooctene Tags with Improved Stability for Dielsâ€"Alder Chemistry in Living Systems. *Bioconjugate Chemistry* **24**, 1210-1217 (2013).
5. Versteegen, R.M. et al. Click-to-Release from trans-Cyclooctenes: Mechanistic Insights and Expansion of Scope from Established Carbamate to Remarkable Ether Cleavage. *Angewandte Chemie International Edition* **57**, 10494-10499 (2018).
6. te Velde, G. et al. Chemistry with ADF. *Journal of Computational Chemistry* **22**, 931-967 (2001).
7. Lee, C., Yang, W. & Parr, R.G. Development of the Colle-Salvetti correlation-energy formula into a functional of the electron density. *Physical Review B* **37**, 785-789 (1988).
8. Stephens, P.J., Devlin, F.J., Chabalowski, C.F. & Frisch, M.J. Ab Initio Calculation of Vibrational Absorption and Circular Dichroism Spectra Using Density Functional Force Fields. *The Journal of Physical Chemistry* **98**, 11623-11627 (1994).
9. Vosko, S.H., Wilk, L. & Nusair, M. Accurate spin-dependent electron liquid correlation energies for local spin density calculations: a critical analysis. *Canadian Journal of Physics* **58**, 1200-1211 (1980).
10. Becke, A.D. Density-functional thermochemistry. III. The role of exact exchange. *The Journal of Chemical Physics* **98**, 5648-5652 (1993).
11. Klamt, A. Conductor-like Screening Model for Real Solvents: A New Approach to the Quantitative Calculation of Solvation Phenomena. *The Journal of Physical Chemistry* **99**, 2224-2235 (1995).